Letícia de Pinho Leite

CONTRIBUTION OF TRIBBLES PROTEIN FAMILY MEMBERS IN GLIOBLASTOMA CELLS

UAlg
UNIVERSIDADE DO ALGARVE

Faculdade de Medicina e Ciências Biomédicas

2023

Letícia de Pinho Leite

CONTRIBUTION OF TRIBBLES PROTEIN FAMILY MEMBERS IN GLIOBLASTOMA CELLS

Master in Oncobiology

Molecular Mechanisms of Cancer

Work developed under the supervision of:

Bibiana I. Ferreira, PhD

Wolfgang Link, PhD

Faculdade de Medicina e Ciências Biomédicas

2023

CONTRIBUTION OF TRIBBLES PROTEIN FAMILY MEMBERS IN GLIOBLASTOMA CELLS

Authorship Statement

I declare to be the author of this work, which is original and unpublished. Authors and papers consulted are properly cited in the text and are listed in the included references.

Letícia de Pinho Leite

Acknowledgments

My grandmother once told me that those who have wings fly, “just like butterflies.". It's been 6 years since I flew away from home. However, in addition to wings, sometimes we do need a little push. First, I would like to thank my supervisor Bibiana Ferreira. Indeed, her encouragement allowed me to complete this thesis since sometimes she believed in me more than I did myself. Also, thanks to Professor Wolfgang, who invited me to be part of the project.

This work would have been even more difficult if it wasn’t for the collaboration of my lab colleagues. To Ana Luísa, Gisela, Bruno, and Alexandra thank you for helping practically and emotionally. A special thanks to Alba, with whom I shared (many) cell plates and also a lot of laughs!

Certainly, the support of my friends, near or far, was fundamental during this year. Ada, Letícia, Ana, Laisla, Malu, Victor, Andreia, Gamarra, Vanda and Clau, thank you! The pressure on the way to obtaining the long-awaited MSc title has been eased with affection, long conversations, tight hugs, and a few glasses of wine.

Finally, a special thanks to my parents. To Papy, from whom I always say I inherited the will to knowledge, and to Mami, my biggest supporter who, even from afar, makes me smile every day.

With a little tear in my eyes, thank you!

Letícia Leite

Abstract

Glioblastoma (GBM) is the most lethal and common form of brain tumor. Currently, the standard treatment comprises surgery, radiotherapy, and chemotherapy with temozolomide (TMZ). However, its prognosis is very deficient due to acquired resistance to therapy and frequent tumor recurrence. Despite research advances, GBM remains largely incurable, with an average survival expectation of 15 months. To improve patients' response to treatment there is an urgent need for new therapeutic strategies.

Tribbles family members (TRIB1, TRIB2, and TRIB3) are pseudokinases known to regulate essential processes such as cell survival and proliferation by modulating signaling pathways. The upregulation of Tribbles has been correlated with a poor prognosis in different types of cancer, such as colorectal and breast cancer, although little is known about their role in GBM.

Previous studies have linked high levels of Tribbles with the progression of different tumors. Preliminary data from our laboratory identified the correlation of high mRNA levels in GBM, resulting in a worse prognosis. Thus, we hypothesized that Tribbles proteins have a tumorigenic role in GBM. Our project focused on generating cell-based tools that allowed the modulation of Tribbles protein levels on GBM cells.

Our results showed that we successfully generated knock-out (KO) GBM lines for TRIB2 and TRIB3. Assays with the generated KO lines demonstrated that inhibition of TRIB3 resulted in decreased proliferation and cell viability in GBM cells. Furthermore, the reduction of TRIB2 levels caused arrest in the mTOR signaling pathway. In general, our results lead to the understanding that Tribbles proteins contribute to the tumorigenesis of GBM cells.

Keywords: cancer; glioblastoma; temozolomide; Tribbles; TRIB2; TRIB3.

Resumo

Os gliomas têm como origem as células da glia e são o tipo mais comum de cancro do cérebro. Segundo a Organização Mundial da Saúde, gliomas podem ser classificados em quatro graus de acordo com sua malignidade. Os gliomas de grau IV são também denominados de glioblastoma (GBM), sendo o tipo mais letal. Pacientes com GBM apresentam uma expectativa de vida de aproximadamente 15 meses, sendo que apenas entre 0,5 e 4,7% dos pacientes sobrevive após 5 anos de diagnóstico. A letalidade deste tipo de tumor pode ser em grande parte explicada devido a sua complexidade. De um ponto de vista molecular, três vias de sinalização encontram-se frequentemente alteradas neste tipo de tumor: via PI3K/AKT, via RB e via P53.

Atualmente, o tratamento padrão para pacientes de GBM compreende cirurgia, radioterapia e quimioterapia com temozolomida (TMZ). No entanto, devido à sua alta complexidade, as células de GBM tornam-se invasivas e adquirem resistência à terapia. Como consequência, cerca de 90% dos pacientes sofre com o reaparecimento tumoral. Nesse sentido, é de extrema relevância a descoberta de biomarcadores que nos possibilitem uma melhora no prognóstico e a identificação de alvos terapêuticos. Estas descobertas permitiriam o desenvolvimento de tratamentos mais eficazes a fim de aumentar a sobrevida dos pacientes de GBM.

Os membros da família Tribbles (TRIB1, TRIB2 e TRIB3) são denominados de pseudoquinases por falta de um domínio catalítico que os permita fosforilar outras proteínas. As proteínas Tribbles estão envolvidas na regulação de processos essenciais (como proliferação, diferenciação e metabolismo celular) através da modulação de vias de sinalização, como por exemplo PI3K/AKT. Dessa forma, a desregulação dos seus níveis está associada a diferentes doenças, entre elas o cancro. Vários estudos descreveram a relação entre sobre-expressão de membros da família Tribbles e a progressão tumoral. Como exemplo, elevados níveis de expressão de TRIB2 está relacionado com pior prognóstico em melanoma, cancro do pâncreas, cancro do pulmão e leucemias. Em relação à TRIB3, altos níveis desta proteína

estão associados à tumorigénese em carcinoma renal, retinoblastoma e cancro da bexiga. No entanto, ainda pouco se sabe em respeito a relação entre proteínas Tribbles e GBM.

Análises preliminares de dados da expressão de mRNA em gliomas realizadas pelo estudante de doutoramento Bruno Santos indicaram que os níveis de mRNA de TRIB1/2/3 estão associados ao grau e à malignidade de gliomas. Isto é, GBMs apresentavam altos níveis de Tribbles, bem como um pior prognóstico. Em associação, esta mesma categoria apresentava também reduzidos níveis de proteínas FOXOs. Levando em consideração esses dados e o papel tumorigénico das proteínas Tribbles em outros tipos de cancro, nossa hipótese é que os membros de Tribbles contribuem para a progressão tumoral de GBM. Portanto, nos propusemos a gerar linhas celulares com níveis de expressão de Tribbles modulados a fim de estudar o papel dos membros dessa família na biologia do GBM.

Conseguimos atingir com sucesso nosso objetivo principal de criar ferramentas que nos permitiriam estudar o efeito da modulação das proteínas Tribbles em GBM. Através da tecnologia CRISPR/Cas9, a partir de linhas celulares de GBM, geramos uma linha *knock-out* (KO) para TRIB3 (U-118 TRIB3 KO) e uma linha KO para TRIB2 (LN-229 TRIB2 KO).

Durante este projeto, estudos realizados com a linha U-118 TRIB3 KO demonstraram que a inibição de TRIB3 nessas células levou a uma redução na viabilidade celular. Ainda, nossos resultados indicam que a redução da viabilidade associada ao TRIB3 ocorre devido a diminuição da proliferação celular, e não de um aumento de morte celular. Em relação ao *status* das vias de sinalização que poderiam estar a resultar no fenótipo observado, não observamos diferenças na regulação da via de sinalização AKT/mTOR e de MAPK/ERK após redução de TRIB3.

Somado a estes dados, também analisamos o comportamento celular após 72h de exposição ao tratamento com TMZ. Demonstramos que, apesar das células com inibição de TRIB3 não apresentarem aumento à sensibilidade ao tratamento com TMZ, devido à diminuição da viabilidade celular causada em

níveis basais, pacientes com baixos níveis de TRIB3 poderiam ser mais beneficiados à terapêutica com TMZ.

Em relação as células KO para TRIB2, devido à falta de tempo, não nos foi possível realizar estudos para avaliar fenotipicamente o efeito da inibição de TRIB2 em células de GBM. No entanto, resultados preliminares da caracterização de níveis de proteínas nessas células demonstrou que a redução de TRIB2 foi capaz de inibir a via mTOR. Entretanto, ainda é preciso aumentar a replicabilidade do experimento e analisar outros parâmetros a fim de podermos confirmar um papel tumorigénico de TRIB2 em GBM.

Em resumo, nossos resultados dão-nos indícios que os membros da família de proteínas Tribbles contribuem para a progressão tumoral em GBM. A identificação de biomarcadores e alvos farmacológicos no contexto de GBM é de extrema importância para o desenvolvimento de estratégias terapêuticas que melhorem o prognóstico deste tipo de cancro ainda tão letal. Assim, a geração de ferramentas que possam ajudar a possivelmente identificar a família de proteínas Tribbles como oncogenes em GBM confere um caráter relevante a este projeto.

Palavras-chave: cancro; glioblastoma; temozolomida; Tribbles; TRIB2; TRIB3.

Table of Contents

Acknowledgments iv

Abstract v

Resumo vi

Table of Contents ix

List of Figures xii

List of Tables xiv

Abbreviations xv

1. INTRODUCTION 1

1.1. Cancer 1

1.2. Gliomas 4

1.3. Glioblastoma 5

1.3.1. GBM cell biology 7

1.3.2. GBM classification 13

1.3.3. Risk factors for GBM development 17

1.3.4. GBM diagnosis 18

1.3.5. GBM treatment 19

1.3.6. GBM therapy resistance 22

1.4. Tribbles protein family members 24

1.4.1. Tribbles members protein structure 25

1.4.2. Mechanism of action of Tribbles proteins and implication in cancer 27

1.4.3. TRIB3 29

1.4.4. TRIB2 33

1.4.5. Tribbles and glioblastoma 37

2. HYPOTHESIS AND OBJECTIVES 39

3. MATERIALS AND METHODS 41
3.1. Cell culture 41
3.1.1. Cell line cryopreservation 42
3.1.2. Cell counting 42
3.2. Assessment of protein levels by Western Blot 43
3.2.1. Protein extraction 44
3.2.2. Protein quantification and calibration 44
3.2.3. Polyacrylamide gel electrophoresis (SDS-PAGE) 46
3.2.4. Protein transfer to PVDF membranes 47
3.2.5. Immunodetection 48
3.3. Quantitative Reverse Transcription Polymerase Chain Reaction analysis of mRNA levels 49
3.3.1 RNA extraction and purification 50
3.3.2. cDNA synthesis 50
3.3.3. RT-qPCR 51
3.4. Gene modulation 52
3.4.1. Cell transfection for gene modulation 53
3.4.2. Generation of knock-out cell lines by CRISPR/Cas9 55
3.5. Crystal Violet Staining 57
3.6. Trypan Blue exclusion assay 58
4. RESULTS 59
4.1. Tribbles' antibodies validation 59
4.2. GBM cell line screening 63
4.2.1. Characterization of GBM cell line panel at mRNA level 63
4.2.2. Characterization of GBM panel cell line panel at proteomic level 65
4.3. Generation of U-118 TRIB3 knockout cell line 66
4.4. Tribbles protein profile in U-118 TRIB3 KO cell line 67

4.5. TRIB3 KO cells have reduced viability in the U-118 cell line 68

4.6. TRIB3 inhibition decreases cell proliferation but does not induce cell death in the U-118 cell line 69

4.7. Status of signaling pathways involved in cell proliferation in U-118 cell line upon TRIB3 abrogation 71

4.8. TRIB3 inhibition does not affect AKT and ERK pathways under starvation in the U-118 cell line 73

4.9. U-118 cell viability and cell death upon TMZ treatment after TRIB3 inhibition…….. 74

4.9.1 Absence of TRIB3 expression does not alter cell sensitivity to TMZ 75

4.9.2. U-118 TRIB3 KO cell death by Trypan Blue exclusion assay upon TMZ treatment 76

4.10. Characterization of TRIB2 silencing in LN-229 78

4.11. Generation of LN-229 TRIB2 KO cell line 79

4.12. LN-229 TRIB2 KO cell line protein characterization 80

4.13. Characterization of TRIB2 overexpression in U-87 82

5. DISCUSSION 84

5.1. TRIB3 inhibition 86

5.2. TRIB2 inhibition 90

6. CONCLUSIONS AND FUTURE PERSPECTIVES 93

7. BIBLIOGRAPHY 95

APPENDIX 115

List of Figures

Figure 1.1 - Hallmarks of cancer. 4
Figure 1.2 - Distribution of brain and other CNS tumors by histology type. 6
Figure 1.3 - Schema of the GBM pathogenesis and its progression. 7
Figure 1.4 - Representation of the RAS/MAPK and PI3K/AKT signaling pathways activated by RTK. 9
Figure 1.5 - Representation of P53 and RB pathways. 11
Figure 1.6 - Frequent genetic alterations in three critical signaling pathways of GBM. 13
Figure 1.7 - Common molecular alterations in primary and secondary GBM. .. 15
Figure 1.8 - Molecular characteristics of GBM subtypes. 16
Figure 1.9 - Schema of human brain anatomy. 18
Figure 1.10 - Schema of Tribbles' structure. 25
Figure 1.11 - Canonical structure of a kinase domain. 26
Figure 1.12 - Representation of the proposed interaction of TRIB3 with the AKT pathway. 30
Figure 1.13 - Proposed model of TRIB2-mediated drug resistance. 37
Figure 2.1 - Flowchart representing the steps of the project. 40
Figure 3.1 - Scheme of Neubauer chamber counting. 43
Figure 3.2 - Scheme of Bradford assay for protein quantification. 45
Figure 3.3 - Representation of the "sandwich" assembly for protein transfer. .. 47
Figure 3.4 - Stages of RT-qPCR for RNA detection. 50
Figure 3.5 - Representation on how we modulated Tribbles in GBM cell lines. 53
Figure 3.6 - Map image for pSpCas9(BB)-2A-Puro (PX459) V2.0 used in CRISPR/Cas9 KO. 56
Figure 4.1 - Expression levels of Tribbles members in UACC-62 after siRNA. 61
Figure 4.2 - Levels of FOXOs proteins in UACC-62 after silencing RNA expression. 62
Figure 4.3 - Transcriptomic profile of GBM cell line panel regarding Tribbles and FOXOs. 64
Figure 4.4 - Tribbles and FOXOs protein levels in GBM cell line panel. 66
Figure 4.5 - Selection of U-118 TRIB3 KO clones. 67

Figure 4.6 - Tribbles and FOXOs protein levels in U-118 TRIB3 KO clones. ... 68
Figure 4.7 - TRIB3 reduces cell viability in U-118 cell line. ... 69
Figure 4.8 - Evaluation of cell proliferation and cell death between U-118 WT and TRIB3 KO cells. ... 70
Figure 4.9 - Phosphorylation levels of key proteins from AKT and MAPK pathways in U-118 WT and TRIB3 KO cells. ... 72
Figure 4.10 - Phosphorylation levels of key proteins from AKT and MAPK pathways in U-118 WT and TRIB3 KO cells upon starvation. ... 74
Figure 4.11 - TMZ concentration for IC50 in U-118 cell line. ... 75
Figure 4.12 - Cell viability of U-118 TRIB3 KO cells after TMZ treatment. ... 76
Figure 4.13 - Cell death by Trypan Blue of U-118 TRIB3 KO cells upon TMZ treatment. ... 77
Figure 4.14 - Protein levels of siTRIB2 on LN-229 cell line. ... 79
Figure 4.15 - Selection of LN-229 TRIB2 KO clones. ... 80
Figure 4.16 - Protein levels of LN-229 after TRIB2 modulation. ... 82
Figure 4.17 - Protein characterization after TRIB2 overexpression in U-87 cell line. ... 83

List of Tables

Table 1.1 - Summary of TRIB2 role in different human cancers. 36
Table 3.1 - Panel of GBM cell lines and their characteristics……42
Table 3.2 - Cell lysis buffer composition 44
Table 3.3 - Composition of 1 gel for SDS-PAGE. 46
Table 3.4 - List of primary and secondary antibodies used in Western Blot in this study. 48
Table 3.5 - Volume of reagents used for the qPCR technique per well. 51
Table 3.6 - List of primers used for RT-qPCR in this study. 52
Table 3.7 - List of siRNA used for gene silencing. 55

Abbreviations

A

ABC: ATP-binding cassettes

AML: acute myeloid leukemia

ATP: adenosine triphosphate

ATRX: Alpha Thalassemia/Mental Retardation Syndrome X-Linked

B

BSA: Bovine Serum Albumin

BV: Bevacizumab

C

CDK: cyclin-dependent kinase

CDKN2A: cyclin-dependent kinase inhibitor 2A

cDNA: complementary DNA

CO_2: carbon dioxide

CRISPR/Cas9: Clustered Regularly Interspaced Short Palindromic Repeats

CSC: cancer stem cell

CT: computed tomography

CNS: central nervous system

D

DMEM: Dulbecco's Modified Eagle's Medium

DMSO: Dimethyl sulfoxide

E

ECL: enhanced chemiluminescence

ECM: extra-cellular matrix

EDTA: ethylenediaminetetraacetic acid

EGFR: epidermal growth factor receptor

EGTA: ethylene glycol-bis (2-aminoethylether) tetraacetic acid

EMT: epithelial-mesenchymal transition

F

FBS: Fetal Bovine Serum

FDS: U.S. Food and Drug Administration

FOXO: forkhead box O

G

GABRA1: Gamma-aminobutyric acid type A receptor alpha1 subunit

GAPDH: glyceraldehyde 3-phosphate dehydrogenase

GBM: Glioblastoma

GEF: guanine nucleotide exchange factor

gRNA: guided-Ribonucleic acid

GSC: glioma stem cell

GSH: glutathione

H

H_2O_2: hydrogen peroxide

HRP: horseradish peroxidase

I

IARC: The International Agency for Research on Cancer

IDH: isocitrate dehydrogenase

IHME: Institute for Health Metrics and Evaluation

K

KO: knock-out

M

MAPK: mitogen-activated protein kinase

MGMT: O6-methylguanine transferase

miRNA: microRNAs

MMP2: matrix metalloproteinase2

MMP4: matrix metalloproteinase4

MRI: magnetic resonance imaging

MTIC: 5-(3-Methyl-1-triazine)imidazole-4-carboxamide

mTOR: mammalian target of rapamycin

mTORC1: mTOR complex 1

mTORC2: mTOR complex 2

N

NaF: sodium fluoride

NAPDH: nicotinamide adenine dinucleotide phosphate

NEFL: Neurofilament light

NF1: Neurofibromin 1.

NHEJ: non-homologous end joining repair

NSCLC: small cell lung cancer

NTC: No-template controls

O

OS: overall survival

OSCC: oral squamous cell carcinoma

OVO4: sodium orthovanadate

P

PBS: Phosphate Buffered Saline

PDGFR: platelet-derived growth factor receptor

PFA: paraformaldehyde

PFS: progression-free survival

PI3K: phosphatidylinositol 3-kinase

PIC: Protease Inhibitors Cocktail

PTEN: phosphatase and tensin homolog

PVDF: polyvinylidene difluoride

R

RB: retinoblastoma

ROS: reactive oxygen species

RT: radiation therapy

RTK: receptor tyrosine kinase

RT-qPCR: Quantitative Reverse Transcription Polymerase Chain Reaction

S

SCL12A5: Solute Carrier family 12 member 5

SDS: sodium dodecyl sulfate

SHH: Sonic Hedgehog

siRNA: short interfering RNA

T

TBS-T: Tris-Buffer saline 0,1% Tween

TCGA: The Cancer Genome Atlas

TEMED: tetramethylethylenediamine

TMZ: temozolomide

TP53: tumor protein 53

TRIB2: Tribbles homolog 2

TRIB3: Tribbles homolog 3

TSC: tuberous sclerosis complex

TSG: tumor suppressor genes

TTF: Tumor Treating Fields

V

VEGF: vascular endothelial growth factor

W

WHO: The World Health Organization

WT: wild-type

OTHERS

α-KG: α-ketoglutarate

1. INTRODUCTION

1.1. Cancer

Cancer is the second leading cause of death globally, only behind cardiovascular diseases, according to the Institute for Health Metrics and Evaluation (IHME)[1]. The global cancer rate is growing every year due to the aging population and the increasing prevalence of cancer risk factors worldwide. The International Agency for Research on Cancer (IARC) estimated about 19,2 million new cases in 2020 and predicts about 28,8 million new cases by 2040, an increase of ≈ 49%[2]. Not only the incidence but mortality rates are predicted to suffer an increase of ≈ 60%, from about 10 million to 16,1 million in the same period[3].

The cancer burden continues to grow globally. The scope of the disease includes not only massive physical damage but also puts an emotional and financial strain on the individual, the family, and the healthcare system. Therefore, it is crucial to develop effective strategies that help to overcome this complex disease. Improving diagnostic tools for accessible early detection, such as the discovery of biomarkers, in association with quality and personalized medicine are factors to help obtain an earlier prognosis and improve a patient's life.

Cancer comprehends a group of diseases characterized by uncontrolled, abnormal cell growth. It is a multi-step process by which cells acquire capabilities and become “masters of their own destinies”, as Hanahan and Weinberg stated[4]. The process of tumorigenesis is progressive and involves a series of alterations and specific characteristics that lead to transforming a normal cell into a cancer cell.

In fact, all cells are susceptible of becoming malignant, but it takes years to reach a lethal metastatic stage. Briefly, this multi-step process initiates with a sequence of random mutations and epigenetic alterations that accumulate and dictate unbalanced cell proliferation[5]. The uncontrolled cell growth will eventually give rise to a small tumor. Sequentially, additional mutation accumulates, giving

rise to other characteristics related to the malignant phenotype, such as evading apoptosis. The stage in which the tumor has not yet invaded neighboring tissues is called carcinoma *in situ*. The invasion phase begins when the cells acquiring the ability to induce angiogenesis, leading to a greater supply of oxygen and nutrients. Finally, when the tumor is able to invade neighboring tissues, the metastatic phase occurs[6].

Genes involved in signaling pathways that control cell proliferation, cell cycle, cell survival and genomic stability are tumor-triggering. The first mutation that gives a cell a selective growth advantageous occurs on a gatekeeper gene[7]. Usually, it affects oncogenes or tumor suppressor genes (TSGs)[8]. During carcinogenesis, oncogenes suffer gain of function mutations, being overexpressed, whereas TSGs suffer inactivating mutations, losing their function.

The more a cell proliferates, the more likely it is to mutate. Therefore, those cancer cells start accumulating other mutations, which can be categorized as driver or passenger mutations. Driver mutations influence the cancer phenotype, whereas the passenger ones do not. On average, a solid tumor accumulates 33 to 66 mutations[7]. The combination of all mutations turns each cancer singular and heterogenous and explains its complexity.

Following the uncontrolled proliferation, the cells consequently acquire other characteristics that contribute to the cancer phenotype, becoming transformed cells. Typically, a transformed cell has a clonal growth capacity, is independent of surrounding growth stimuli, has adhesion-independent proliferation, and loses contact inhibition[6]. In addition to these transformations, cancer cells also accumulate other characteristics. These characteristics have been described as the Hallmarks of Cancer[4].

One of the hallmarks is that tumor cells have *sustaining proliferative signaling*. The secretion of growth factors that activates the cell cycle, the overexpression (or mutated active form) of receptors of those growth factors, or alterations that affect proteins involved in the cell cycle are changes that lead to the sustained proliferation of the cancer cells[9]. Not only tumor cells have increased signals to grow, they also can *evade growth suppressors*, such as loss of function of TSGs[10], resulting in uncontrolled growth.

Typically, normal cells suffer a programed cell death under specific reasons, such as DNA damage and apoptosis-inducing stresses[11]. However, this process is limited in cancer due to mutations in stress sensors or effectors of apoptosis or autophagy[12]. Therefore, cancer cells can also *resist cell death*. Other characteristic of cancer cells is their *replicative immortality.* Normal cells have a finite ability to divide due to the lack of activity of the enzyme telomerase, causing telomere shortening. However, cancer cells can bypass this obstacle by activating this enzyme responsible for adding repeated segments to the telomere[13].

Moreover, due to uncontrolled growth, tumor cores often have low oxygen and nutrient supply. To overcome this, cancer cells rewire signaling pathways that *induce processes like angiogenesis*[14]. Therefore, cancer cells can create newly formed vessels that allow reoxygenation of tumors and nutrient availability. In addition, to sustain uncontrolled growth, cancer cells also shift their energy metabolism. By *deregulating cellular energetics*, tumor cells can degrade glucose through glycolysis, even in the presence of oxygen[15].

Tumor cells also present alterations in structural proteins that transform the interactions between the cells' extra-cellular matrix (ECM), leading to an epithelial-mesenchymal transition (EMT). These modifications help their migratory and invasive phenotype and *activate invasion and metastasis*[16]. Moreover, tumors are also infiltrated with immune system cells that *promote inflammation* and release proinflammatory agents that end up helping the tumor progression[17]. Normally, the immune system is involved in inhibiting the formation of many tumors in the body. Therefore, cancer cells must be able to *avoid immune system destruction* for cancer to develop[18].

The acquisition of the characteristics necessary for tumor formation is partly due to *genome instability and mutation*. This susceptibility of cancer cells can occur by defects in the DNA repair machinery or increased levels of molecules that promote DNA damage[19].

All these capabilities mentioned have been validated to be part of the core set of the Hallmarks of Cancer[4]. In 2022, Hanahan proposed to incorporate two more emerging hallmarks (unlock phenotypic plasticity and senescent cells) and

two enabling characteristics (nonmutational epigenetic reprogramming and polymorphic microbiomes)[20] (Figure 1.1).

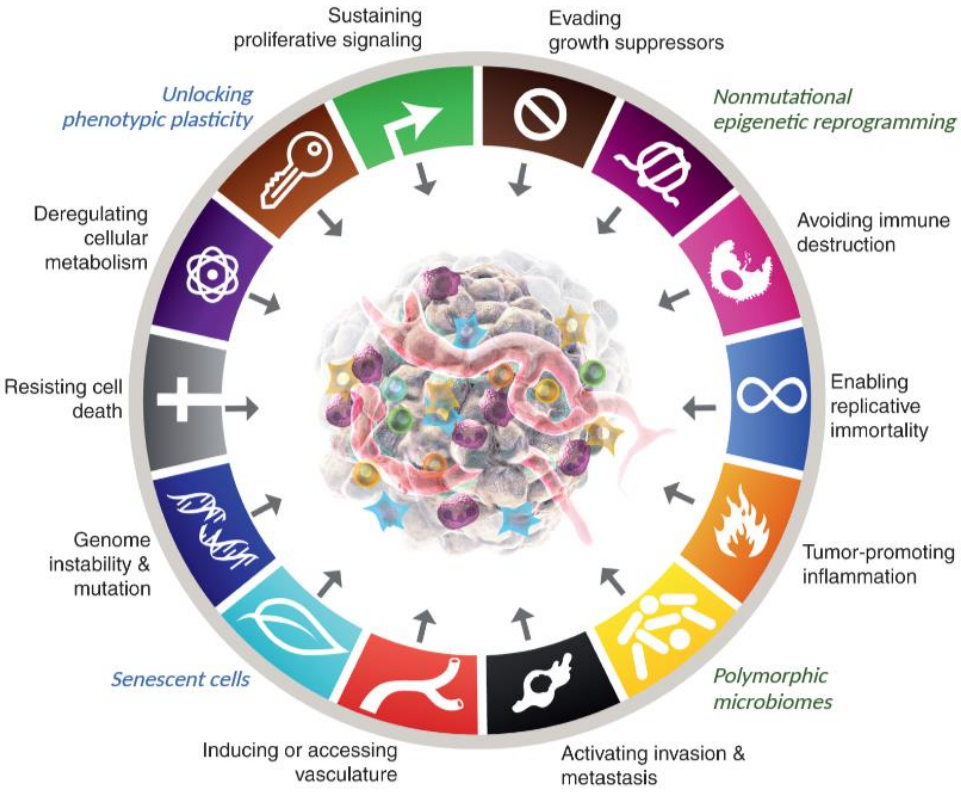

Figure 1.1 - Hallmarks of cancer.

This diagram shows the 10 hallmarks (in black) of cancer consolidated and described by Hanahan and Weinberg. In blue, two emerging hallmarks and in green, two enabling characteristics proposed for Hanahan in 2020. Adapted from Hanahan, 2020.

1.2. Gliomas

Gliomas are solid tumors that originate from the glial cells and account for the majority of malignant brain tumors[21]. Brain tumors, although relatively rare, have high mortality and low survival rate[22]. For comparison, breast and prostate cancer presented respectively about 7.3 and 4.6 times more prevalence than brain cancer in the year 2020[23]. In short, this can be explained in part by the reduced cell proliferation in central nervous system (CNS) cells, which decreases the likelihood of mutation occurring. In addition, the presence of the blood-brain barrier (BBB) also plays a role in reducing the prevalence of brain cancers by

limiting the entry of toxic substances and potentially carcinogenic agents into the brain[24,25]. These aspects also present an obstacle to the treatment of brain tumors as the BBB limits the entry of therapeutic agents into the brain, making it difficult for drugs to effectively target and treat cancer cells[26].

It is estimated that more than 251.000 people worldwide died from brain cancer in 2020. In Europe, the IACR estimated 67.114 new cases and 53.680 cases of death caused by brain tumors in the same period, reflecting a mortality rate of ≈ 80%[23]. Globally, the mortality rate is expected to increase to 85% by 2040[3].

Although a new classification for brain tumors was published in 2021[27], the most used classification is the one from 2016[28]. Gliomas are classified according to their morphologic and molecular features. From histologic criteria, gliomas can be originated from astrocytes, oligodendrocytes, or have a mixed origin. The World Health Organization (WHO) incorporated molecular analysis and classifies gliomas from grades I to IV according to their increasing level of malignancy. Grade I are non-invasive tumors. Grades II to IV are diffuse infiltrating gliomas. Grade IV glioma is also known as glioblastoma (GBM), and it is the most aggressive and lethal kind of glioma, also being the most common type[29]. GBM displays similarity to different glial lineages, so the cellular origin is not yet clear[30,31].

1.3. Glioblastoma

GBM is the most frequent and aggressive kind of glioma, representing about 45% of all gliomas. Compared to all malignant brain and other CNS tumors, GBM also ranks as the most common, comprising nearly 50% of the cases[32] (Figure 1.2). Despite being the most common type of brain tumor, its incidence is considered rare, at 3,2 / 100.000 people per year[32]. In addition to that, GBM has the worst glioma prognosis, with a median overall survival (OS) of approximately 15 months[33] and only 0.05% to 4.7% of patients surviving five years past diagnosis[34], making GBM a lethal disease.

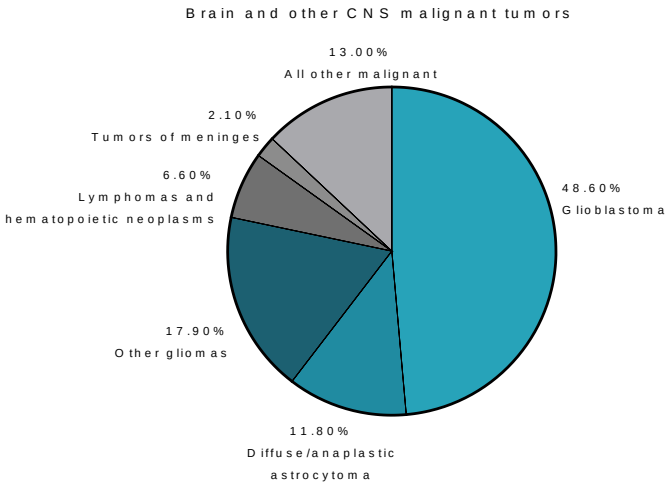

Figure 1.2 - Distribution of brain and other CNS tumors by histology type.

Data from the Central Brain Tumor Registry of the United States showed that Glioblastoma accounts for almost half of the cases (48.6%) of malignant tumors patients. Data from 2013 to 2017. Figure adapted from Ostrom *et al.*, 2021.

GBMs can be distinguished from low-grade gliomas by having some striking features. This type of grade IV tumor expresses necrosis and microvascular proliferation. However, its hallmark is rapid cell proliferation with high infiltrating capacity. As a result, GBMs display intrinsic heterogeneity, reflected in the presence of different cells of varying morphology[35]. The presence of stem-like cells also contributes to cellular heterogeneity in this type of tumor[36]. These stem-like cells are capable of self-renewal and tumor initiation and will be discussed later. All these characteristics involved in GBM pathogenesis and progression are in accordance with the Hallmarks of Cancer proposed by Hanahan[20] already described in the text and are schematized in Figure 1.3.

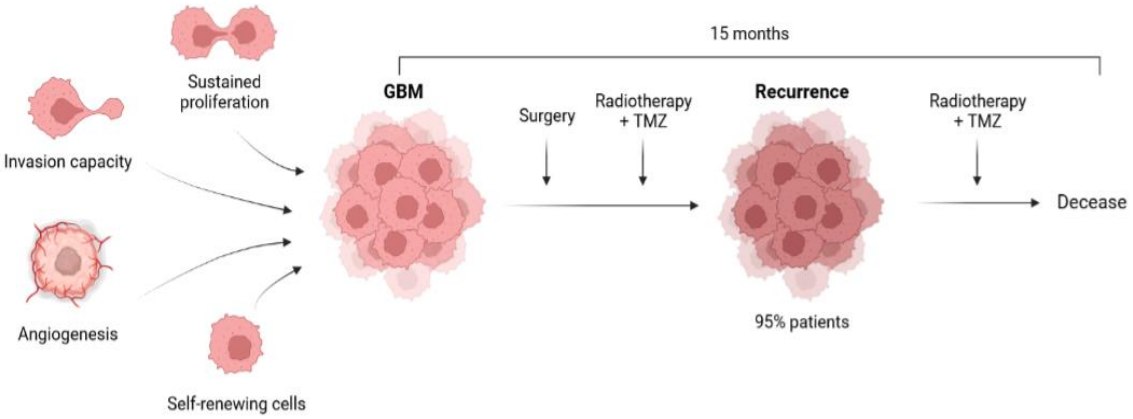

Figure 1.3 - Schema of the GBM pathogenesis and its progression.

GBMs are characterized by a rapid cell proliferation with great invasion capacity. In addition to that, this type of tumor expresses microvascular progression by promoting angiogenesis and stem-like cells with self-renewing capacity. Despite treatment with surgery followed by radiotherapy and chemotherapy with temozolomide (TMZ), about 95% of patients suffer from recurrence partially due to invasive cells and intense intratumoral variability. On average, the life expectancy of people diagnosed with GBM is 15 months. Figure created with BioRender.com.

1.3.1. GBM cell biology

From a molecular perspective, in the past year, patients with GBM have been detected with numerous genetic and epigenetic alterations, reflecting the complexity of this kind of tumor[37]. Three core pathways have been recurrently documented as altered in a study made by The Cancer Genome Atlas (TCGA) Research Network: (i) receptor tyrosine kinase (RTK) signaling in 88% of the cases; (ii) retinoblastoma (RB) pathway in 77% of the cases; and (iii) protein 53 (P53) pathway, in 87% of cases[38]. These signaling pathways are involved in the cell proliferation process[10,39]. Changes in the components of these pathways can lead to a hyperactivated state. It culminates in contributing to the maintenance of cell proliferation and subsequent tumor progression.

1.3.1.1. RAS and PI3K/AKT pathways

In normal cells, RTK signaling regulates cellular processes such as growth, survival, differentiation, and migration through the activation of mitogen-activated protein kinase (RAS/MAPK) and phosphatidylinositol 3-kinase (PI3K/AKT) pathways[39,40]. Growth factors bind to RTK and cause its dimerization, promoting a cross-phosphorylation that activates the receptor. This activation triggers a signaling by the phosphorylation of intracellular proteins.

In the case of the RTK/RAS pathway, RTK recruits GRB adaptor protein that in turn binds to SOS, a guanine nucleotide exchange factor (GEF) protein that can activate RAS by promoting the binding of Ras to GTP. RAS-GTP activates a phosphorylation cascade of the mitogen-activated protein kinase (MAPk) module, a cascade of three serine/threonine kinases – RAF, MEK1/2, and ERK1/2. The phosphorylation of ERK1/2 results in the activation of many downstream targets involved in the regulation of cell proliferation, such as Cyclin D complexes with Cdk4/6[39] (Figure 1.4).

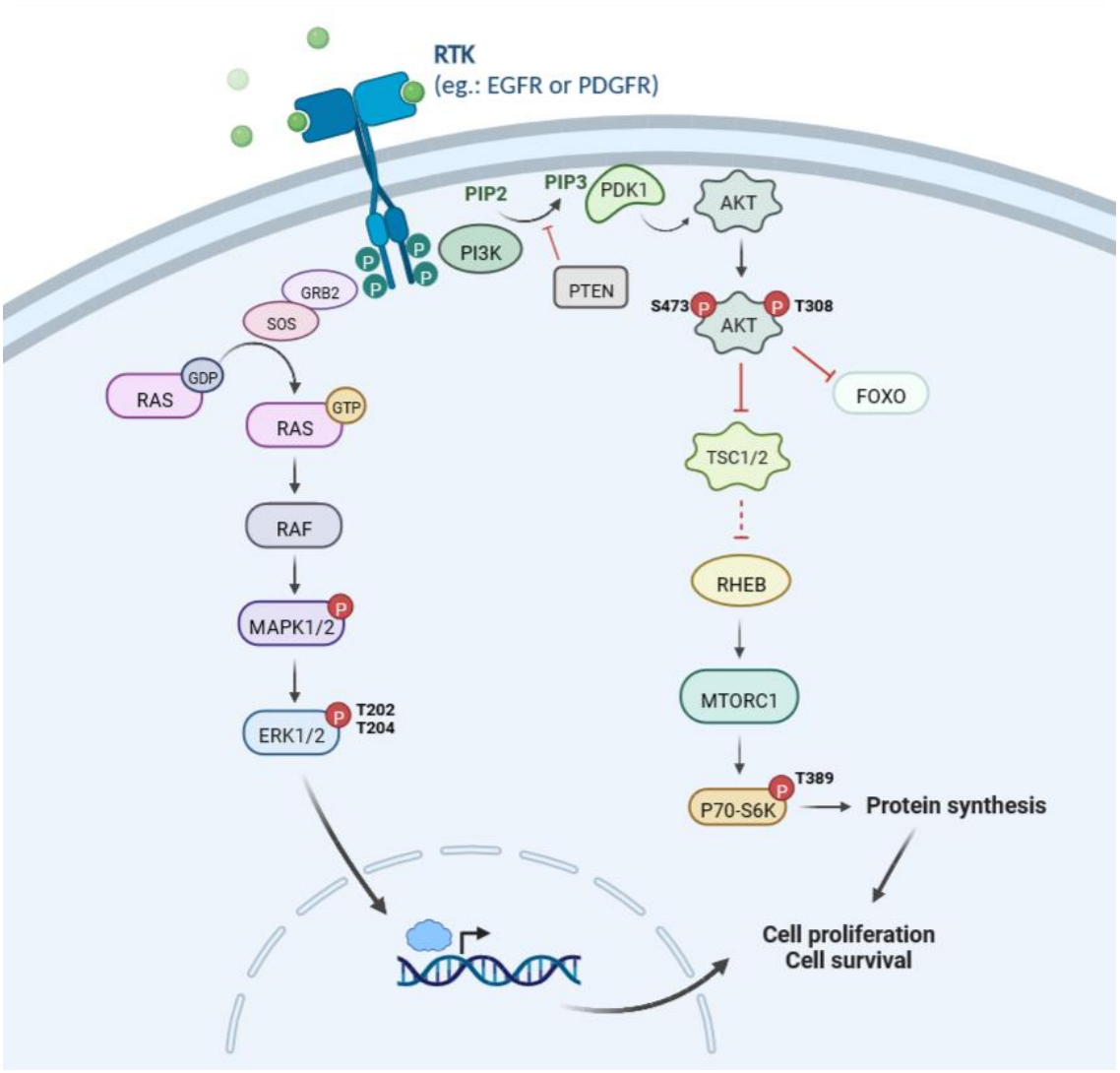

Figure 1.4 - Representation of the RAS/MAPK and PI3K/AKT signaling pathways activated by RTK.

Schematic representation of RTK activation and the resultant downstream signaling. Black arrows indicate activation whereas red arrows indicate inhibition. Described in detail in the introduction. Overactivation of these pathways can lead to an oncogenic phenotype. Figure created with BioRender.com.

On the other hand, RTK dimerization can also activate PI3K, a lipid kinase that catalyzes the phosphorylation of phosphatidylinositol 3,4-bisphosphate (PIP_2) to phosphatidylinositol 3,4,5-triphosphate (PIP_3). The tumor suppressor phosphatase and tensin homolog deleted on chromosome 10 (PTEN) antagonizes the PI3K/AKT pathway by reconverting PIP_3 back to PIP_2[41] (Figure 1.4).

PDK1 and AKT contain pleckstrin homology domains that bind to PIP_3 promoting AKT phosphorylation. The activation of AKT has several downstream effects that result in anti-apoptotic or pro-cell proliferation events[42].

AKT directly phosphorylates the forkhead box O (FOXO) family proteins. FOXOs are a family of transcription factors composed of FOXO1, FOXO3, FOXO4, and FOXO6. In the absence of growth factors, FOXOs translocate into the nucleus and can promote the transcription of several genes related to cell death, cell cycle, autophagy, and metabolism. When phosphorylated, FOXO1, FOXO3, and FOXO4 are retained in the cytoplasm, inhibiting their transcriptional activities[43].

One of the key effectors downstream of AKT is the mammalian target of rapamycin (mTOR). mTOR forms two complexes characterized by different binding proteins, mTOR complex 1 (mTOR1) and mTOR complex 2 (mTOR2). The phosphorylation of tuberous sclerosis complex (TSC) by AKT releases RHEB protein that, in turn, leads to the activation of mTOR. Activated mTORC1 can phosphorylate p70-S6K, leading to protein translation and cell growth[40].

In GBM, frequent genetic alterations were found in these major signaling pathways. RTK, such as epidermal growth factor receptor (EGFR) and platelet-derived growth factor receptor (PDGFR), are commonly activated due to gene amplification or mutation[44,45]. These alterations in RTK converge in the stimulation of downstream signaling pathways RAS/MAPK and PI3K/AKT. Other mutations on these proteins also contribute to the over-activating of these pathways. For example, loss of function of the PTEN protein and AKT amplification are also common in GBM[38,46]. These alterations can lead to an oncogenic phenotype by activating invasion and uncontrolled proliferation. Studies have demonstrated that the activation of both AKT and RAS in neural progenitors induced GBM formation in the murine model[47]. Also, the activation of the AKT pathway resulted in the progression from an anaplastic astrocytoma to GBM[48]. Moreover, inhibition of the PI3K/AKT pathway has been shown to inhibit the growth of GBM cells[49] (Figure 1.6, A).

1.3.1.2. P53 pathway

The P53 is a transcription factor induced in response to DNA damage, for example, and regulates a set of genes that leads either to cell cycle arrest or apoptosis. P53-target genes include CDK inhibitor P21 and MDM2, which in turn are negative regulators of P53. MDM2 binds to P53, inhibiting its transcription and catalysis of its ubiquitination for further degradation. P53 and MDM2 have an autoregulatory feedback loop in normal cells that regulates both activities[50] (Figure 1.5).

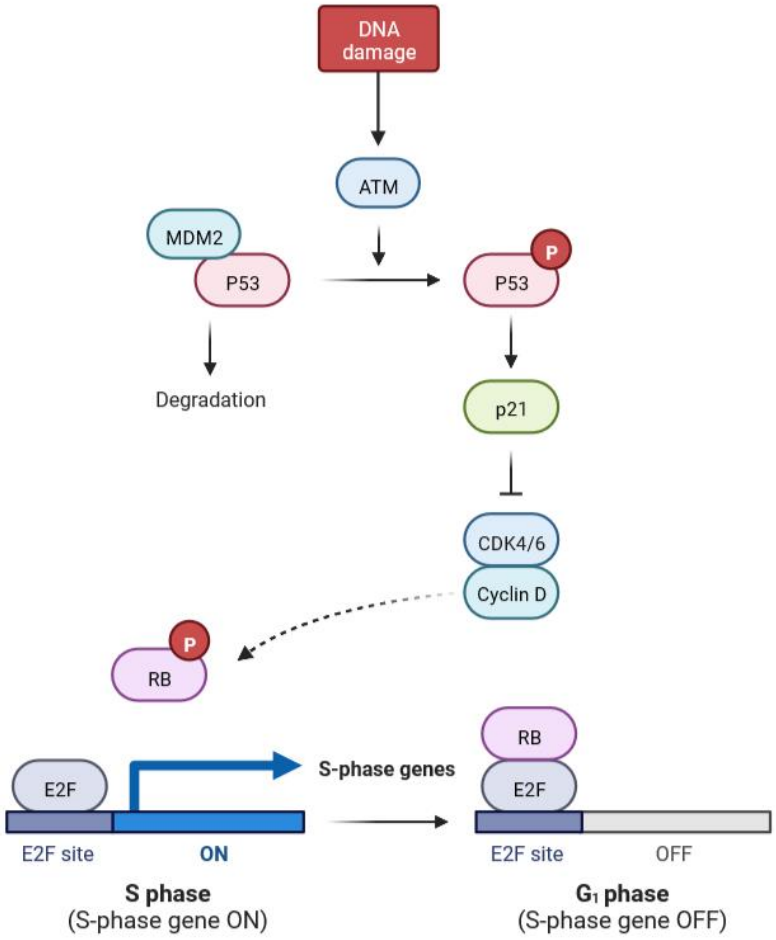

Figure 1.5 - Representation of P53 and RB pathways.

Schematic representation of P53 pathway and downstream signaling affecting RB pathway. DNA damage results in P53 phosphorylation. Consequently, a complex of CDK-Cyclin is inhibited and cannot phosphorylate RB. In turn, RB inhibits the transcription of genes necessary for the S phase. Therefore, the cell cycle stops. Described in detail in the introduction. Figure created with BioRender.com.

Inactivating mutations of P53 and amplifications of MDM2 are alterations frequently found in GBM cells[38] (Figure 1.6, B). As a result, the P53 pathway is disrupted and can no longer control the cell cycle. Wang *et al.* described that transfection of P53 and P21 in GBM cells resulted in reduction of tumor cell growth and *in vitro* colony formation[51]. Moreover, a study comparing GBM cell lines differing in P53 and PTEN status showed that the cell lines mutated in both P53 and PTEN resulted in the highest invasion rates[52]. These studies demonstrate the capacity of tumor suppressors of regulating GBM growth.

1.3.1.3. RB pathway

In normal cells, RB can restrict cell proliferation by suppressing gene expression through inhibition of E2F, a transcription factor that can induce the cell to enter the S-phase. However, phosphorylation of RB by a complex of cyclin-dependent kinases (CDK) 4/6/2 and Cyclin D can inactivate RB, releasing E2F to be activated[53]. Therefore, the deregulation of this pathway leads to sustained of proliferative signaling (Figure 1.5).

RB acts as a tumor suppressor gene and is commonly mutated in GBM cells, inactivating its function[54] (Figure 1.6, C). In addition, a negative regulator of this pathway, cyclin-dependent kinase inhibitor 2A (CDKN2A), is also found to be mutated in GBM cells. CDK2A competes with cyclin for CDK binding, preventing RB phosphorylation[38]. A study showed an association between low CDKN2A expression and high-grade gliomas in patients' samples[55]. Furthermore, overexpression of CDKN2A was able to inhibit the colony-forming activity in GBM cells[55].

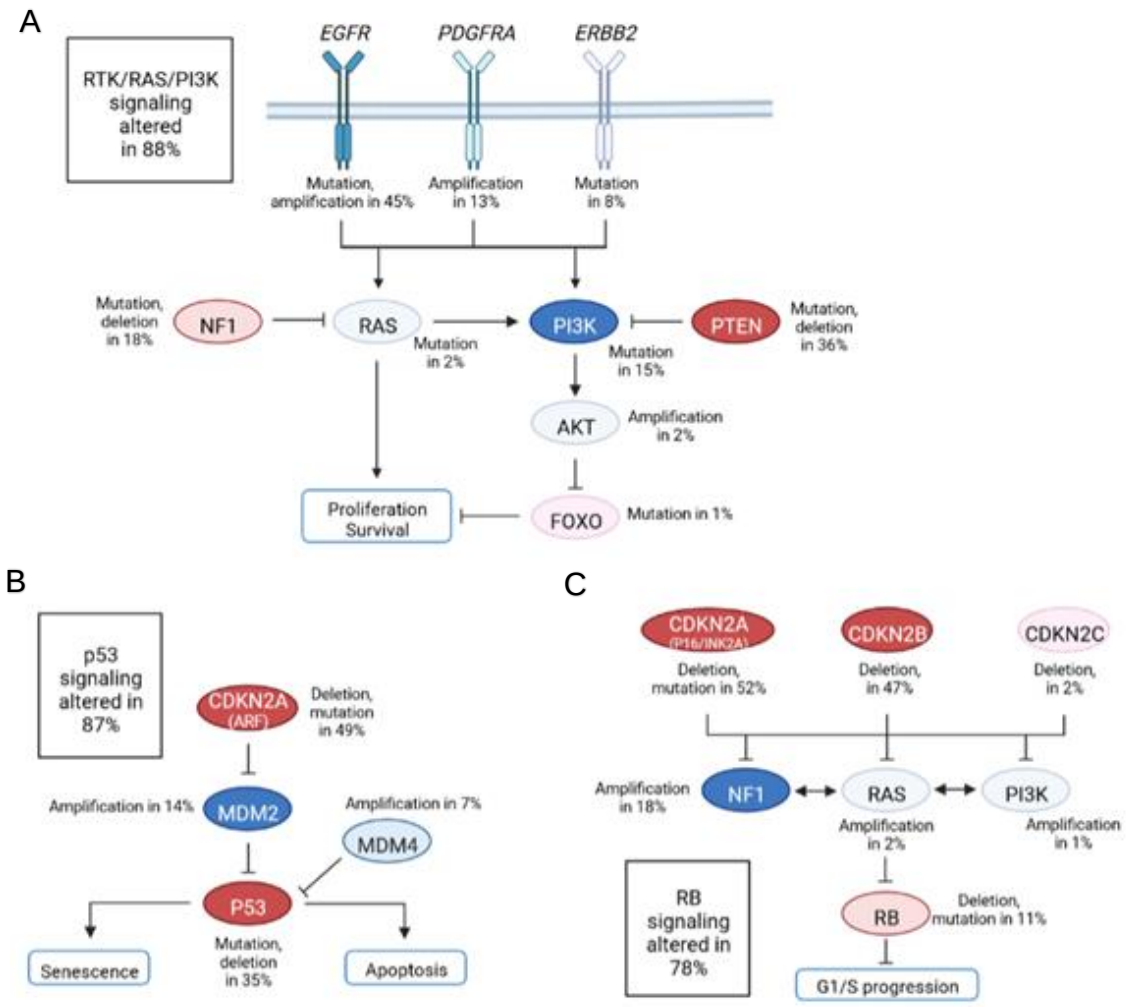

Figure 1.6 - Frequent genetic alterations in three critical signaling pathways of GBM.

(A) RTK/RAS/PI3K pathway; **(B)** p53 pathway; **(C)** RB pathway. The type of mutation and the frequency is indicated in each case. Blue indicates activating alterations, with darker shades corresponding to higher percentages. Red indicates inactivating alterations, with frequently altered genes showing deeper shades of red. Adapted from McLendon *et at.*, 2008. Figure created with BioRender.

1.3.2. GBM classification

Depending on the presence or not of a precursor lesion, this tumor can be classified into two subtypes. Primary GBM arises *de novo*, without previous lesions, and comprehends most of GMB (≈ 90%). Secondary GBM develops through the progression from a prior lower-grade glioma, such as a diffuse astrocytoma[56].

These two subtypes normally also differ in the status of isocitrate dehydrogenase (IDH) mutation. IDH is an enzyme that acts in the citric acid cycle and can be found in three isoforms: IDH1, IDH2, and IDH3. IDH1 is an enzyme that catalyzes the oxidative decarboxylation of isocitrate to α-ketoglutarate (α-KG) with the release of nicotinamide adenine dinucleotide phosphate (NADPH)[57]. NAPDH, in turn, is also a cofactor in the synthesis of glutathione (GSH), an abundant intracellular antioxidant. Thus, GSH is related to mechanisms of detoxification and protection of cells against reactive oxygen species (ROS)[58].

Mutations in IDH1 were found in most cases (78%) of secondary GBM patients[59]. Moreover, patients with mutated IDH1 showed better OS compared to patients with the wild-type (WT) form[60]. The most frequent IDH1 mutation in gliomas results in the loss of the enzyme's catalytic activity by substituting arginine, crucial for the recognition of isocitrate, into histidine in position 132 (R132H)[61]. Studies have shown that overexpression of mutated IDH1 R132H in GBM cells led to decreased GSH levels and increased intracellular ROS levels. As a result, the accumulation of ROS induced apoptosis and inhibition of cell proliferation[62]. These findings of the mutated IDH form as a protective factor contribute to a better understanding of the association between its occurrence and a favorable prognosis.

On the other hand, primary GBM typically presents the wild-type (WT) form of IDH, which is correlated with the worst outcome. In this way, IDH status has become a molecular marker for GBM and its aggressiveness[63]. However, Jiao *et al*. described a group of patients with mutated IDH in different grades of gliomas with a poor prognosis[64]. Therefore, it is essential to discover other biomarkers or molecular signatures that may provide a better prognostic.

GBMs with mutations in IDH1 are also associated with mutation in the a-thalassemia/mental-retardation-syndrome-X-linked (ATRX) gene[65]. ATRX encodes a protein involved in chromatin remodeling[66]. Mutations in this gene are related to the maintenance of telomere length by non-telomerase mechanisms and affect epigenetic regulatory functions[67]. ATRX appears mutated in about 57% of cases of secondary GBM[68].

Furthermore, a study revealed that 74% of GBM IDH1-WT patients had mutations in the Telomerase Reverse Transcriptase (TERT) gene[69]. The TERT gene encodes the enzyme telomerase. As previously mentioned, this enzyme is responsible for preventing telomere shortening by adding sequences to the chromosomal ends[13]. Mutations in the TERT gene promoter increase telomerase activity that aids in telomere lengthening and are associated with poor prognosis in GBM patients[69],

The frequency of other mutations and the genomic profile also differentiate primary from secondary GBM. In this way, primary GBM frequently presents EGFR amplifications, CDKN2A and RB deletions, loss of chromosome 10, and PTEN mutations. On the other hand, the secondary GBM most found alterations are P53 mutation, hypermethylation of RB promoter, and PDGFR overexpression[70]. These alterations are summarized in Figure 1.7.

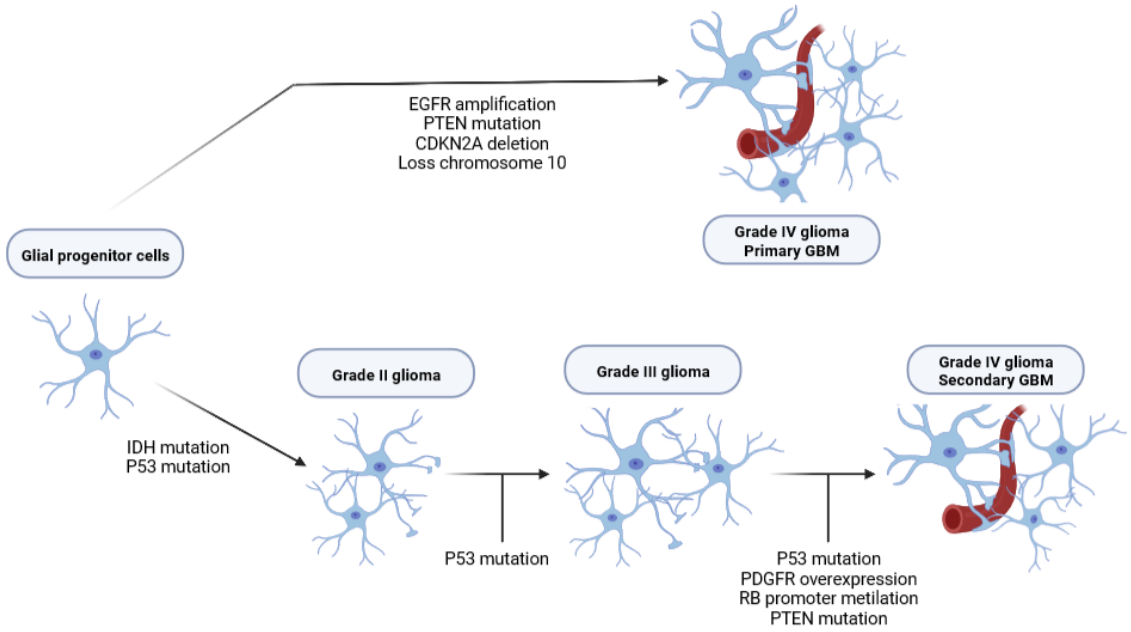

Figure 1.7 - Common molecular alterations in primary and secondary GBM.

Description of frequent genetic alterations that leads to primary and secondary GBM progression. Loss of chromosome 10 is frequent in both primary and secondary GBM, whereas P53 mutations are more frequent in the pathway leading to secondary GBM. Adapted from Ohgaki *et al.*, 2004. Created with BioRender.com.

Primary and secondary GBM also differ in the average age of patients at diagnosis. Usually, primary GBM is diagnosed in patients over 60 years old, whereas secondary GBM is more common in patients over 45 years old[71]. Although GBM is diagnosed at an average age of 64 years, this type of tumor can occur at any age, including childhood. However, pediatric GBM is considered a rare disease[72]. In terms of gender, primary GBMs develop more frequently in men and secondary GBMs in female patients[70].

In 2010, Vernaak *et al*. described a new molecular classification for GBM based on gene expression studies. Integrated genomic analysis has categorized primary and secondary GBM into four subtypes: Pro-neural, Neural, Classical, and Mesenchymal. These subtypes were characterized by patterns of specific genetic alterations[45]. The principal molecular alterations are described in Figure 1.8.

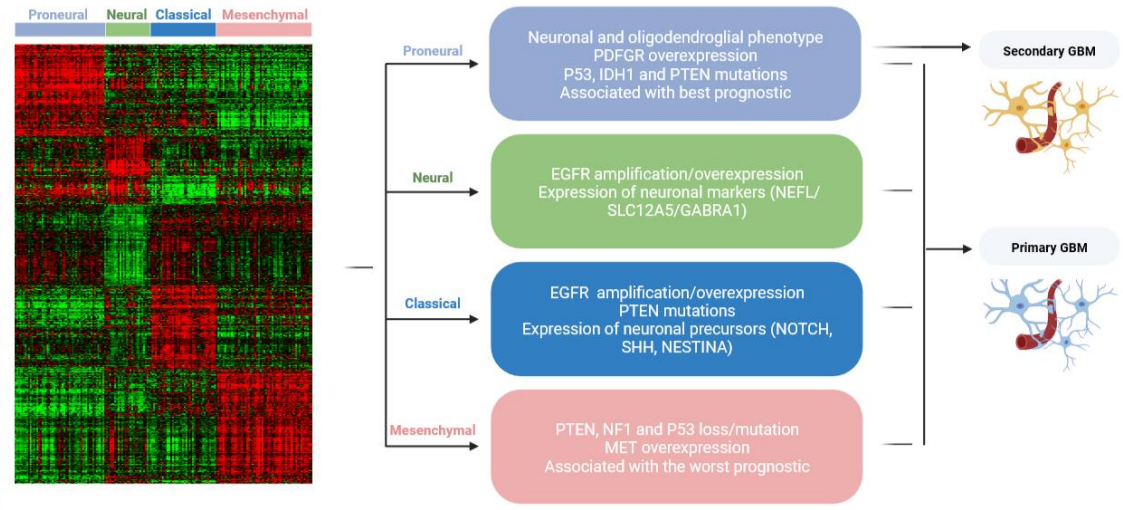

Figure 1.8 - Molecular characteristics of GBM subtypes.

Molecular characteristics of GBM subtypes. Gene expression levels of 840 genes from 173 TCGA GBM patients' samples. In red, genes that are overexpression and in green gene that has low expression. From this data analysis, a summary scheme of the main molecular alterations found in each subtype. Figure adapted from Verhaak *et al.*, 2010 and Agnihotri *et al.*, 2013. Created with BioRender.com.

NEFL: Neurofilament light; SLC12A5: Solute Carrier family 12 member 5; GABRA1: Gamma-aminobutyric acid type A receptor alpha1 subunit; SHH: Sonic Hedgehog; NF1: Neurofibromin 1.

Several studies based on the genetic alterations present in GBM progression resulted in the definition of molecular profiles that categorize this type of cancer. These classifications allowed us to better understand GBM biology and may contribute to reducing intratumoral heterogeneity. The advances in the characterization of GBM subtypes present prognostic and predictive potential. However, biopsy or surgical resection is necessary to perform the genomic analysis that determines a patient's tumor subtype. Due to the invasive nature of these approaches and the associated risks, in addition to the enormous genetic alterations to be tested, this method is not commonly used with GBM patients. Therefore, it is not yet possible to stratify GBM patients in a way that would allow offering personalized therapies according to their molecular alterations.

1.3.3. Risk factors for GBM development

So far, the research carried out to find associations between environmental and occupational exposures with the development of GBM is still inconclusive. Cigarette smoking, for example, is statistically proven to have a high carcinogenic effect on the lungs, esophagus, and oral cavity[73]. However, regarding the nervous system and the development of GBM, no significant association was found[74].

It is noteworthy that cigarette consumption is a source of exposure to components such as nitrosamines. In addition to cigarettes, nitrosamine can also be derived from eating processed meats. Studies have shown that the intake of these components may increase the risk of developing gliomas[75]. Nevertheless, other studies diverge from these results and demonstrate that processed meat does not increase adult glioma risk[76].

One risk factor that does seem to have an impact on the development of brain tumors is ionizing radiation[77,78]. Exposure to ionizing radiation can damage genetic material directly and cause the formation of free radicals. As a result, there is an increase in the occurrence of mutations in DNA[79].

Regarding the effects of electromagnetic radiation, such as waves emitted by microwave ovens and cell phones, the results are still controversial[80,81]. Due to the relatively short period of massive use of smartphones and inconclusive results, more research is still needed to verify whether there is an increased risk of GBM associated with the use of these devices.

1.3.4. GBM diagnosis

Clinical description of new GBM patients can vary depending on the size and location of the tumor and the anatomic brain structures involved. GBM most often develops in the supratentorial and rarely in the infratentorial area. The most frequent region for GBM development is in the frontal lobe (42%)[68,82] (Figure 1.9). However, the patients often present symptoms such as headaches, seizures, and neurological deficits due to increased intracranial pressure[83].

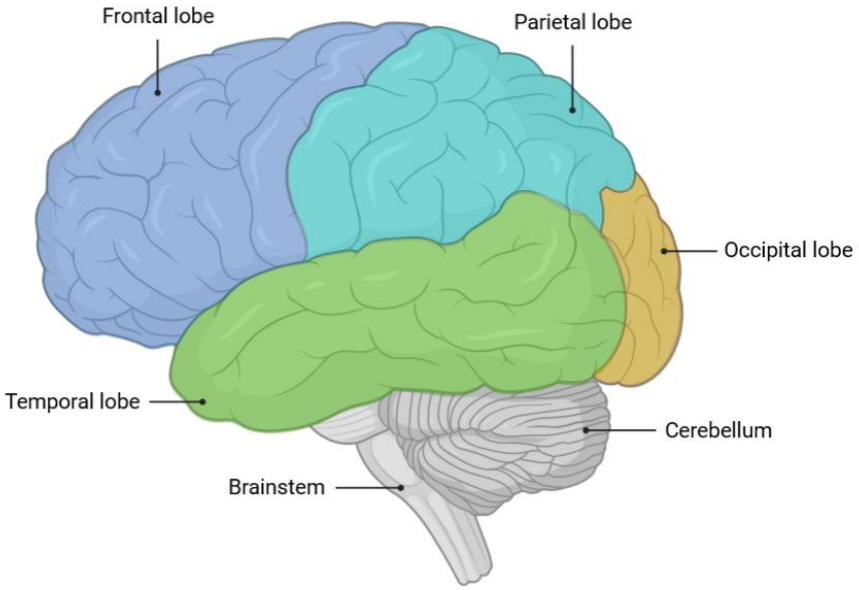

Figure 1.9 - Schema of human brain anatomy.

Divisions of the human brain. The supratentorial area is represented in color (comprehends frontal, parietal, occipital, and temporal lobes). The infratentorial area is represented in grey and is composed of the cerebellum and brainstem. The most frequent location of GBM development is in the frontal lobe (blue). Figure created with BioRender.com.

Upon presentation with neurological symptoms, initial diagnostic for GBM includes computed tomography (CT) or magnetic resonance imaging (MRI) scan. Morphological and anatomic aspects and parameters such as the presence of cellularity, necrosis, and edema surrounding the tumor are evaluated to differentiate GBM from low-grade tumors[84]. In addition, histopathological analysis from biopsy allows the confirmation of the GBM diagnostic.

1.3.5. GBM treatment

A multiple-modality approach is required for the treatment of newly diagnosed GBM. The first phase of the treatment requires surgical resection of the tumor. Studies showed that the surgery helps to relieve the intracranial pressure in the brain and also prolongs the OS rate[85]. However, an extensive resection is usually incomplete due to the infiltrating nature of the tumor. Therefore, primary tumor mass cannot be entirely removed by radical resection, and the application of complementary treatment to eliminate the remaining cells is required to avoid later disease progression or recurrence of the tumor[33].

The standard concurrent treatment after surgery includes the administration of radiation therapy (RT) and chemotherapy with temozolomide. Studies showed that the surgical resection associated with only RT results in median survival of 12.1 months[86]. However, adjuvant therapy of RT in association with TMZ after surgery extended the median survival to 14.6 months, resulting in a benefit of 2.5 months[86].

Normally, during the concomitant phase with radiotherapy, TMZ is administered daily for 42 days at a dosage of 75 mg/m^2. After a 1-month rest period, adjuvant treatment with TMZ is administered for 6 months. Initially, a dose of 150 mg/m^2 is given daily for five days followed by 23 days without treatment (totaling a cycle of 28 days). For the remaining 5 months, if supported by the patient, the dose is increased to 200 mg/m^2 [86].

TMZ is a small lipophilic molecule that can cross the BBB and function as a DNA alkylating agent. When absorbed, it undergoes hydrolysis at physiological

pH to form the active metabolite 5-(3-Methyl-1-triazine)imidazole-4-carboxamide (MTIC)[87]. As a result, MTIC can further methylate purine residues in the DNA. In turn, the methylation causes breaks in the DNA double-strand, which inhibits the cell cycle at the G2/M phase and eventually induces cell apoptosis[87].

The primary cytotoxic target of TMZ is O6-methylguanine. The effectiveness of TMZ action depends on the expression of the enzyme O6-methylguanine transferase (MGMT), a DNA repair protein that catalyzes the removal of methyl groups from the O6 position of guanine[88]. Removing the methyl group confers resistance for the tumor cells to alkylating agents. In this way, a high expression of MGMT produces resistance to the induction of apoptosis promoted by TMZ[89]. However, when MGMT is epigenetically silenced, the expression of the enzyme is reduced, which is related to an increased sensitivity of GBM cells to the TMZ[90]. Thus, the methylation of the MGMT promoter constitutes a predictive factor of the response to TMZ treatment in GBM[91].

Other factors may be predictive of glioma patient survival. Studies have shown that a complete and extensive resection surgery, when possible, has a better outcome for patients and a longer progression-free survival (PFS) rate[92]. In addition, the patient's age and the size of the tumor mass are also used as prognostic predictors. Less advanced age patients have better survival[93]. Regarding tumor size, those greater than 5 cm are normally associated with worse outcomes[93].

Despite the aggressive multimodal treatment that a GBM patient must undergo, GBM is still a deadly disease, with a median survival of only about 15 months[94] and less than 5% of patients surviving five years after diagnosis[34]. Furthermore, about 90% of patients experience a recurrence in less than a year[95]. In the past years, new strategies for treating GBM patients are emerging.

One of the most promising approaches is based on the use of electrical fields with alternating polarity, called Tumor Treating Fields (TTF). TTF was approved by the U.S. Food and Drug Administration (FDA) in 2011 for the treatment of recurrent GBM and in 2015 as treatment in association with TMZ after surgery for newly diagnosed supratentorial GBM. This technology delivers low-intensity, intermediate-frequency alternating electrical fields to tumor cells

and interrupts cell division resulting in apoptosis[96]. The approval use of TTF for specific cases was given after a study with 315 GBM patients showed an increased PFS of 7.1 months after TFF plus TMZ treatment against four months of PFS in the group treated only with TMZ[97].

Other treatments have also been studied upon the recurrence of GBM, besides the TFF approval. For example, in 2009, Bevacizumab (BV) was approved for recurrent disease. BV is a monoclonal antibody that targets vascular endothelial growth factor (VEGF), a protein important for angiogenesis. Although trials showed increased PFS, the OS had no significant effects[98], and the occurrence of life-threatening side effects such as blood clots and intracranial hemorrhage were reported[99].

Clinical trials with agents that affect frequently signaling pathways altered in GBM are also being studied including EGFR inhibitors such as erlotinib, gefitinib, and dacomitinib[100–102]. As mentioned earlier, EGFR is a receptor tyrosine kinase capable of regulating the RAS/MAPK and PI3K/AKT pathways. Although mutations in this receptor are commonly present in GBM progression, targeting it has been challenging. Phase I and II clinical trials with these inhibitors given as single-agent therapies did not significant improve OS and PFS in GBM patients[100,101]. More studies are still needed involving drug delivery to cross the BBB and pre-clinical settings as well[103]. Improving this knowledge will help to target these critical pathways.

The field of immunotherapy has shown progress in the treatment of GBM, especially with the use of tumor vaccines. A phase III clinical trial demonstrated favorable results for GBM patients treated with dendritic cell vaccines[104]. This dendritic cell vaccine is loaded with autologous tumor cell lysate and stimulates the immune response of the patient, being fully personalized. Trial results showed significant improvements in OS in both newly diagnosed and recurrent GBM patients[104].

1.3.6. GBM therapy resistance

As already described, the difficulty of a complete tumor resection may cause tumor cell populations to remain around the cavity. The presence of tumor cells with stem-like properties in these populations may contribute to therapy resistance and tumor recurrence. Advances in GBM genomic studies allowed us to reveal the complexity of the cells within the tumor[38]. Some studies have shown that extracellular vesicles (EVs) released from tumor cells can carry prooncogenic signals to neighboring cells contributing to maintaining intratumoral heterogeneity[105]. Therefore, this heterogeneous nature of GMB makes it extremely challenging to achieve an effective therapeutic target and leads to the development of resistance in nontarget clones.

Several groups demonstrated that brain tumors contain self-renewing tumorigenic cells, called cancer stem cells (CSCs)[36,106]. Moreover, these CSC were described as resistant to the standard GBM chemotherapy[107], relating their role in the disease progression and recurrence. CSC cells isolated from GBM, also called glioma stem cells (GSCs), are tumor cells capable of forming heterogeneous glial tumors[108]. These cells can undergo successive symmetric and asymmetric divisions, self-renew their population, and generate more differentiated progenitors that constitute the majority tumor population[109]. Therefore, CSCs play a critical role in tumor initiation, progression, therapy resistance, and ultimately disease recurrence.

The presence of CSCs in the tumor microenvironment is related to EMT, a process that makes the cancer cells more able to migrate and invade[110]. In addition, CSCs play a crucial role in the progression of GBM by suppressing the immune system, preventing the immune cells from access to nutrients such as glucose and oxygen, and promoting angiogenesis[111]. As a result, the CSCs are more drug-resistant and have increased potential for metastasis[112].

Different propositions rely on the capabilities of CSCs to treatment resistance. CSCs are normally found in the G0 phase, a quiescent state. As alkylating agents like TMZ target proliferating cells, CSCs become less susceptible to this kind of drug[113]. Moreover, the high expression of ATP-binding

cassettes (ABC) helps to expel chemotherapeutic agents from the cell interior. Efflux transporters like ABC act as a mechanism for protecting stem cells and play a role in tumor cells' multidrug resistance[114]. High levels of MGMT were also found to be expressed in CSCs, collaborating with the TMZ resistance as already described[115].

In general, the ability of CSCs to migrate and evade therapeutic intervention leads to the persistence of these cells within the tumor and thus contributes to the recurrence after treatment. Consequently, CSCs have emerged as a promising target for the development of new treatment strategies[116].

A recently published study described a network of rhythmic activity in glioblastomas[117]. Hausmann *et al.* showed the presence of a small plastic population of glioblastoma cells that present rhythmic oscillation of Ca2+ that connects them. These periodic oscillations would be able to activate signaling pathways such as the MAPK and the NF-kB cascade. Furthermore, the pharmacological interference of this rhythmic activity impairs global communication, being able to result in reduced cell viability, decrease tumor growth in mice, and extended animal survival[117].

In summary, the standard conventional therapy for GBM patients includes resection surgery followed by radiotherapy and chemotherapy with TMZ. Although many patients' tumors initially respond to this approach, there is currently no efficient therapy for GBM recurrence (that happens in most cases), making GBM a lethal disease. In addition, the heterogeneity of GBM is a crucial burden for the failure of current therapy. Therefore, it is necessary to identify molecular markers that aid in targeting cancer cells that evade primary therapy and develop new combinatorial personalized treatments that may improve GBM patients' survival.

1.4. Tribbles protein family members

An important regulation of signaling networks occurs through protein phosphorylation. Protein kinases, in association with the Ubiquitin system, are responsible for post-translation modifications on proteins that result in their activation or degradation. As a result, they modulate signaling pathways that control most biological processes in eukaryotic cells, such as cell differentiation, growth, and death[118,119].

Typically, protein kinases possess a conserved kinase domain fold that catalyzes the transference of phosphate from adenosine triphosphate (ATP) to target proteins in specific residues (serine, threonine, or tyrosine)[120]. However, about 10% of kinases lack one or more canonical domains required for phosphorylation, being called pseudokinases[121]. Despite losing their catalytic activity and therefore not being able to phosphorylate other proteins, pseudokinases can still modulate cellular processes through protein-protein interactions, acting as allosteric regulators or scaffolding proteins[122,123]. However, several cases described an affinity for ATP binding even with the loss of the catalytic domain[124]. In this way, instead of directly phosphorylating target proteins, pseudokinases act as adaptors to regulate and integrate signaling pathways important for cellular processes and are often found dysregulated in various diseases, including cancer[125,126].

Members of the Tribbles protein family are serine/threonine pseudokinases composed of three isoforms, TRIB1, TRIB2, and TRIB3. They are named after the homologs of the *Drosophila* pseudokinase Tribbles (Trbl) and indeed share highly conserved domains[127]. Trbl was first shown as a regulator in coordinating mitosis and morphogenesis during *Drosophila* development, inducing the degradation of CDC25 homolog String by promoting proteasome-mediated degradation[128].

In mammals, this family of pseudokinases is ubiquitously expressed in the body, although with different expression patterns, as each isoform expression is highly regulated and context-dependent[129]. Furthermore, the expression of each isoform varies according to the developmental phase[130]. Regarding their cellular

location, studies have shown that the Tribbles family can act both in the cytoplasm and in the nucleus. However, TRIB1 and TRIB3 are frequently detected in the nucleus, whereas TRIB2 is found mainly in the cytoplasm[131]. A recent study from the host lab showed that TRIB2-GFP is expressed in both the nucleus and the cytoplasm and inhibition of the CRM1-mediated nuclear export by leptomycin B did not affect its subcellular localization. These data suggest that TRIB2 is not a substrate of the CRM1 export receptor[132].

1.4.1. Tribbles members' protein structure

In mammalian cells, Tribbles family members are three-domain proteins characterized by an N-terminal PEST region, an atypical pseudokinase core (without the catalytic domain), and a C-terminal tail that binds E3 ligases[127] (Figure 1.10).

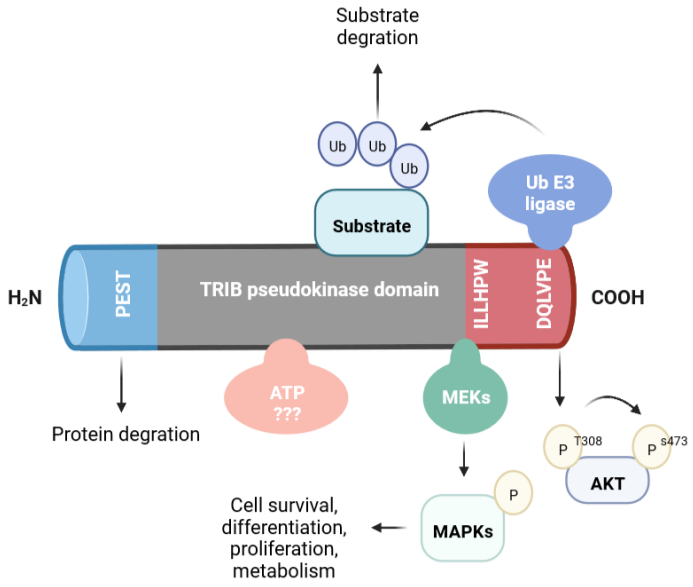

Figure 1.10 - Schema of Tribbles' structure.

Tribbles are three-domain proteins. The N-terminal PEST region mediates degradation to control protein turnover. The pseudokinase domain serves as a scaffolding region for substrate proteins. The C-terminal contains binding motifs involved in interactions with MEKs and ubiquitin E3 ligases. C-terminal is also involved with AKT interaction, which promotes phosphorylation of serine 473. Adapted from Eyers *et al.*, 2017 and Mayoral-Varo *et al.*, 2021. Figure created with BioRender.com.

The N-terminal PEST domain characterizes each TRIB variant by distinct motifs. This fragment is very high in serine and proline content. The abundance of these amino acids is involved with the stability, regulation, and cellular localization of the proteins[133,134]. Some studies have associated the proline-rich region with other functions, such as an anchoring site for SH3 or WW domains of other proteins[135].

A protein kinase usually has the canonical catalytic domain. This domain is, in general, composed of the N-lobe and the C-lobe (Figure 1.11). The N lobe is formed by five β chains (where motifs responsible for ATP union are located) and one α helix (important for the transition from the active state to the inactive state of the kinase). Regarding the C lobe, it is composed of six α helices, where the activation loop and the catalytic loop are located. In this activation loop, also called loop A, is the DFG motif, responsible for chelating Mg^{2+} that regulates ATP binding[136].

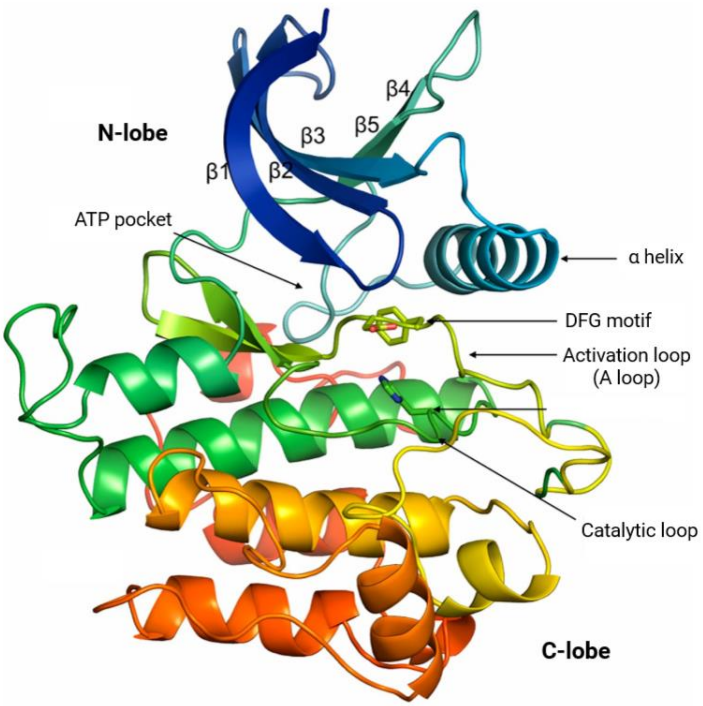

Figure 1.11 - Canonical structure of a kinase domain.

The figure illustrates the structure of a typical protein kinase domain. It is possible to observe the different elements that make up the N and C lobes and the ATP binding site of the kinase domain. Adapted from Modi and Dunbrack, 2019.

Members of the Tribbles family of proteins are known to have an atypical pseudokinase domain. This domain differs from a conventional kinase domain in the absence of the DFG motif (Asp-Phe-Gly), which chelates the Mg^{2+} ion regulating ATP binding necessary for the catalytic activity[137]. Due to these alterations, TRIB2 and TRIB3 show low affinity to ATP, whereas TRIB1 has no affinity[127].

The TRIB C-terminal tail contains two unique sequences: the HPW (F/L) and DQXVP (D/E). These sequences are related to protein-protein interactions. It was described that the HPW (F/L) sequence is involved in the binding of MEK1 as well as other MAPKK to Tribbles[138,139]. On the other hand, the DQXVP (D/E) promotes the interaction with ubiquitin E3 ligases, including COP1[140]. This domain is characteristic of Tribbles family members and has not been described in other protein kinases[127].

1.4.2. Mechanism of action of Tribbles proteins and implication in cancer

The characteristic lack of enzyme activity of the Tribbles pseudokinases prevents the phosphorylation capacity of these proteins. However, members of the Tribbles family retain the ability to interact with signaling proteins. Therefore, they can modulate different signaling pathways, such as those involved in cell proliferation[141], cell differentiation[142], metabolism[143,144], inflammation[145], immunity[146], stress response[147], and drug resistance[148].

Tribbles protein members can act in different ways. They can function as protein scaffolds, can lead to protein degradation by binding to ubiquitin ligases and further ubiquitylation of substrates[149], can stabilize proteins by suppressing sumoylation[150], and can bind to signaling molecules, such as MEK and AKT, affecting signal pathways[138]. Tribbles proteins could have redundant and non-overlapping functions[130]. However, the functional role of each isoform, as their expression pattern, depends on the tissue and the cell type in which they are expressed. For example, studies described that TRIB2 could promote the phosphorylation of AKT and activate the pathway, inducing drug resistance[151].

Nevertheless, other groups demonstrated that TRIB3 has the opposite effect on the AKT axis. By inhibiting AKT phosphorylation in neuronal cells, TRIB3 can induce cell death in Parkinson's disease[152].

Even in the same context, each member of Tribbles has differences in functional role and expression levels, as described in acute myeloid leukemia (AML). Analysis of expression levels in hematopoietic cells showed that TRIB1 is highly expressed in granulocyte/monocyte and B-cell lineages. However, TRIB2 was significantly increased in T-cells. Regarding TRIB3, high expression levels were found in the erythrocyte lineage[153]. Studies indicate that TRIB1 and TRIB2, but not TRIB3, can promote tumor progression of AML through regulation of the ERK pathway and degradation of CEBPα, a transcription factor involved in the differentiation of myeloid cells[154–156]. Therefore, TRIB1 and TRIB2 appear to have an oncogenic role in AML.

The upregulation of TRIB3 was associated with the worst outcome for non-small cell lung cancer (NSCLC) patients by regulation of Notch signaling[157]. Furthermore, in colorectal cancer patients, high expression of TRIB3 was related to susceptibly recurrence and poor overall survival[158].

An oncogenic role was also associated with TRIB2 as a promoter of tumor progression in liver cancer cells. It was shown that TRIB2 could reduce the expression of TCF4 and β-catenin through associated-ubiquitin E3-ligases, resulting in negative regulation of the Wnt signaling[140]. Moreover, high levels of TRIB2 favored the survival and proliferation of melanoma cells by activating AKT and, consequently, inhibiting FOXO[159]. Studies showed that the E3 ubiquitin ligase COP1 domain of TRIB2 promotes phosphorylation of AKT at serine 473 and activates the pathway. As a direct target, FOXO3 is phosphorylated by AKT, being repressed[151].

On the other hand, TRIB3 was found to be acting as an inhibitor of AKT[160]. Studies demonstrated that TRIB3 loss facilitated hyperphosphorylation of AKT at serine 473 by mTORC2. Consequently, it led to FOXO3 repression and contributed to enhanced tumorigenic features on TRIB3-deficient cells[161]. Thus, it demonstrates that TRIB3 could have a tumor-suppressing role. Therefore,

depending on the cell context and the family member, Tribbles proteins might exhibit an oncogenic or tumor suppressive behavior in tumor progression.

Tribbles' members could be used as valuable molecular biomarkers for prognosis and prediction of response to therapeutic in different kinds of tumors. For example, high expression of TRIB2 is correlated with antiapoptotic BCL-2, which confers sensitivity to therapy in blood cancer[162]. Therefore, TRIB2 could be used as a predictive biomarker for treatment response in these patients.

Overexpression of TRIB3 was correlated with the promotion of tumorigenic properties, such as cell proliferation and migration, in renal cell carcinoma[163]. In gastric cancer, TRIB3 overexpression is also positively correlated with VEGF-A expression and angiogenesis, resulting in a higher incidence of tumor recurrence[164].

Studies suggest that high expression of TRIB2 could confer a resistance mechanism for tumor cells. The induced phosphorylation of AKT by TRIB2 results in activation of the pathway and thus FOXO inhibition. Therefore, the expression of FOXO targets, which include genes involved in apoptosis, is also reduced. These findings suggest that drugs that induce apoptosis can be attenuated by TRIB2[151]. In this way, TRIB2 could serve as a predictive biomarker in cancer.

1.4.3. TRIB3

Tribbles homolog 3 (TRIB3, also known as NIPK or SIKP3) pseudokinase is the most studied member of the Tribbles family. Studies from the past years have shown that TRIB3 has multiple effects on critical metabolic processes, including glucose and lipid metabolism, inflammation, oxidative stress, apoptosis, and proliferation[165,166]. Indeed, TRIB3 deregulation has been linked to pathological conditions, such as metabolic disorders and cancer[167]. Studies suggest that TRIB3 has different metabolic functions and interacts with several transcriptional mediators. For example, it has been shown that TRIB3 is a negative regulator of AKT[168]. Indeed, Salazar *et al*. proposed that TRIB3 interacts with AKT and inhibits its phosphorylation on serine 472 by mTORC2 (Figure 1.12,

A). Moreover, inhibition of TRIB3 facilitates the AKT hyperphosphorylation by mTORC2, thus subsequent inactivation of FOXO3[161] (Figure 1.12, B). In this way, TRIB3 acts as an inhibitor of the PI3K/AKT/mTOR pathway. Moreover, TRIB3 has been described to interact with other pathways, such as TGF-β, MAPK, and JAG1/NOTCH[169,170].

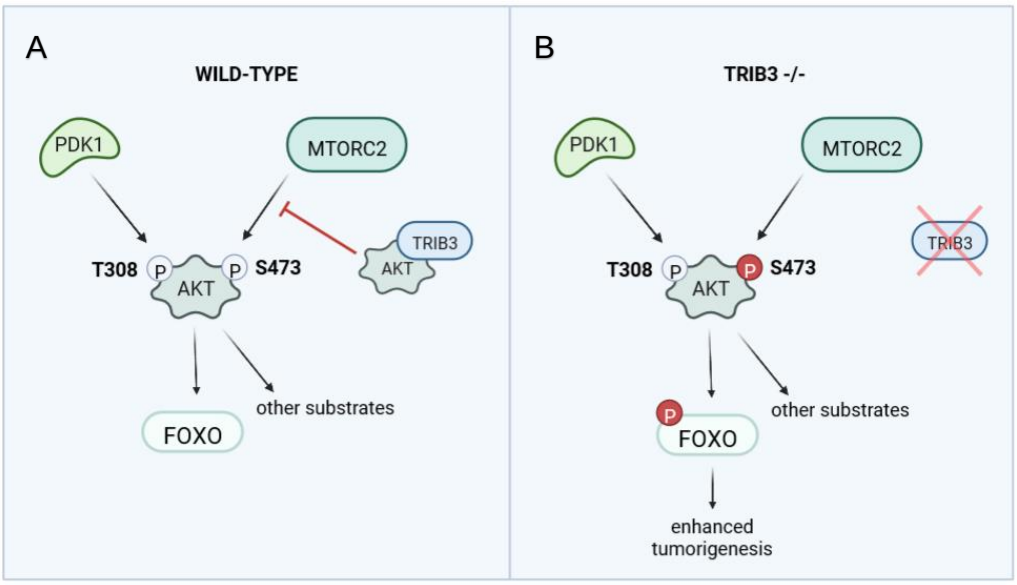

Figure 1.12 - Representation of the proposed interaction of TRIB3 with the AKT pathway.

Proposed role of TRIB3 acting as tumor suppressor in the AKT pathway. **(A)** In a wild type cells, TRIB3 interacts with AKT and disturbs its phosphorylation by mTORC2. **(B)** After inhibiting TRIB3, AKT is hyper-phosphorylated by mTORC2. Sequentially, AKT inactivates FOXO by phosphorylating it. Inactivation of FOXO contributes to enhanced tumorigenic features of TRIB3-deficient cells. Adapted from Salazar *et al*., 2014. Figure created with BioRender.com.

Since TRIB3 can act in several cellular pathways and is involved in different cell processes depending on the context, it is essential to study how TRIB3 is regulated to understand how its modulation generates different responses. The mRNA that codes to TRIB3 is formed by four exons located on chromosome 20 (20p13-p12.2), and the translated protein is composed of 358 amino acids with approximately 45 kDa. TRIB3 expression can be regulated at the level of mRNA processing. The 5' UTR of the gene is an important site of regulation for gene expression levels[171], and different human TRIB3 mRNA

transcript variants have been reported due to alternative transcription initiation and alternative splicing of the first exon[172].

At a protein level, TRIB3 can be regulated by post-translational modifications. These modifications could affect the protein stability or modulate TRIB3 interactions with other proteins. Studies demonstrated that TRIB3 protein could be regulated by acetylation[173], methylation[174], and phosphorylation[175]. However, the most known post-translational modification that TRIB3 protein can suffer is ubiquitination. TRIB3 ubiquitination results in proteasome-mediated degradation of TRIB3 and was reported to occur by interaction with different E3-ubiquitin ligases[176,177].

TRIB3 has been described to be expressed in a range of cells and tissues. For example, in mammal cells, TRIB3 is highly expressed in the spleen, heart, lung, kidney, prostate, skin, white adipose tissue, liver, small intestine, stomach, skeleton muscle, hematopoietic tissues, thymus, and neurons[129]. By interacting with different molecules, TRIB3 can modulate distinct pathways and affect several cellular functions.

1.4.3.1. TRIB3 functions and role in cancer

It is estimated that TRIB3 is a regulator of cellular responses to stresses. For example, in prostate carcinoma cells, the lack of glucose or amino acids results in increased TRIB3 protein levels, acting as a nutrient sensor[178]. Moreover, in a hypoxic environment, a hallmark of solid tumors, TRIB3 is overexpressed in multiple human tumors such as colorectal and prostate cancer[179]. Furthermore, it is known that TRIB3 is induced by endoplasmic reticulum (ER) stress through ATF4 and CHOP. Indeed, overexpression of both ATF4 and CHOP activated TRIB3 promotor activity in HEK293 cells[180]. In fact, Ord *et al.* described that TRIB3 could act in a negative feedback loop, reducing the levels of ATF4 and CHOP[172].

Some other studies also relate the role of TRIB3 to the regulation of cell survival processes. Depending on the cellular context involved, TRIB3 has been

described as a promoter of apoptosis in chondrocytes[181], pancreatic beta cells[182], neuronal cells[183,184], and endometrial cancer cells via inhibition of AKT[185] and also in human monocyte-derived macrophages[186]. On the other hand, studies showed that TRIB3 enhances cell viability in glucose-deficient conditions in HEK293 cells[187]. Moreover, TRIB3 also acts as an anti-apoptotic factor in erythroid progenitor cells starved of erythropoietin[188] and contributes to the survival of primary cultured mast cells[189]. In this sense, it is also estimated that TRIB3 plays a role in modulating the immune response.

TRIB3 is also involved in cell cycle regulation. Sakai *et al*. demonstrated that the levels of Cdc25A protein, an activator of cyclin-dependent kinases (CDKs), are suppressed by the over-expression of TRIB3, whereas TRIB3 knockdown enhances endogenous Cdc25A levels[190]. In fact, the decrease of Cdc25 expression by TRIB3 leads to G2 cell cycle arrest[128,191]. Furthermore, TRIB3 can regulate the cell cycle at other levels, such as inhibiting Cyclin B1 transcription, which also causes cell cycle arrest[192].

TRIB3 is associated with underlying molecular mechanisms of a wide variety of cancers and seems to have dual roles, such as acting as an oncogene or as a tumor suppressor gene in carcinogenesis[193].

Acting as an oncogene, TRIB3 is associated with a poor prognosis in different cancers such as colorectal cancer[194], non-small cell lung cancer[157], renal cell carcinoma[163], and oral squamous cell carcinoma (OSCC)[195]. In this context, a few mechanisms have been described. Overexpression of TRIB3 supported cell proliferation *in vitro* by promoting AKT and mTOR phosphorylation and thus activating the AKT signaling pathway in OSCC. Conversely, TRIB3 knockdown decreased AKT and mTOR phosphorylation[195]. This mechanism was also described by Bao *et al.* in retinoblastoma cells, where overexpression of TRIB3 promoted cell proliferation and invasion by AKT and mTOR phosphorylation[196]. In lung cancer cells, it was found that TRIB3 could interact with EGFR and affect its stability, thus promoting NSCLC progression[197]. Other studies in lung cancer also showed that TRIB3 could interact and activate β-catenin recruitment, resulting in lung cancer progression[198]. JAG1/Notch is another pathway described as being regulated by TRIB3. In fact, Notch 1 was downregulated by TRIB3 knockdown in adenocarcinoma cell lines, inhibiting the cell's malignant

behavior[157]. Finally, TRIB3 was described to interact with and stabilize SMAD3. Knockdown of TRIB3 inhibited migration and invasion *in vitro* in hepatocellular carcinoma cells[199].

Wennemers *et al*. described that TRIB3 mRNA levels are not correlated with TRIB3 protein levels in breast cancer[134]. Curiously, it was found that high levels of TRIB3 mRNA were associated with a poor prognosis, while high levels of TRIB3 protein were associated with a good prognosis for breast cancer patients[200]. However, TRIB3 mRNA and protein levels were found to be correlated in tumor samples from colorectal cancer patients[158].

Nevertheless, TRIB3 has also been described as a suppressor of proliferation and invasion in other tumor contexts, such as endometrial cancer[185]. Therefore, TRIB3 could act as a tumor suppressor. In fact, overexpression of TRIB3 promoted apoptosis and suppressed the proliferation of endometrial cancer cells, in addition to decreasing the levels of matrix metalloproteinase (MMP) 2 and 9[185].

1.4.4. TRIB2

A taxonomic analysis described Tribbles homolog 2 (TRIB2) as the most ancestral member of the Tribbles protein family[127]. TRIB2 can regulate a wide range of signaling pathways and is associated with various cellular processes, such as apoptosis, cell proliferation and differentiation, inflammation, and drug resistance[146,201,202]. Therefore, TRIB2 presents diverse roles in healthy and pathological processes, such as metabolic diseases, neurological disorders, and cancer[203].

Although the structure of TRIB2 is similar to other members of the Tribbles family, there are some peculiarities. For example, the N-terminal domain of TRIB2 is more evolutionarily conserved across different species than the other isoforms[131]. As previously mentioned, the N-terminal domain is rich in serine and proline, and that the abundance of these amino acids is related to the stability and regulation of Tribbles. Studies have shown that the phosphorylation of serine-

83 present in this domain by p70S6 kinase is essential for the ubiquitination of TRIB2 mediated by Smurf-1[133]. Phosphorylation and ubiquitination in this region, called TRIB2 degradation domain (TDD), was linked to the stability of the TRIB2 protein in human liver cells[133].

The catalytic pseudokinase domain also shows a difference. The α-helix present in the N-lobe of TRIB2 contains three unusual cysteine residues that are not found in TRIB1 or TRIB3[204].

As with the other isoforms, TRIB2 expression is dependent on context and cell type. However, it has already been reported that TRIB2 is expressed in the heart, lungs, thymus, brain, skin, kidneys, spleen, and T and B lymphocytes[129].

TRIB2 expression can be regulated in different manners. The activation or repression of TRIB2 can occur by transcriptional factors and through microRNAs (miRNAs)[205,206], for example. The expression of TRIB2 was described to be regulated cyclically during the cell cycle. However, the underlying mechanism still needs to be established[207].

1.4.3.1. TRIB2 functions and role in cancer

TRIB2 can regulate different downstream pathways that control processes like stem cell pluripotency, cell survival, and cell cycle. To do so, TRIB2 can interact with a wide range of proteins, such as OCT4, CDC25, MAPK, AP4, and AKT[208].

The pseudokinase TRIB2 has been described as a regulator of stem cell fate decisions. In embryonic stem cells, TRIB2 can interact with OCT4, a transcription factor related to induced pluripotent stem cells. TRIB2 increases OCT4 activity, being an important factor in the maintenance of self-renewal ability in embryonic stem cells and for pluripotency induction[209]. In terms of stem cell differentiation, studies have shown that gene silencing of TRIB2 in mesenchymal stem cells was able to increase adipocyte differentiation *in vitro*[210]. Another study demonstrated that the suppression of adipocyte differentiation by TRIB2 was related to the inhibition of AKT and degradation of transcription factor C/EBP[211].

Down-regulation of C/EBP by TRIB2 is also related to the hematopoiesis process. During this process, TRIB2 is overexpressed in B cells, natural killers, and CD4+ T cells[212].

During reproduction, TRIB2 also appears to have a regulatory role. Studies have shown that, in granulosa cells, TRIB2 is involved in the regulation of gene expression and signaling pathways relevant to ovarian follicular development[213]. TRIB2 expression levels vary during oocyte maturation. While TRIB2 levels tend to decrease, TRIB1 and 3 levels tend to increase during the process. This variation may indicate that TRIB2 is more involved in cell proliferation than in oocyte maturation[214].

Oscillations on TRIB2 levels were also described during the cell cycle process. In this context, TRIB2 can interact with CDC25, promoting its ubiquitination and consequent degradation. The resulting decrease in CDC25 levels led to the arrest of the cell cycle in HeLa cells[207].

MAP kinases, such as p38, were described to be activated by TRIB2. p38 can control cell cycle regulators that are hyperactivated in myeloid leukemia. By activating this p38 pathway, TRIB2 demonstrated a tumor suppressor role in myeloid leukemia[215] (as summarized in Table 1.1). On the other hand, other groups demonstrated that TRIB2 can induce the progression of acute myeloid leukemia via the degradation of C/EBP. Thus, TRIB2 would also play an oncogene role in myeloid leukemia[216]. The apparent contradictory role of TRIB2 in leukemia progression could be explained by TRIB2 expression levels and their correlation with different subtypes of leukemia. For example, leukemia patients with deletions on chromosomes 5 or 7 show overexpression of TRIB2, whereas TRIB2 expression is decreased in patients with translocations on chromosomes 9 or 11[212].

Table 1.1 - Summary of TRIB2 role in different human cancers.

Cancer type	TRIB2 function	Target	References
Leukemia	Tumor suppressor	p38	(215)
	Oncogenic	C/EBP	(216)
Colorectal	Oncogenic	AP4/p21	(217)
Liver	Oncogenic	C/EBP, YAP	(219)
Melanoma	Oncogenic	FOXO	(159)

Elevated expression of TRIB2 was found in colorectal cancer tissues. Interaction of TRIB2 with AP4 induced the downregulation of p21 levels, resulting in decreased senescence and apoptosis of colorectal cancer cells. These findings associate TRIB2 with oncogene functions[217]. TRIB2 has also been described as upregulated in hepatocellular carcinoma[218]. Studies have pointed to TRIB2 as a direct target of the Wnt pathway. In turn, the activation of TRIB2 relieves the liver tumor suppressor protein C/EBPα-mediated inhibition of YAP transcriptional activation in liver cancer cells[219].

TRIB2 is also strongly related to melanoma progression. Studies have shown that TRIB2 expression is correlated with disease stage and clinical prognosis, and may be a valuable biomarker for the treatment response[220]. Indeed, it has been shown that TRIB2 is a FOXO repressor and contributes to the carcinogenic phenotype in melanoma. Furthermore, in melanoma xenograft models, the inhibition of TRIB2 was able to reduce tumor growth[159].

The inhibition of FOXO by TRIB2 is also related to mechanisms of resistance to therapies. Indeed, the interaction between TRIB2 and AKT can induce AKT phosphorylation on serine 473, resulting in FOXO inhibition[151]. It results in increased MDM2 activity, which degrades p53, a transcription factor of apoptotic genes. Thus, drugs that induce apoptosis by these genes can be attenuated by TRIB2, conferring a resistance mechanism to tumor cells with high expression of TRIB2 (Figure 1.13)[151]. In addition, studies from our laboratory have described two natural compounds capable of promoting FOXO nuclear

translocation, as well as the transcription of FOXO target genes. Thus, the use of this type of compound may be effective in reversing drug resistance mediated by TRIB2[221].

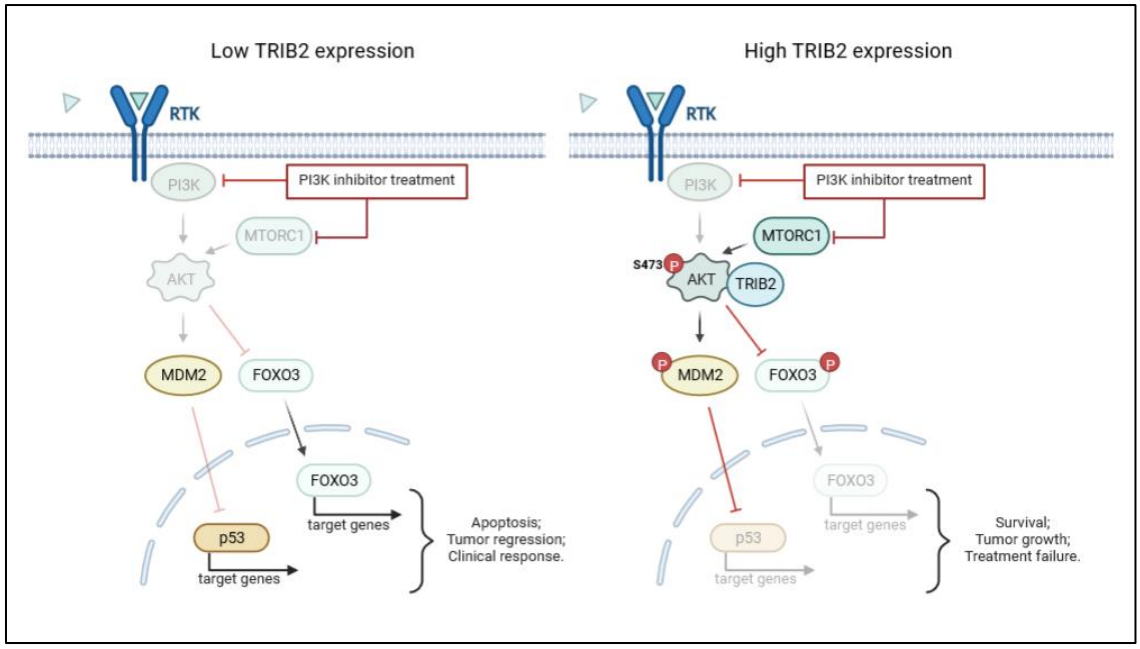

Figure 1.13 - Proposed model of TRIB2-mediated drug resistance.

Schematic representation of the resistance mechanism mediated by TRIB2. On the left side, when TRIB2 levels are low, the treatment can inhibit AKT activation. Consequently, MDM2 does not inhibit the transcription of p53-target genes. In addition, FOXO3 can translocate into the nucleus and promote the transcription of FOXO-target genes. On the right side, when TRIB2 is expressed in high levels, it induces AKT activation. As a result, MDM2 is phosphorylated and inhibits the transcription of p53-target genes. Moreover, FOXO3 is also phosphorylated and remains on the cytoplasm, not being able to promote the transcription of its target genes. Adapted from Hill *et al*., 2017. Figure created with BioRender.com.

1.4.5. Tribbles and glioblastoma

Regarding the role and regulation of Tribbles protein members in GBM, the existing literature is still limited. A few studies have been published in the last decade. In 2020 Tang *et al*. described that TRIB3 overexpression of TRIB3 increased cell proliferation migration and invasion of GBM cells. Accordingly, the silencing of TRIB3 resulted in decreased tumorigenic properties. Moreover, they suggested that this oncogenic phenotype caused by TRIB3 was due to a suppress of autophagic flux by TRIB3[222].

Two studies associated Tribbles with treatment resistance in GBM cells. In 2015 it was published that inhibition of TRIB1 could attenuate radioresistance in GBM cells. The study showed that irradiation could upregulate TRIB1 in GBM cell lines, and this increase of TRIB1 could interfere with irradiation-induced apoptosis by binding to the p53 promoter[223]. In 2019, another study suggested that high levels of TRIB2, in combination with MAPK, could indicate a poor prognosis and chemoresistance to TMZ in GBM cells[202].

Recently, a single-cell RNA-seq data analysis identified TRIB2 as a glioma neoplastic cell marker in GBM samples, indicating that TRIB2 could potentially become a drug target in GBM[224].

Together, these data suggest that Tribbles protein family members could be involved in both tumorigenesis and resistance to therapy in GBM cells. Thus, further studies about the role of Tribbles members in GBM should be relevant in the context of this lethal disease.

2. HYPOTHESIS AND OBJECTIVES

GBM is one of the most lethal and common forms of brain tumor, demonstrating a poor prognosis due to acquired resistance to treatment and frequent recurrence. Tribbles protein family members are known to be involved in a wide range of tumors, and their upregulation is correlated with poor prognosis in some types of cancers. However, little is known about the role of Tribbles in GBM.

Unpublished data obtained in the host laboratory show that transcript expression of Tribbles family members increases in glioma with the tumor grade, being highest in GBM. Moreover, higher levels of Tribbles mRNA are also associated with a worse prognosis. The host lab also observed that lower expression of FOXO3/4 mRNA also contributes to bad prognosis in glioma. High levels of TRIB1/2/3 and low levels of FOXO3/4 transcripts are predominantly found in GBM samples.

Based on these preliminary data and the known relevance of Tribbles in tumorigenesis, this project aims to delve into the study of the role of Tribbles in GBM. Our **main hypothesis** is that the members of the Tribbles protein family have an oncogenic role in GBM, supporting tumorigenic properties in GBM cells.

Therefore, the **main objective** of this project is to generate cellular-based tools that will be crucial to carry out a range of assays to validate our hypothesis. To achieve this objective, we proposed the following **specific objectives**:

1. Generate GBM knockout cell lines for Tribbles' members based on CRISPR/Cas9 system.
2. Characterize these generated cell lines phenotypically.

A diagram representing our approach to achieving our main objective is shown in Figure 2.1.

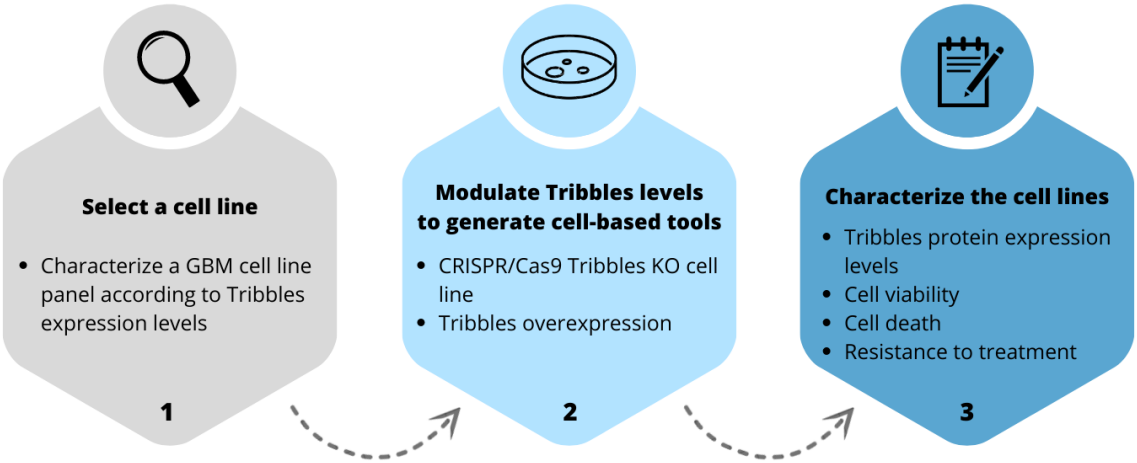

Figure 2.1 - Flowchart representing the steps of the project.

The main object of this project is to generate cell-based tools of GBM cell lines. Modulation of Tribbles expression levels in GBM cell lines will help us to understand if indeed Tribbles have an oncogenic role in GBM progression.

3. MATERIALS AND METHODS

3.1. Cell culture

This project's scope includes understanding the role of Tribbles protein family members in GBM biology. To achieve this, we have selected a panel of GBM cell lines that will be used hereafter. The cell lines used in this study are characterized according to Table 3.1.

All the cell lines were maintained under standard culture conditions at 37°C and 5% carbon dioxide (CO_2) and were cultivated with Dulbecco's Modified Eagle's Medium (DMEM) with High Glucose, 4 mM L-glutamine and sodium pyruvate (HyClone, USA), supplemented with 10% Fetal Bovine Serum (FBS) (Corning, USA) and 1% Penicillin – Streptomycin (100X) (PanReac AppliChem, Germany).

All the cell lines used grow on a single layer. When the cells reached about 80% confluence, they were transferred to a new culture plate at a 1:6 or 1:10 dilution. After removing the medium, the cells were washed with Phosphate Buffered Saline (PBS) (VWR, USA) and incubated with 1x Trypsin 0.25% EDTA solution (Santa Cruz Biotechnology, USA) at 37°C. Trypsin is a proteolytic enzyme that digests adhesive proteins and releases adherent cells into the medium. After 5 minutes, complete DMEM with serum is added to inactivate the reaction. Next, the cells are detached from the plate, and it is possible to re-seed in a new plate diluted in a fresh medium. We used 60- or 100-mm culture dishes (SPL Life Sciences, Korea) to seed the cells.

The cells were manipulated inside a Class II Laminar Flow Hood (Telstar, UK) to provide a sterilized environment. All the materials used for cell maintenance were autoclaved and sterilized previously. DMEM, PBS, and Trypsin were preheated in a 37°C bath.

Table 3.1 - Panel of GBM cell lines and their characteristics.

	A-172	LN-18	LN-229	U-118 MG	U-87-MG
ORIGIN	ATCC	ATCC	ATCC	ATCC	ATCC
TISSUE	Brain	Brain	Brain	Brain	Brain
CULTURE PROPERTIES	Adherent	Adherent	Adherent	Adherent	Adherent
DISEASE	Glioblastoma	Glioblastoma	Glioblastoma	Glioblastoma	Glioblastoma
GENE DELETION	PTEN	CDKN2A	CDK2NA	-	-
GENE FUSION	ABL1-CBFB	-	-	-	-
MUTATION	IDH1; TP53	PIK3CB; TP53	LIFR; RAD21; TERT; TP53	IDH1; PTEN; TP53	IDH1; NF1; PTEN; TERT; TP53

3.1.1. Cell line cryopreservation

Long-term storage of cell lines is maintained in freezers at -180°C with 90% DMEM and 10% of cryoprotective agent Dimethyl sulfoxide (DMSO) (VWR, USA) to prevent dehydration. The process of freezing the cells is done gradually up to -180°C to avoid the formation of ice crystals that can cause the rupture of the cell membrane.

The process of cell thawing is done more rapidly to avoid cell exposure to high DMSO concentrations, which is toxic[225]. The cryo-vials were directly from the storage to a 37°C bath wash for about 1 minute. Once thawed, cells were transferred to a 15 mL conical tube with medium to centrifuge for 5 minutes at a speed of 216.3 *g* to remove DSMO residues. Cells were resuspended with fresh DMEM and seeded onto 100 mm culture plates with a pre-warmed medium.

3.1.2. Cell counting

For specific applications, we do need a specific cell number. For that, we stained the cells with Trypan Blue (Sigma Aldrich, USA) (1:1), a dye that can penetrate the membrane of dead cells, but not the living ones. Hence, dead cells

appear dyed in blue, and viable cells in white. Once labeled, cells were counted in a Neubauer Chamber (Marienfeld, Germany). Cells from the four quadrants of the chamber were counted according to Figure 3.1 and the cell concentration by mL was obtained as follows:

$$Cell\ concentration\ /\ mL\ = \frac{(A + B + C + D)}{4} \times\ dilution\ factor\ \times\ 10^4$$

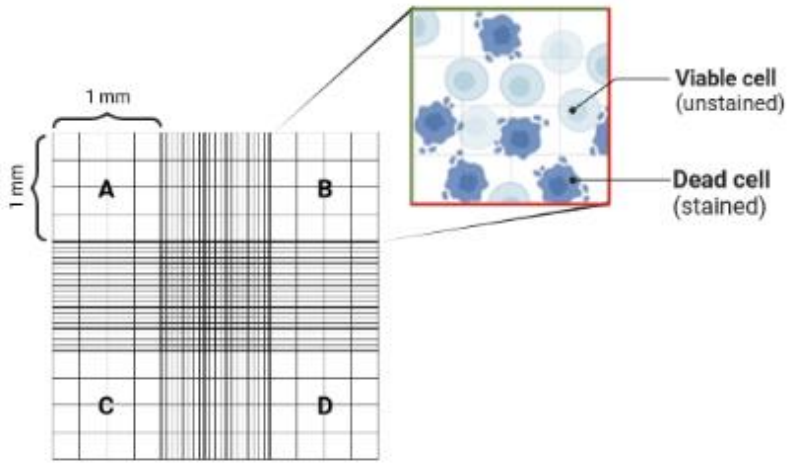

Figure 3.1 - Scheme of Neubauer chamber counting.

We counted the cells from each quadrant (A, B, C and D) and calculate the average number. We included cells touching the top or right edges (in green) but not those touching the bottom or left edges (in red). Each quadrant of the chamber represents the volume of 1 x 10^{-4} ml. Created with BioRender.com.

3.2. Assessment of protein levels by Western Blot

The evaluation of protein relative expression of the studied cell lines was performed by Western Blot. In this technique, the use of specific antibodies allows the identification of proteins after their separation by molecular weight on a polyacrylamide gel by electrophoresis.

3.2.1. Protein extraction

We obtained pellets from the GBM cell lines used in this study when they were at 80% confluent by centrifuging the cells for 5 minutes at 216.3 *g*. To collect the protein lysates, the pellets were resuspended in 80 – 120µl of lysis buffer, depending on the pellet size. The components of the lysis buffer are described in Table 3.2. The lysis buffer help to lysate the cell membrane to extract all the proteins avoiding their degradation. Once resuspended, the samples were vortexed 4 times at 5-minute intervals. Finally, they were centrifuged at 16.200 *g* for 20 minutes at 4°C. The supernatant containing all the proteins was collected into a 1,5 ml centrifuge tube.

Table 3.2 - Cell lysis buffer composition

Cell Lysis Buffer
1M Tris pH 7.5
5M sodium chloride (NaCl)
5% Triton X-100
1M β-glycerophosphate
0.5M ethylenediaminetetraacetic acid (EDTA)
0.5M ethylene glycol-bis (2-aminoethyl ether) tetraacetic acid (EGTA)
1M sodium fluoride (NaF)
200mM Pyrophosphate
100mM sodium orthovanadate (OVO4)
10nM Calyculan A
Protease Inhibitors Cocktail (PIC) (Sigma Aldrich, USA)

3.2.2. Protein quantification and calibration

To measure the concentration of total protein obtained in our samples we performed the Bradford Assay (Alfa Aesar, USA). This method relies on the binding of protein molecules in a dye that changes its color according to protein

concentration. The resultant blue color from the unknown samples is measured at 595nM and compared with a standard sample.

The calibration curve was prepared with Bovine Serum Albumin (BSA) (Thermo-Fisher Scientific, USA) in known concentrations between 2000 and 0 µg/mL, according to the schema in Figure 3.2. The samples were diluted 1:15 in Milli-Q H_20. The calibration curve and the diluted samples were analyzed at a 96-well plate. 250 µl of Bradford reagent was added to each well. After 10 minutes of incubation at room temperature, the absorbance was measured at 595 nm using SpectraMax iD3 (Molecular Devices, USA).

The final concentration of all the samples were normalized for the same concentration of 4 µg/µl. The data was analysed with Microsoft® Excel® 365.

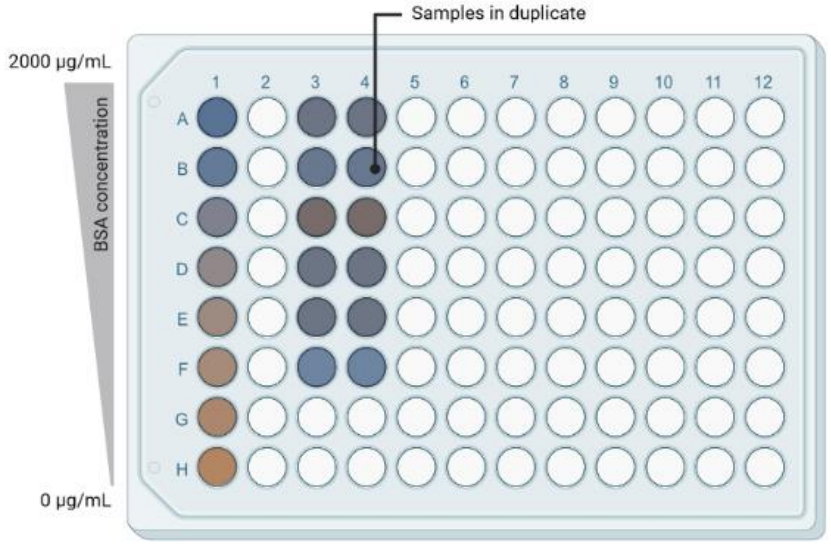

Figure 3.2 - Scheme of Bradford assay for protein quantification.

Protein quantification was done by Bradford assay in a 96-well plate. Calibration curve was calculated using BSA in serial dilution from 2000 to 0 µg/ml. Bradford reagent is added to each sample. The resultant colour corresponds to protein amount and was measured at 595nM. Each reaction is set up in duplicate to check for reproducibility. Figure created with BioRender.com.

After quantifying the samples, they were calibrated and prepared for electrophoresis. We added Laemmli loading buffer that contains sodium dodecyl sulfate (SDS), β-mercaptoethanol, glycerol, Bromophenol blue, and Tris 1M pH 6.8. SDS is a detergent that disrupts non-covalent bonds and provides a negative charge to them. The negative charge will allow the proteins to migrate toward the positive electrode in response to an electrical impulse. β-mercaptoethanol breaks covalent bonds helping to denature the protein structure. Glycerol is used to give density and bromophenol blue dyes the samples. Finally, the samples were heated for 5 minutes at 99,8°C for helping the protein denaturation.

3.2.3. Polyacrylamide gel electrophoresis (SDS-PAGE)

For the electrophoresis, we prepared an acrylamide gel to run the samples. The gel is composed of two parts: a stacking (on the top) and a running gel (at the bottom). The stacking gel has a lower concentration of acrylamide and lower pH compared to the resolving gel. It has the function of concentrating the proteins and lining them up.

The gels were prepared according to the laboratory protocol, as described in Table 3.3. Ammonium persulfate (APS) is necessary for the polymerization of acrylamide, whereas tetramethylethylenediamine (TEMED) (AppliChem, Germany) catalyzes it. A running gel of 10% acrylamide, ideal for studying proteins of 15-100kDa, was prepared due to the molecular weight of studied proteins, which ranged between 35 and 97kDa.

Table 3.3 - Composition of 1 gel for SDS-PAGE.

Stacking gel		**Running gel (10%)**	
1M Tris pH 6.8	312,5 µl	1M Tris pH 8.8	3 ml
dH_20	2,6 ml	dH_20	2,9 ml
40% bis-acrylamide	312,5 µl	40% bis-acrylamide	2 ml
10% SDS	25 µl	10% SDS	80 µl
25% APS	12,5 µl	25% APS	32 µl
TEMED	7,5 µl	TEMED	12 µl

Once the gel was polymerized, the samples were loaded. The total amount of protein varied according to the experiment. We loaded 3 µl of the protein ladder NZYColour Protein Marker II (NZYTECH, Portugal) to map the molecular weight of each protein.

The run occurred in an electrophoresis chamber (BioRad, USA) filled with running buffer (constituted by 1x Tris, glycine, and SDS). The system was subjected to an 85V voltage until the samples reached the running gel. Then, the voltage was increased to 145V to allow proteins to migrate until the bottom of the gel. The molecules migrate according to their size. Smaller proteins migrate faster whereas larger proteins are slower and therefore higher up in the gel.

3.2.4. Protein transfer to PVDF membranes

After separating the proteins according to their size, they were transferred to a polyvinylidene difluoride (PVDF) (Cytiva, Germany) membrane. To do so, we used a cassette forming a “sandwich” consisting of a sponge, filter paper, gel, PVDF membrane, filter paper, and sponge, according to Figure 3.3. The cassette is placed inside a chamber submerged with Transfer buffer (composed of 1x Tris, glycine, and methanol). A 75V current was applied for 90 minutes in ice.

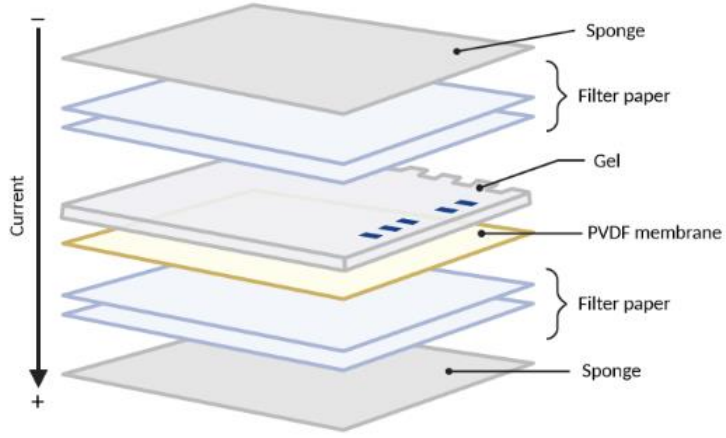

Figure 3.3 - Representation of the "sandwich" assembly for protein transfer.

After running, the proteins are separeted by molecular weight on the acrylamide gel. To transfer them to a PVDF membrane, a “sandwich” in the same order as representated is made. A voltage of 75V were applied in the system for 90 minutes so the proteins can migrate from the gel to the membrane. Created with BioRender.com.

3.2.5. Immunodetection

After the protein transference, the membrane carries all the proteins from the sample. Before proceeding directly with the immunodetection, it is important to block the membrane. The blocking is important to avoid unspecific binding besides the interested antibody. For that, the membrane was incubated with 5% non-fat milk in 1x Tris-Buffer saline 0,1% Tween (TBS-T) solution for 1 hour rocking at room temperature. Next, the membrane was washed 3 times with TBS-T.

For the immunodetection, specific antibodies were used for the interest proteins, as detailed in Table 3.4. The membranes were incubated with the primary antibody overnight on a roller at 4°C. The primary antibody recognizes and binds specifically to the epitope of the protein of interest.

Table 3.4 - List of primary and secondary antibodies used in Western Blot in this study.

Primary Antibodies				
Antibody	**Dilution**	**Specie**	**Reference**	**Company**
Actin	1:1000 milk	Goat	sc-1616	Santa Cruz Biotechnology
AKT total	1:1000 BSA	Rabbit	CST #9272	Cell Signaling
ERK1/2 total	1:300 BSA	Rabbit	sc-94	Santa Cruz Biotechnology
FOXO1	1:500 BSA	Rabbit	CST 2880	Cell Signaling
FOXO3	1:500 BSA	Rabbit	CST 12829	Cell Signaling
FOXO4	1:500 BSA	Rabbit	CST 9472	Cell Signaling
FOXO6	1:500 BSA	Rabbit	PA5-106411	Invitrogen
FOXO6	1:500 BSA	Rabbit	PA5-35117	Invitrogen
GAPDH	1:5000 BSA	Rabbit	sc-25778	Santa Cruz Biotechnology
P-AKT (Ser 473)	1:1000 BSA	Rabbit	CST #4060	Cell Signaling
P-ERK1/2 (Thr202/Tyr204)	1:1000 BSA	Rabbit	CST #4370	Cell Signaling
P-S6K (Thr389)	1:500 BSA	Rabbit	CST #9234	Cell Signaling
S6K total	1:1000 BSA	Rabbit	sc-230	Santa Cruz Biotechnology
TRIB1	1:1000 BSA	Rabbit	09-126	Millipore
TRIB2	1:1000 milk	Rabbit	CST 13533	Cell Signaling
TRIB3	1:1000 BSA	Rabbit	ab 75846	Abcam
Tubulin	1:15000 BSA	Mouse	T9026	Sigma

Secondary Antibodies

Antibody	Dilution	Specie	Reference	Company
Anti-Goat IgG	1:10000 milk	Donkey	sc-2020	Santa Cruz Biotechnology
Anti-Mouse IgG	1:10000 milk	Sheep	NA931	GE Healthcare
Anti-Rabbit IgG	1:10000 milk	Donkey	NA934	GE Healthcare

The next day, the membranes were washed with TBS-T three times. Following, they were incubated with the secondary antibody (described in Table 3.4) rocking for 1 hour at room temperature. The secondary antibody is species-specific and binds to the primary antibody. The enzyme horseradish peroxidase (HRP) is conjugated with the secondary antibody, necessary for posterior detection. The membranes were then washed again three times with TBS-T.

Finally, the membranes were incubated with a home-made enhanced chemiluminescence (ECL) solution for 3 minutes protected from the light. The ECL solution contains luminol 250 mM, acid coumaric 90 mM, 1 M Tris pH 8.5, 30% hydrogen peroxide (H_2O_2), and H_2O. Basically, the luminol will be oxidated by H_2O_2 in a reaction that emits light, and it is catalyzed by the HRP enzyme. The luminescence production is proportional to the amount of secondary antibody conjugated with HRP and therefore indirectly measures the presence of the target protein. The signal was detected by ChemiDoc XRS+ (BioRad, USA). The images were analyzed in Image Lab 5.2.1. The protein bands were quantified by densitometry with Image-J.

3.3. Quantitative Reverse Transcription Polymerase Chain Reaction analysis of mRNA levels

Gene expression evaluation of GBM cell lines was assessed by Quantitative Reverse Transcription Polymerase Chain Reaction (RT-qPCR). This technique enables the detection of specific mRNA molecules presents in a sample. Basically, RNA is first extracted from the cells, and the complementary DNA (cDNA) is synthesized and then amplified, as schematized in Figure 3.4. Monitoring the PCR products is possible because of the addition of a fluorescent

dye to the cDNA molecules throughout the process. The measured fluorescent emitted allows for quantifying the levels of the target gene expression.

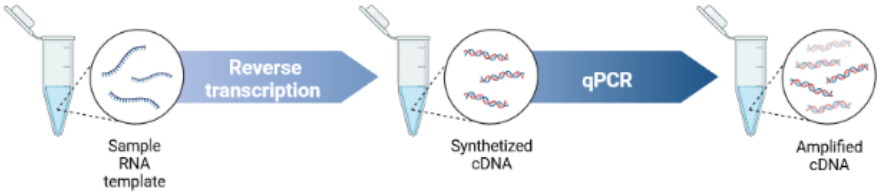

Figure 3.4 - Stages of RT-qPCR for RNA detection.

RT-qPCR allows to detect specific RNA molecules from a sample for gene expression evaluation. First, the RNA obtained from the cells acts as template for the synthetization of cDNA by reverse transcription. Then, the binding of fluorescent dye to cDNA molecules during the PCR reaction enables to quantify the PCR product. The measured emitted fluoresce is proportional to the target gene expression. Figure created with BioRender.com.

3.3.1 RNA extraction and purification

RNA was collected from GBM cultures at 80% confluency. The cell pellet was collected by centrifugation at 216.3 *g* for 5 minutes.

To extract RNA from the pellets, the cells were lysed with lysis buffer containing 1% of 2-mercaptoethanol. The RNA purification was performed using PureLink™ RNA Mini Kit (Invitrogen, USA), according to the manufacture's protocol in annex I. The total concentration of the purified RNA was assessed in NanoDrop2000c Spectrophotometer (Thermo-Scientific, USA). The tubes were stored at -80°C for posterior use since RNA is very unstable and easily degradable.

3.3.2. cDNA synthesis

To proceed with the RT-qPCR, first, we need to convert the purified RNA into cDNA. To do so, the NZY First-Strand cDNA Synthesis Kit (NZYTECH, Portugal) was used. The manufacturer protocol followed is in annex II. The

quantity of RNA used was 2µg. The additional step of adding RNase was done to degrade the RNA template in cDNA-RNA hybrids after the first-strand cDNA synthesis. The thermal reaction was performed using C1000 Touch Thermal Cycler (BioRad, USA). The cDNA product was then diluted into 1:10 in dH_20 and the remaining volume was stored at -20°C.

3.3.3. RT-qPCR

The synthesized cDNA was used as the template for the qPCR. For this technique, we used iTAq Universal SYBR Green Supermix Kit (BioRad, USA). The manufacturer protocol and instructions were followed and can be assessed in annex III. The experimental design of the plate was previously prepared. The volumes of the reagents used are described in Table 3.5. First, the Mastermix was prepared and pipetted into a 384 well-plate. Then, the samples of cDNA products were added. The sequence of the primers previously designed used is detailed in Table 3.6. We used triplicated samples to reduce technical variability. No-template controls (NTC) were also included as negative controls. For normalization, housekeeping gene expression was also evaluated. We used glyceraldehyde 3-phosphate dehydrogenase (GAPDH) as a reference gene in this study.

Table 3.5 - Volume of reagents used for the qPCR technique per well.

Reagent	Volume (µl) / well
iTaq Universal SYBR Green Supermix	1,25
Forward primer (10µM)	0,5
Reverse primer (10µM)	0,5
Nuclease free H_20	2,8
DNA template	5,0
Total volume	**20,0**

Table 3.6 - List of primers used for RT-qPCR in this study.

Gene	Direction	Sequence 5' > 3'
FOXO1	Forward	AAGAGCGTGCCCTACTTCAA
	Reverse	CTGTTGTTGTCCATGGATGC
FOXO3	Forward	ACAAACGGCTCACTCTGTCC
	Reverse	TCTTGCCAGTTCCCTCATTC
FOXO4	Forward	GCCTGGGGAAATCAGTCATA
	Reverse	GCCTCGTTGTGAACCTTGAT
FOXO6	Forward	ACCTCATCACCAAAGCCATC
	Reverse	AGCATCCACCACGAACTCTT
GAPDH	Forward	CAATGACCCCTTCATTGACC
	Reverse	TTGATTTTGGAGGGATCTCG
TRIB1	Forward	ATCGCCGACTACCTGCTG
	Reverse	GTAATGTTGCTGTGCGATGG
TRIB2	Forward	GACTCCGAACTTGTCGCATT
	Reverse	ATGAGCAGACAGGCAAAAGC
TRIB3 (I)	Forward	TGCCCTACAGGCACTGAGTA
	Reverse	GTCCGAGTGAAAAAGGCGTA
TRIB3 (II)	Forward	TCAAGCTGTGTCGCTTTGTC
	Reverse	AGGCCCGTGAGCTGAGTAT

The RT-qPCR reaction occurred in a C100 Touch Thermal Cycler CFX384 Real-Time System machine (BioRad, USA). The reaction protocol was set as follows: first, a polymerase activation period of 30 seconds at 95°C; then, for amplification, 40 cycles of 5 seconds at 95°C for denaturation, followed by 30 seconds at 60°C for annealing and extension. Finally, 5 seconds starting at 65°C until 95°C for the melting curve analysis. The results were analyzed using Bio-Rad CFX Maestro 1.0 software.

3.4. Gene modulation

To understand the role of Tribbles protein family members in GBM biology, we wanted to modulate Tribbles in GBM cell lines. To do so, we decided to (i) create a TRIB3 KO cell line and (ii) a TRIB2 KO cell line with Clustered Regularly Interspaced Short Palindromic Repeats (CRISPR/Cas9) system, (iii) a TRIB2

silenced cell line with short interfering RNA (siRNA) and (iv) induce TRIB2 overexpression (as schematized in Figure 3.5).

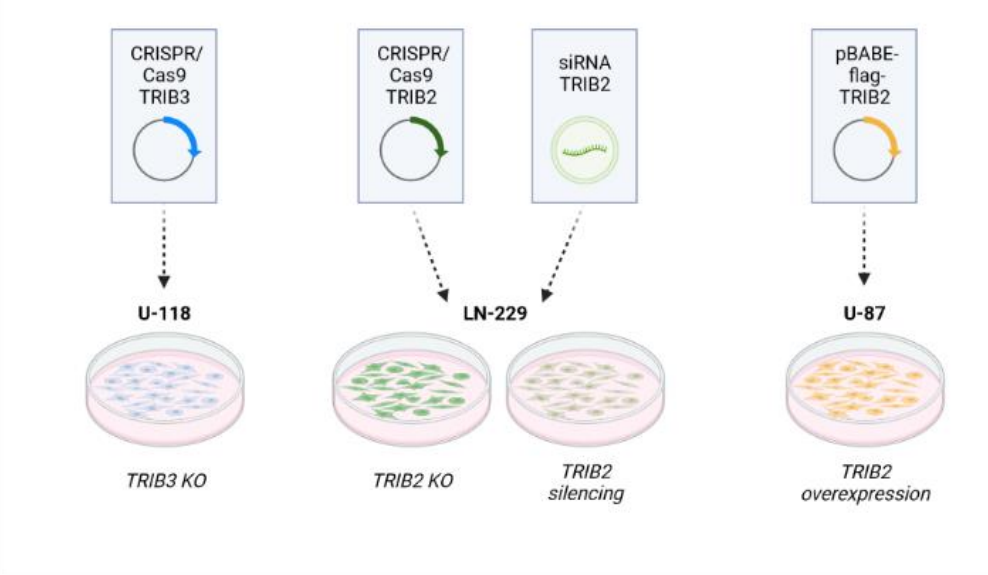

Figure 3.5 - Representation on how we modulated Tribbles in GBM cell lines.

We decided to have different approaches to modulate Tribbles proteins in GBM cell lines. We generated U-118 TRIB3 KO cell line and LN-229 TRIB2 KO cell line using CRISPR/Cas9 system. Besides, we silenced TRIB2 in LN-229 using siRNA. Moreover, we overexpressed TRIB2 in U-87 with plasmids. Figure created with BioRender.com

3.4.1. Cell transfection for gene modulation

3.4.1.1 Cell transfection with plasmid vectors

We used plasmids to generate the KO cell lines and to promote protein overexpression. For the insertion of the plasmids into the studied cells, we used Lipofectamine 2000 (Invitrogen, USA). For the generation of the U-118 TRIB3 KO cell line, we plated 0,4 x 10^6 cells in 60mm dishes. In the case of LN-229 TRIB2 KO cell line generation, 0,3 x 10^6 cells were plated in 60 mm dishes. To induce TRIB2 overexpression, we plated 0,4 x 10^6 LN-229 cells in 60 mm dishes. On the next day, the cell lines were about 80% confluent, and we proceed following the manufacturer's protocol.

Briefly, we diluted 3 µg of the plasmid to be transfected into 250 µl of Opti-MEM (Gibco, USA) and 10 µl of Lipofectamine reagent into 250 µl of Opti-MEM. After 5 minutes, both dilutions were mixed and incubated for 20 minutes. We then added the DNA-lipid complex to the cells and incubated them in standard conditions.

For the KO generation with CRISPR/Cas9, we transfected the plasmid pSpCas9(BB)-2A-Puro (PX459) V2.0 (Addgene plasmid #62988). For the overexpression of TRIB2, we used the plasmid pBABE-flag-TRIB2.

3.4.1.2. Cell transfection with siRNAs

Short-interfering RNAs (siRNAs) are used to knock down gene expression to study protein function in different cell types. siRNA are small molecules normally composed of 21 base pairs length. These molecules can bind to specific mRNAs and act as a post-transcriptional control mechanism, causing gene silencing through repression of translation.

This biological approach was used to help validate the specificity of the antibodies used in this project in the UACC-62 melanoma cell line. Moreover, siRNAs were used to modulate TRIB2 in the LN-229 GBM cell line by silencing TRIB2 gene expression.

To do so, 0,4 x 10^6 cells of each cell line were plated in 60 mm the day before the transfection. On the next day, the cells were about 80% confluent and suitable for being transfected. We used different SMARTpools from Dharmacon, USA, as described in Table 3.7. For transfecting siRNA, we used DharmaFECT transfection reagent according to the manufacturer's protocol. Briefly, we diluted 15 µl of siRNA [5 µM] into 285 µl of OPTI-mem and 6 µl of DharmaFECT reagent into 294 µl. After 5 minutes, the dilutions were mixed and incubated for 20 minutes. Finally, the transfection mixture was added to the cells. Corresponding analyzes were performed 48 hours after transfection. The non-targeting sequence siRNA (non-targeting siRNA) was used as a negative control for the siRNA experiment. It is designed and chemically modified to have no known

mRNA targets in the cells used. It was used for determining the non-specific effects of siRNA delivery to provide a baseline to compare to siRNA-treated samples.

Table 3.7 - List of siRNA used for gene silencing.

Gene	Name	Reference
FOXO1	SMARTpool ON-TARGETplus Human FOXO1 siRNA	SO-2871756G
FOXO3	SMARTpool ON-TARGETplus Human FOXO3 siRNA	SO-2871756G
FOXO4	SMARTpool ON-TARGETplus Human FOXO4 siRNA	SO-2871756G
FOXO6	SMARTpool ON-TARGETplus Human FOXO6 siRNA	SO-2871756G
TRIB1	SMARTpool ON-TARGETplus Human TRIB1 siRNA	SO-2997341G
TRIB2	SMARTpool ON-TARGETplus Human TRIB2 siRNA	SO-30736607G
TRIB3	SMARTpool ON-TARGETplus Human TRIB3 (57761) siRNA	SO-2997341G
Non-targeting siRNA	ON-TARGETplus Non-targeting siRNA	D-001810-01-05

3.4.2. Generation of knock-out cell lines by CRISPR/Cas9

To study the effects of TRIB3 and TRIB2 modulation on GBM, we generated a U-118 TRIB3 KO cell line and an LN-229 TRIB2 KO cell line using the CRISPR/Cas9 system, a tool that allows gene editing with high precision. CRISPR/Cas is part of the microbial adaptive immune system that has been adapted to edit the genome. It relies on RNA-guided nucleases to cleave specific sites on target genes. After cleavage, the cell uses the non-homologous end joining repair (NHEJ) mechanisms that can lead to the formation of non-functional genes.

The introduction of the CRISPR/Cas9 machinery into the cells was done by Lipofectamine transfection as described in the previous point. In this project, we used the plasmid pSpCas9(BB)-2A-Puro (PX459) V2.0 (Figure 3.6). The

advantage of using this plasmid is the presence of the gene encoding Cas9 and the designed guided RNA for the target gene in the same vector.

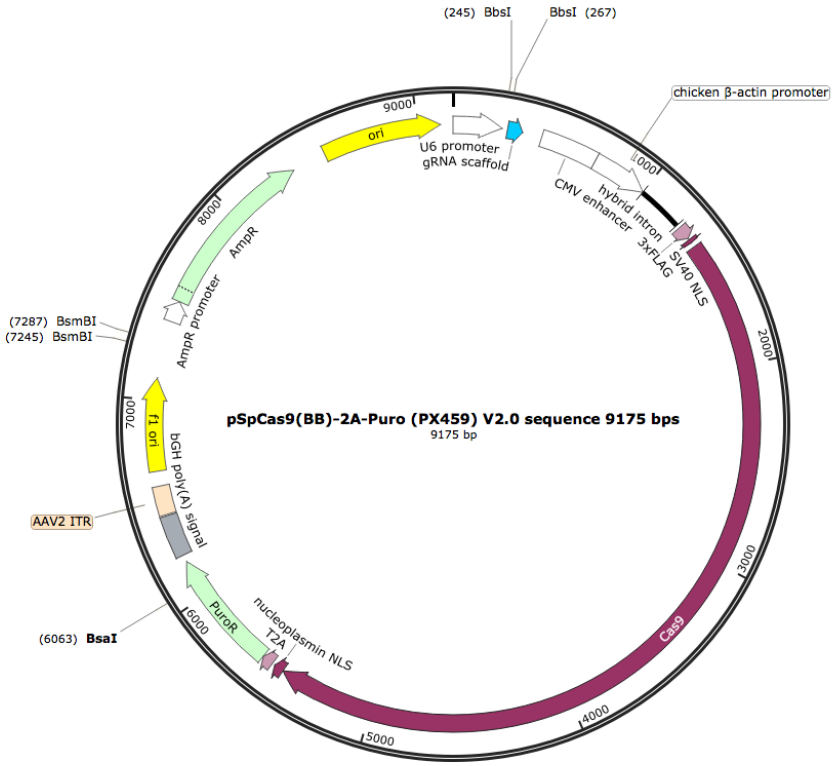

Figure 3.6 - Map image for pSpCas9(BB)-2A-Puro (PX459) V2.0 used in CRISPR/Cas9 KO.

We used plasmid PX459 (Addgene plasmid #62988) as a vector to generate KO cell lines. This figure indicates the region where the gRNA sequence was inserted in blue, after the U6 promoter, and sequence that codes for Cas9 in purple.

The guided RNAs (gRNAs) for TRIB3 and TRIB2 used in this project were previously designed by Dr. Bibiana Ferreira. Two different gRNAs for each gene were used to minimize the off-target probability. For TRIB3 KO, gRNAs #1170 and #1172 were transfected with the vector to U-118 cells. For TRIB2 KO, gRNAs #1167 and #1169 were transfected into the LN-229 cell line. We chose not to disclose the specific sequences of the gRNAs as these results have not yet been published.

To select the cells that had incorporated the plasmid, we treated the cells with Puromycin (1µl/1ml) 48 hours after the transfection, since the plasmid used

has the gene for Puromycin resistance. We maintained selection with this antibiotic for 48h. As a result, only the successfully transfected cells will survive.

To be able to pick colonies formed by clones from one single cell, we performed a serial dilution. We used rings to isolate the clones, trypsinized them, and collected the cell clones to a different plate. We maintained the clones until they reached 80% confluently and then expanded them. This allowed us to generate cell stocks for clone maintenance and to obtain pellets for protein extraction. With this material, we were able to confirm KO efficiency by Western Blot.

3.5. Crystal Violet Staining

To assess the viability of the U-118 TRIB3 KO cells in basal conditions and upon TMZ treatment, we used crystal violet staining. Crystal violet is a triarylmethane dye that binds to ribose-like molecules such as DNA.

For this assay, we plated 1 x 10^4 cells in 24-well in triplicate. Then, the cells were exposed to TMZ or DMSO (which is the drug vehicle) for 72 hours. After this time, the cells were washed twice with PBS, so the dead cells can be washed away, as they detach from the plate. The remaining cells were then fixed with 400µl of 4% paraformaldehyde (PFA) for 15 minutes at room temperature. Once fixed, they were washed again with PBS three times and stained with a solution of 1% Crystal violet (Panreac, Spain) and 20% methanol for 30 minutes in agitation. Sequentially, the plates were washed with water and left to try overnight. On the next day, the stain was solubilized in 250µl of Triton 0,125% in PBS for 30 minutes in agitation. Then, 200µl of each sample was transferred to a 96-well plate so the absorbance could be read in wavelength of 570nm in SpectraMas iD3 Microplate Reader (Molecular Devices, USA).

As only the attached cells were stained, the measurement of the absorbance is proportional to the number of viable cells on the plate. In other words, a reduction in absorbance related to a control indicates reduced viability.

This assay allows for estimating how different treatments affected the survival of the seeded cells.

3.6. Trypan Blue exclusion assay

Trypan Blue is a dye that can penetrate through the membranes of non-viable cells. Trypan Blue exclusion assay enables us to assess the quantification of cell viability by light microscopic. By differentiating blue non-viable cells from white viable cells, it allows us to quantify cell proliferation and cell death in an assay and infer more information about cell viability.

We performed this assay to analyze if there are differences in cell proliferation and cell death upon TRIB3 abrogation in the U-118 cell line. We quantified the total number of cells and the percentage of cell death of U-118 parental and TRIB3 KO cell lines under basal conditions and upon TMZ treatment.

The cell lines were seeded into a 6-well plate with an amount of 5×10^4 cells per well in DMEM complete. On the next day, the medium was replaced with fresh DMEM containing DMSO (which is the drug vehicle) or TMZ [500 µM] and the cells were incubated for 72 hours. After this time, the cells were trypsinized and collected in a 15 ml conical tube in addition to the medium containing the cells in suspension. After centrifuging for 5 minutes at 216.3 *g*, the cells were resuspended in DMEM. We diluted 10 µl of cell suspension in 10 µl of Trypan Blue (Sigma Aldrich, USA) and 10 ul of this mixture was loaded on a Neubauer chamber. Viable and non-viable cells were counted on the microscope as described in section 3.1.2.

To quantify cell proliferation, we account for the total number of cells (viable + non-viable cells). To quantify cell death, we calculated the percentage of dead cells over the total number of cells. The results were analyzed with GraphPad Prism 7.03.

4. RESULTS

As previously mentioned, the standard therapy for treating GBM is based on surgical resection of the tumor followed by a combined administration of radiotherapy and chemotherapy with the alkylating agent TMZ. However, the average survival of these patients is only slightly improved by these treatments[33]. To improve patients' response to therapy, it is extremely relevant to discover new biomarkers and develop better therapeutic strategies.

Our hypothesis is that TRIB2 and TRIB3 proteins have an oncogenic role in GBM. To achieve our goal, we divided this project into different phases. First, we need to (i) characterize the expression of Tribbles proteins in a panel of glioblastoma cell lines. Then we could select the best cell lines to modulate Tribbles expression. After that, we want to (ii) create tools that allow us to study the effects of the presence or absence of Tribbles proteins on cellular phenotypes. Hence, we generated Tribbles knock-out (KO) cell lines using the CRISPR/Cas9 system to better understand the effect of Tribbles abrogation on GBM cells. Next, we (iii) characterize those GBM cells to study how the KO genes would affect their phenotype.

Data from our laboratory showed that Tribbles' mRNA expression levels correlate with GBM patients' survival. Our analysis demonstrated that high Tribbles levels are often associated with glioma grade, being higher in GBM. Moreover, the phenotype with high levels of Tribbles in association with low levels of FOXO3/4 mRNA is correlated with the worst prognosis. Thus, we hypothesize that Tribbles may contribute to GBM aggressiveness and patients' poor survival.

4.1. Tribbles' antibodies validation

Our aim is to generate isogenic GBM cell lines that express different Tribbles protein levels. To do that, and because there are three different Tribbles family members, we proceed to validate the specificity of different antibodies using siRNA. We transfected different siRNAs against each of the Tribbles family

members in the UACC-62 melanoma cell line (routinely used cell line in the lab that expresses mRNA levels for all Tribbles isoforms, not shown) (see section 3.4.1.2).

Our data shows that siRNA against TRIB2 and TRIB3 successfully reduced protein levels. Our results also show that the antibodies against TRIB2 (CST 13533, Cell Signaling Technology, USA) and TRIB3 (ab 75846, Abcam, UK) are specific for TRIB2 and TRIB3, respectively, without reducing other family members' protein levels (Figure 4.1, A). On the other hand, siRNA against TRIB1 did not have any effect on TRIB1 protein levels using the TRIB1 antibody (Millipore 09-126, Merck, Germany). This might indicate that the antibody is not specific to TRIB1 or that the siTRIB1 is not binding to the TRIB1 isoform in this experiment. We also checked mRNA levels by RT-qPCR to validate the efficiency of siRNA transfection. Our data shows that siRNA indeed reduced TRIB1 mRNA levels compared to the control (Figure 4.1, B). Therefore, TRIB1 might not be specific against TRIB1. It is important to note that the experiment was only performed once, so it is difficult to conclude with certainty.

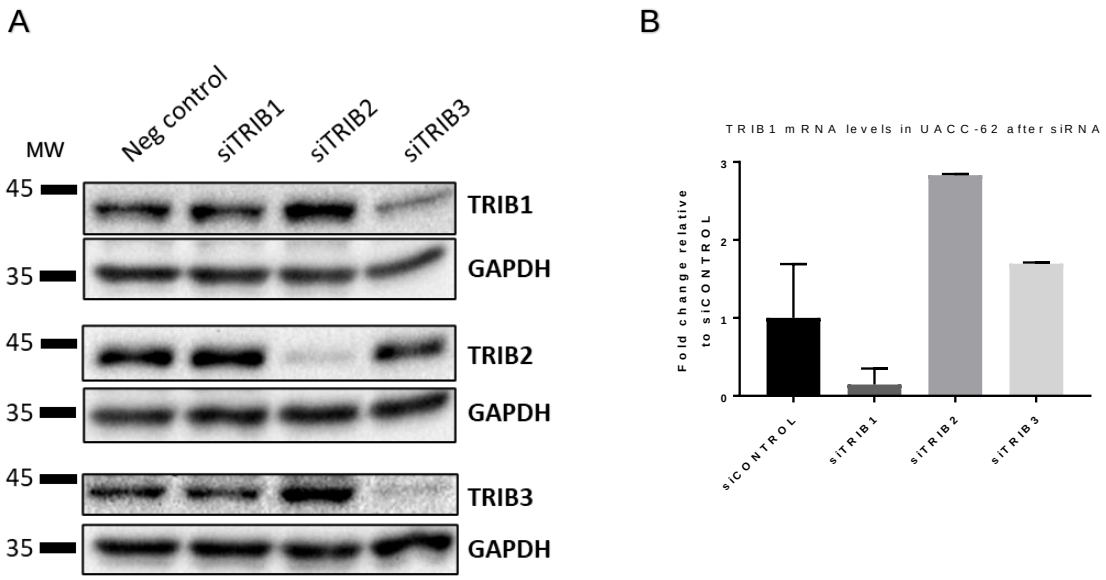

Figure 4.1 - Expression levels of Tribbles members in UACC-62 after siRNA.

(A) Analysis of levels of Tribbles protein in UACC-62 cell line after siRNA transfection by Western Blot. GAPDH was used as loading control. Non-targeting siRNA (Neg control) was used as negative control for the transfection assay. We loaded 60 µg of protein and 3 µg of NZY Blue Protein Marker into the wells. The gels are 10% of acrylamide. The signal was detected by Chemidoc XRS+ System and images were treated in Image Lab 6.1 software. MW = molecular weight. **(B)** TRIB1 mRNA levels in UACC-62 after siRNA quantified by RT-qPCR. Data correspond to TRIB1 mRNA levels normalized to loading housekeeping gene (GAPDH) and are expressed as mean ± SEM fold change of treated condition versus negative control. Data analysed in BioRad CFX Maestro.

As previously mentioned in the introduction section, Tribbles' family members act upstream and modulate different key signaling pathways that regulate the activity of FOXOs proteins. Thus, FOXOs proteins are often used as a possible readout of Tribbles' activation status. With this in mind, we will also evaluate FOXOs' levels in our experiments. Therefore, we also validated the specificity of antibodies against FOXOs proteins.

Because Tribbles proteins act upstream of FOXO and might regulate their activity[161], we also screened for FOXOs' antibodies. Our results demonstrated that siRNA against FOXO1 and FOXO3 translated into a reduction of FOXO1 and FOXO3 protein levels, respectively. Our data also shows that antibodies against FOXO1 (CST 2880, Cell Signaling Technology, USA) and FOXO3 (CST 12829, Cell Signaling Technology, USA) are isoform-specific (Figure 4.2). Regarding FOXO4, our data show that the siRNA against FOXO4 reduces FOXO4 mRNA

levels. Moreover, the FOXO4 antibody (CST 94725, Cell Signaling Technology, USA) is specific for FOXO4 and does not detect other FOXOs' isoforms (Figure 4.2). Silencing of FOXO6 did not show a reduction in FOXO6 protein levels using the FOXO6 antibody PA5-106411 (Invitrogen, USA) (Figure 4.2). This result can be due to an unsuccessful silencing of FOXO6.

Moreover, RT-PCR analysis of these samples showed that levels of FOXO6 were barely detectable (not shown). This result might explain the inefficient siRNA experiment against FOXO6. As a consequence, we were unable to confirm FOXO6 antibody specificity. Taking all of this into account, we chose not to include this antibody during the rest of the study. Until now, tools to analyze FOXO6 activity are scarce because little is known about the role of FOXO6, but we are still in the process of validating alternative antibodies.

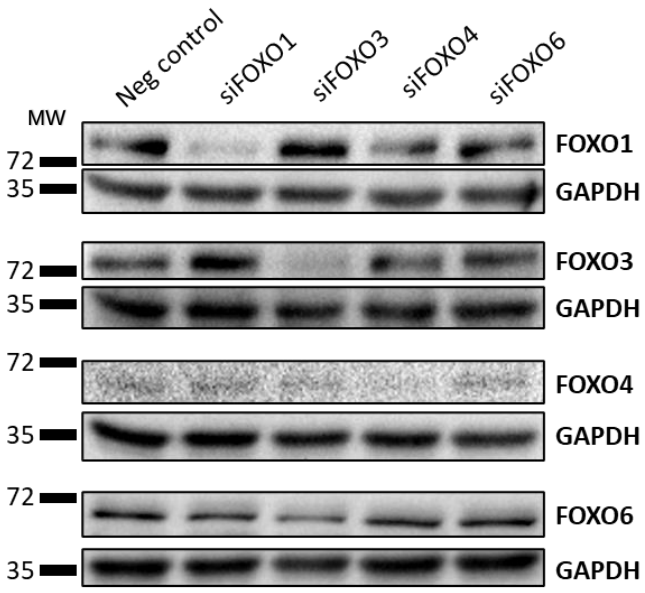

Figure 4.2 - Levels of FOXOs proteins in UACC-62 after silencing RNA expression.

Specificity of FOXOs' antibodies were assessed by siRNA in UACC-62. Protein levels were evaluated by Western Blot. FOXO1 and FOXO3 protein levels were reduced after silencing FOXO1 and FOXO3, respectively. Despite of the low signaling of the band, FOXO4 antibody also showed a reduction of the signal. However, FOXO6 protein levels are not changing and therefore will not be used in the following experiments. GAPDH was used as loading control. Non-targeting siRNA was used as a negative control. Each well was loaded with 60 µg of protein and 3 µg of the NZY Blue Protein Marker. Gels of 10% acrylamide were used. The signal was detected by Chemidoc XRS+ System and images were treated by Image Lab 6.1 software. MW = molecular weight.

4.2. GBM cell line screening

To study the role of Tribbles family members in GBM biology, we wanted to generate isogenic GBM cell lines that express different Tribbles protein levels. To do so, we needed to select suitable cell lines. Therefore, we need to characterize different GBM cell lines according to Tribbles family members' expressions.

We selected a panel of five different GBM cell lines (A-172, LN-18, LN-229, U-118, and U-87) and evaluated Tribbles' mRNA expression levels and endogenous protein levels. It is described that all GBM cell lines from our panel have mutations in the P53 gene. Also, U-118 and U-87 have mutations on the PTEN gene, and A-172 has a deletion on this TSG. A full description of the GBM cell lines can be seen in Table 3.1.

4.2.1. Characterization of GBM cell line panel at mRNA level

To evaluate the expression of Tribbles' mRNA levels in our GMB cell panel, we performed RT-qPCR. We used TRIB1, TRIB2, and TRIB3 specific and previously validated primers, as described in section 3.3. Our results showed that LN-229, U-118, and U-87 cell lines have higher TRIB1 and TRIB2 mRNA levels, whereas A-172 and LN-18 have lower TRIB1 and TRIB2 mRNA levels (Figure 4.3, A, B). Regarding TRIB3 expression, the U-118 cell line showed the highest level of this protein (Figure 4.3, C).

Since data from our lab showed a characteristic phenotype that associates high levels of Tribbles and low levels of FOXOs with GBM aggressiveness, we also decided to verify the transcriptional levels of FOXO1, FOXO3, and FOXO4. Our data also showed that, overall, all the GBM cell lines express higher levels of FOXO3 and FOXO4 compared to FOXO1 expression levels (Figure 4.3, D, E, F).

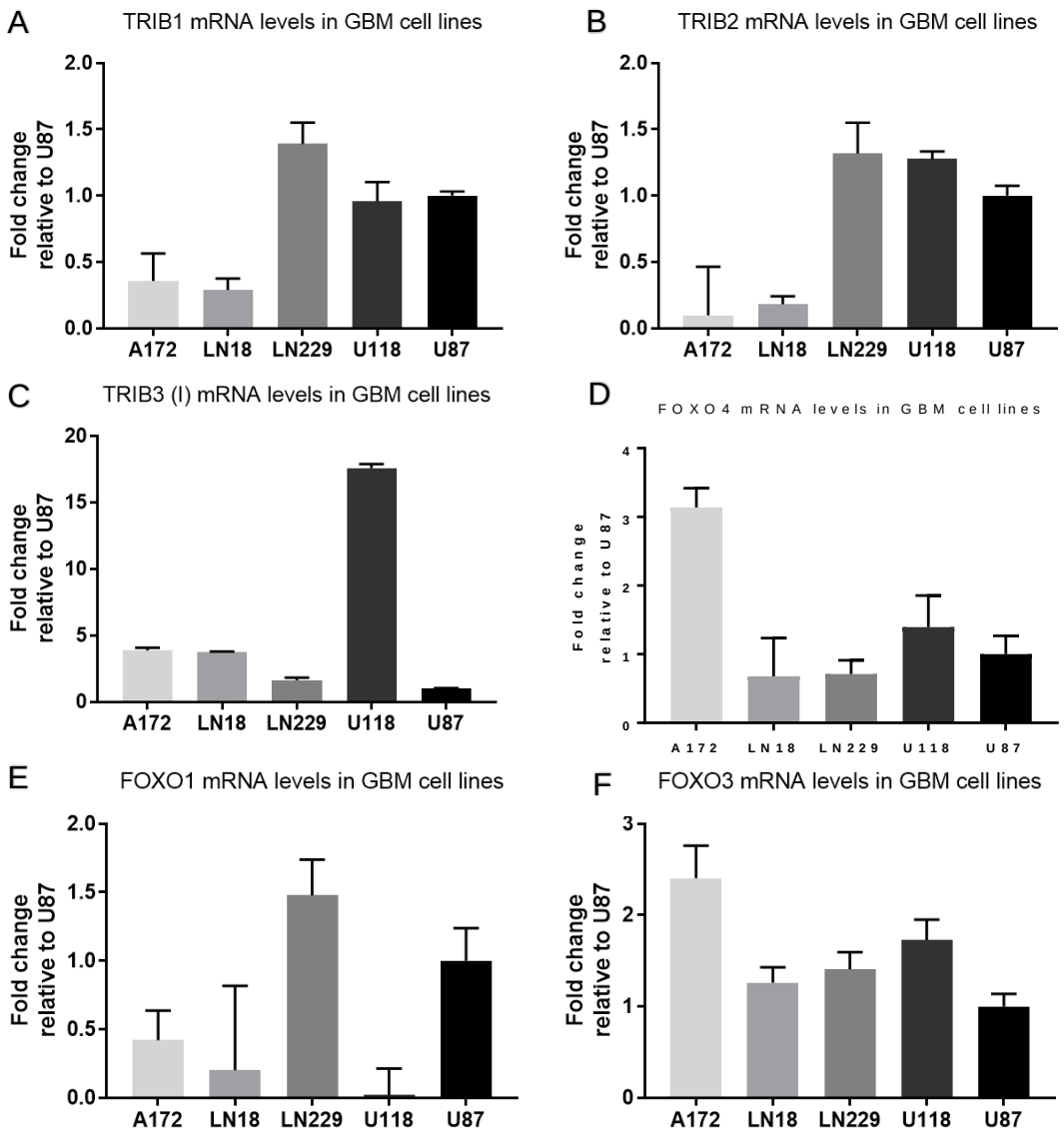

Figure 4.3 - Transcriptomic profile of GBM cell line panel regarding Tribbles and FOXOs.

We used RT-qPCR technique to assess Tribbles (**(A)** TRIB1; **(B)** TRIB2; **(C)** TRIB3 (l)) and FOXOs (**(D)** FOXO4 **(E)** FOXO1; **(F)** FOXO3) mRNA levels in a GBM cell line panel composed by five different cell lines: A-172, LN-18, LN-229, U-118 and U-87. GAPDH was used as housekeeping gene to normalize gene expression. Data are expressed as mean ± SEM fold change related to U87 cell line. Data reflects three technical replicates from one single biological experiment. Results were analysed using Bio-Rad CFX Maestro 1.0 Software.

4.2.2. Characterization of GBM panel cell line panel at the proteomic level

The mRNA levels do not always correlate with the protein levels due to post-transcriptional, post-translational, and protein degradation regulation [226]. However, proteins are the major effectors of cellular functions. Since we are interested in modulating Tribbles protein family members in GBM cells, we evaluated Tribbles protein levels in our panel of GBM cell lines. For that, we used specific antibodies previously validated in section 3.1. Figure 4.4 shows that the U-118 cell line has a high expression of TRIB3 protein. The LN-229 cell line is the only GBM cell line from our panel that seemed to express high levels of TRIB2. Overall, none of the glioma cell lines showed high levels of TRIB1 protein. Taking all the data together, we chose the U-118 and LN-229 cell lines for the following experiments. The U-118 and LN-229 cell lines were used to generate the TRIB3 and TRIB2 isogenic knockout cell lines, respectively. Additionally, we selected the U-87 cell line to generate an isogenic cell line that overexpresses TRIB2 since this cell line showed low levels of TRIB2 protein expression by Western Blot (Figure 4.4).

Regarding FOXOs protein levels, FOXO3 seems to be expressed in all the cell lines tested, although expression levels differ from cell line to cell line. FOXO1 protein expression was only detected in the LN-229 cell line. Interestingly, FOXO4 protein expression was not detected in any of the cell lines tested (Figure 4.4). In fact, this result agrees with findings from Qi *et al*., which described that FOXO4 expression was downregulated in GBM cell lines. Indeed, they showed that FOXO4 was reduced according to glioma's grade, namely, normal brain tissue presented higher FOXO4 levels and grade V glioma (GBM) had the lowest levels[227].

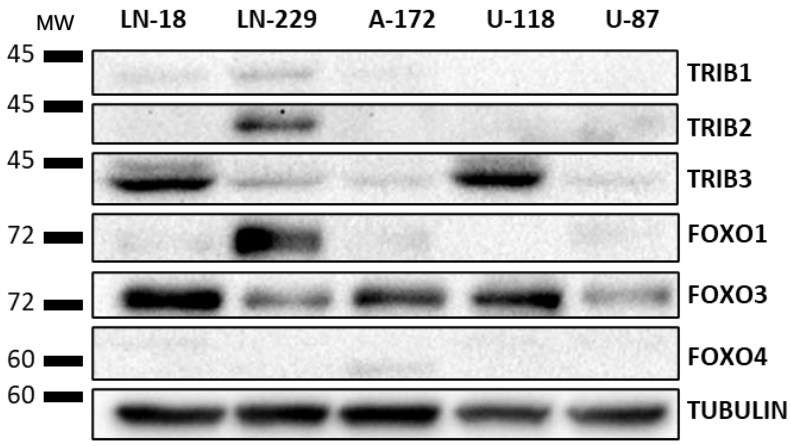

Figure 4.4 - Tribbles and FOXOs protein levels in GBM cell line panel.

We assessed the protein expression levels on our GBM panel by Western Blot. Tribbles and FOXOs proteins were detected using specific antibodies. A total of 80µg of protein and 3 µg of the NZY Blue Protein Marker was loaded onto each well. We used 10% acrylamide gels. Tubulin was used as loading control. The signal was detected by Chemidoc XRS+ System and images were treated in Image Lab 6.1 software. MW = molecular weight.

4.3. Generation of U-118 TRIB3 knockout cell line

Since we aim to create GBM cell-based models to study Tribbles' contribution to GBM development, we decided to generate a TRIB3 knockout (KO) cell line. KO cell lines are powerful tools to study disease mechanisms and investigate the relationship between genotype and phenotype. Since U-118 presented a high expression of TRIB3 protein level (Figure 4.4), we chose to KO TRIB3 in this GBM cell line. The generation of the KO cell line was done using the CRISPR-Cas9 technique. CRISPR-Cas9 is a gene editing tool adapted from the bacterial immune system. This technique uses gRNAs to direct the Cas9 enzyme to cleave a target location in the genome.

The protocol for this experiment has been followed as described in section 3.4.1. Clones were selected and validated by Western Blot using a specific antibody against TRIB3 (ab 75846, Abcam). As previously mentioned, we transfected cells with two different gRNAs against TRIB3 (#1170 and #1172) to minimalize the off-target effects. In total, we tested 16 clones obtained from gRNA

#1170 and 20 clones from gRNA #1172. Figure 4.5 shows five different clones from each gRNA that had been positively selected.

None of the clones from figure 4.5 showed a band of the expected size of TRIB3, which is around 43kDa. For the following experiments, we proceeded with clones #7 and #16 from gRNA #1170 and clones #2 and #6 from gRNA #1172 since they were the only ones that did not show additional bands.

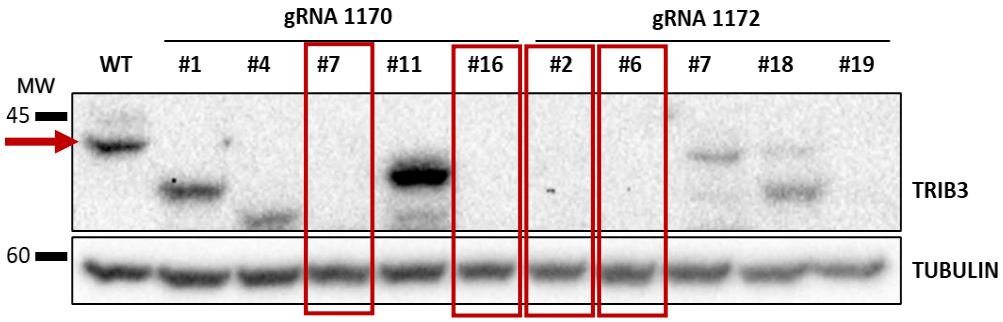

Figure 4.5 - Selection of U-118 TRIB3 KO clones.

U-118 cell line was transfected with plasmid PX459 containing gRNAs #1170 or #1172 for TRIB3 abrogation. First lane was loaded with control sample U-118 WT. The other lanes were loaded with isolated clones obtained after transfection with Lipofactamine 2000. Red arrow indicates the expected band size for TRIB3, which is around 43kDa. Red boxes highlight the selected clones for further experiments. Specific antibody against TRIB3 (ab 75846) was used. A total of 80µg of protein were loaded per well into 10% acrylamide gels. Tubulin was used as reference gene for loading control. The signal was detected by Chemidoc XRS+ System and images were treated by Image Lab 6.1 software. MW = molecular weight.

4.4. Tribbles protein profile in U-118 TRIB3 KO cell line

Considering that Tribbles family members may be functionally redundant, TRIB3 abrogation could be compensated by the other Tribbles family members. Therefore, we decided to analyze TRIB1 and TRIB2 protein levels in the U-118 TRIB3 KO clones and compare them to the U-118 parental cell line (WT).

We saw no differences in the TRIB1 expression levels between WT and the KO clones (#7, #16, #2, #6) (Figure 4.6). As for the TRIB2 protein expression, both clones from U-118 cells transfected with gRNA #1170 (#7, #16) seem to have a slight expression of TRIB2 compared with the WT.

Next, we evaluated the effect of TRIB3 depletion on FOXOs protein levels in U-118 WT and U-118 TRIB3 KO cells GBM cells. We could not detect any differences in FOXO1 expression levels. Concerning FOXO3, the KO cells seem to present a slightly increased expression of the FOXO3 protein levels, especially the clones #2 and #6 of gRNA #1172 (Figure 4.6).

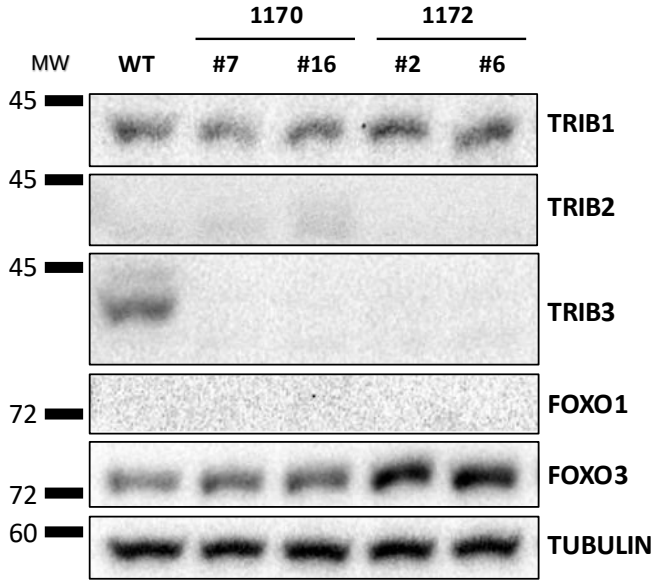

Figure 4.6 - Tribbles and FOXOs protein levels in U-118 TRIB3 KO clones.

First lane corresponds to U-118 WT and was used as control. Second and third lane were loaded with two different clones (#7, #16) transfected with gRNA 1170. Fourth and fifth lanes were loaded with two different clones transfected with gRNA 1172 (#2, #6). Protein levels were assessed with specific antibodies. A total of 80µg of protein were loaded per well in 10% acrylamide gels. Tubulin was used as reference gene for loading control. The signal was detected by Chemidoc XRS+ System (BioRad, USA) and images were treated by Image Lab 6.1 software. Figure representative from 3 experiments that had been performed. MW = molecular weight.

4.5. TRIB3 KO cells have reduced viability in the U-118 cell line

Our hypothesis is that TRIB3 has an oncogenic role in GBM and consequently, TRIB3 abrogation could have a negative impact on cell viability. Therefore, we analyzed how the abrogation of TRIB3 in the U-118 cell line could affect cell viability. To do so, we quantified the number of viable U-118 TRIB3 KO cells by crystal violet staining and compared it to the parental cell line (see section 2.5 for details). The absorbance measure of the staining is proportional to the

number of viable cells attached to the plate. Our results indicate that the two clones from gRNA #1170 (#7 and #16) and the other two clones from gRNA 1172 (#2 and #6) have significantly less viability in comparison with the WT cells (Figure 4.7). Our results show that TRIB3 abrogation decreased U-118 cell viability compared to the parental cell line that does express TRIB3. Indeed, our results agree with another published study by Tang *et al*. that shows that TRIB3 knockdown impairs cell proliferation, whereas overexpression of TRIB3 increases proliferation in GBM cell lines[222].

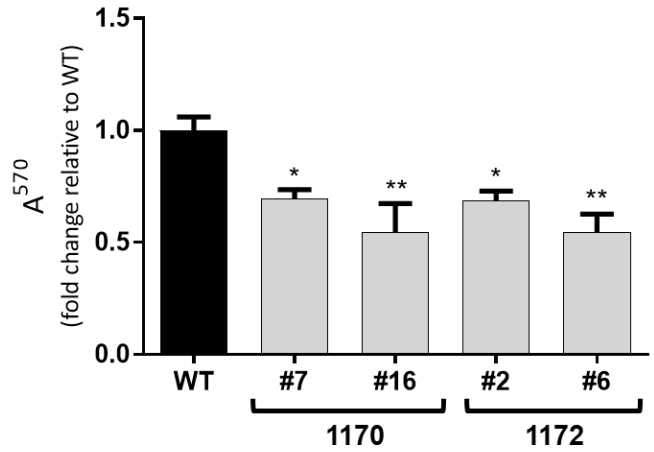

Figure 4.7 - TRIB3 reduces cell viability in U-118 cell line.

U-118 WT and TRIB3 KO clones were stained with crystal violet after 72h in culture. Absorbance was read in a wavelength of 570nm. Parental cell line was used as control (WT). All the four clones tested (#7, #16, #2 and #6) showed a statistically significant decrease in cell viability compared to WT. Statistical analysis was done using the GraphPad Prism 7.03 program. Statistical significance was determined by 1way ANOVA (Dunnett's multiple comparisons) * $p \leq 0.05$; ** $p \leq 0.01$. Data from triplicates of 2 biological replicates.

4.6. TRIB3 inhibition decreases cell proliferation but does not induce cell death in the U-118 cell line

Since the U-118 TRIB3 KO cell line showed lower cell viability than the parental cell line, we wanted to understand whether this was due to less cell proliferation or increased cell death. Therefore, we performed a Trypan Blue exclusion assay in U-118 WT and TRIB3 KO cell lines. Our results showed that all TRIB3 KO clones have a less total number of cells compared to the U-118 WT

cell line. However, only clone #2 from gRNA #1172 reached statistical significance (Figure 4.8, A).

Cell death analysis revealed that, on average, 4,88% of the U-118 parental cell line was non-viable after 72h. Regarding the isogenic TRIB3 KO clones, they varied in a range from 3,4% (in clone #7) to 6,69% (in clone #2) of non-viable cells for the same period. Except for clone #1170 #7, the three other TRIB3 KO clones tended to show a slightly increased cell death rate. However, none of the results were statistically significant, and the standard deviations were very high (Figure 4.8, B).

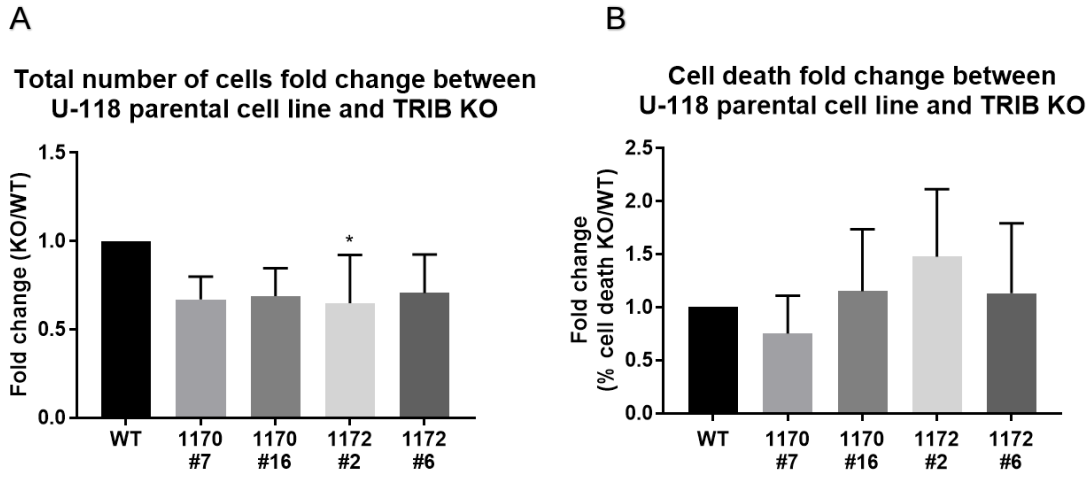

Figure 4.8 - Evaluation of cell proliferation and cell death between U-118 WT and TRIB3 KO cells.

To verify if the difference between cell viability was due to a decrease in the cell proliferation or to an increase in the cell death, we performed a Trypan Blue exclusion assay. **(A)** Total number of cells normalized by WT represented in fold change. **(B)** Percentage of cell death in total number of cells normalized by WT and represented in fold change. Statistical analysis was done using the GraphPad Prism 7.03 program. Statistical significance was determined by 1way ANOVA (Dunnett's multiple comparisons) * $p < 0.05$. N= 4 independent experiments.

Taking all the data together, these results indicate that TRIB3 inhibition decreases cell proliferation in the U-118 GBM cell line, resulting in less cell viability. It is described that down-regulation of TRIB3 can inhibit the proliferation of ovarian cancer cells[228], oral squamous carcinoma cells[195], and renal carcinoma cells[163]. In this sense, our results lead us to believe that TRIB3 may indeed

contribute to the malignant phenotype in GBM. However, it is necessary to understand how the inhibition of TRIB3 can lead to a decrease in cell proliferation.

4.7. Status of signaling pathways involved in cell proliferation in U-118 cell line upon TRIB3 abrogation

Recent studies have shown that TRIB3 is able to activate the AKT/mTOR and MAPK/ERK pathways[196,229]. These pathways are strongly associated with cell proliferation, and their activating status leads to increased cell proliferation. GBM cells often have mutations on these core pathways, as described in the introduction section. Our results showed that U-118 TRIB3 KO clones have less cell viability accompanied by a reduction in cell proliferation. Therefore, we decided to verify if the TRIB3 inhibition is associated with the modulation of AKT and MAPK pathways.

Our results show that all TRIB3 KO cells have increased levels of S6K phosphorylation. However, the quantification of these data did not show to be significant (Figure 4.9, A, C, D). Phosphorylation of AKT at serine 473 did not change depending on the TRIB3 status, indicating that TRIB3 is not able to modulate AKT activity in the U-118 cell line. Analysis of the MAPK pathway revealed that ERK1/2 phosphorylation status was clone-specific and not significant (Figure 4.9, B, D). However, including more biological replicates is necessary to increase the significance and validate our findings.

Taken together, the abrogation of TRIB3 does not appear to interfere with either the AKT or the MAPK pathway in GBM cells. However, these pathways are composed of several intermediate players that, in turn, can be regulated. Thus, it would be valuable to evaluate the status of these other proteins, such as the phosphorylation of MAPK1/2 and the phosphorylation of mTOR, to understand what is indeed happening in these signaling pathways.

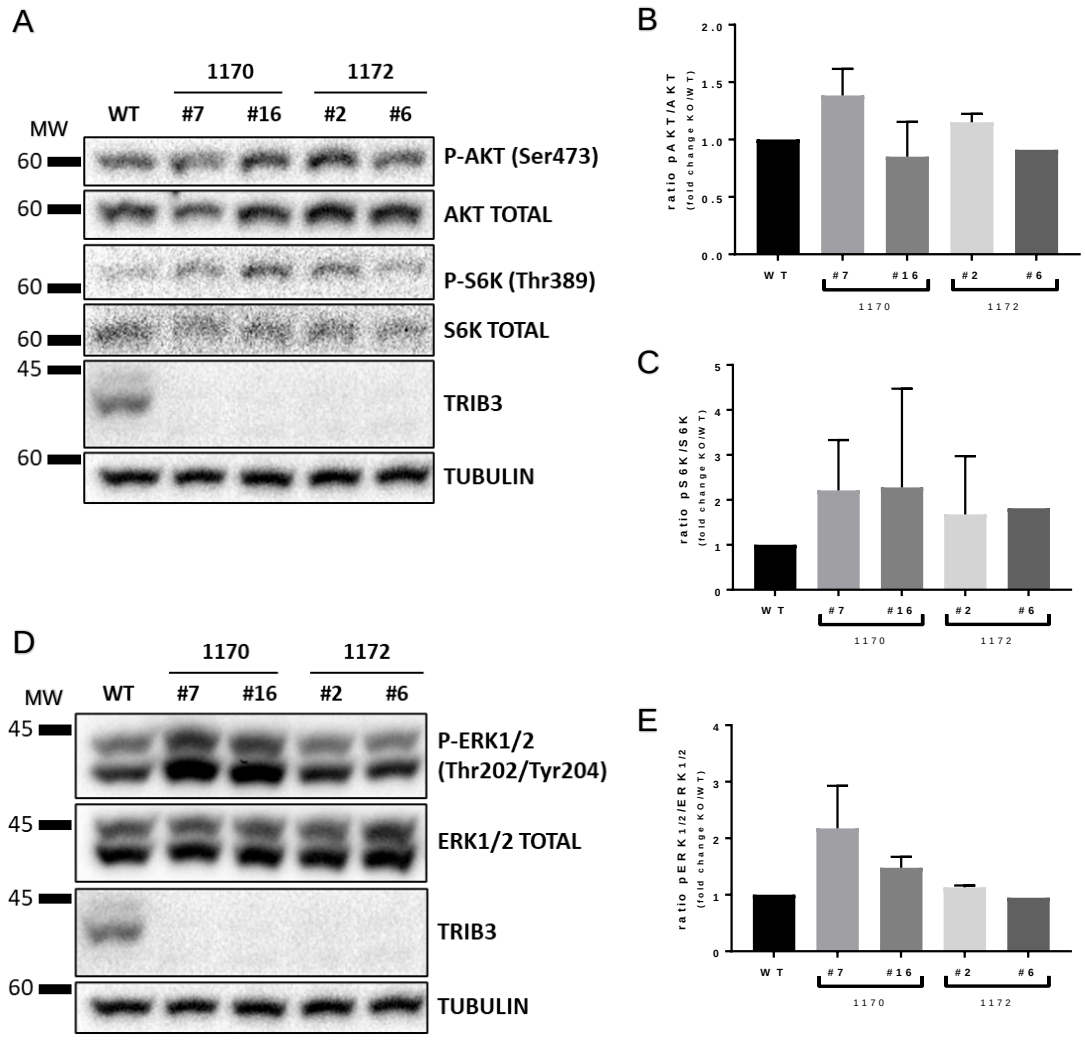

Figure 4.9 - Phosphorylation levels of key proteins from AKT and MAPK pathways in U-118 WT and TRIB3 KO cells.

Phosphorylation levels of key proteins from AKT and MAPK pathways in U-118 WT and TRIB3 KO cells. **(A)** Effect of TRIB3 KO on AKT pathway by analyzing AKT phosphorylation at serine 473 and S6K phosphorylation at threonine 398 in U-118 WT and TRIB3 KO cell line. **(B)** Quantification by densitometry of the levels of AKT phosphorylated in S473 (pAKT Ser473) and **(C)** S6K phosphorylated at threonine 389 (pS6K Thr389). The data correspond to the optical density in arbitrary units for each experimental condition normalized with respect to total AKT and the loading control (tubulin) and total S6K and loading control (tubulin), respectively. **(D)** Effect of TRIB3 KO on MAPK pathway by analyzing ERK1/2 phosphorylation at threonine 202 and tyrosine 204 in U-118 WT and TRIB3 KO cell line. **(E)** Quantification by densitometry of the levels of ERK1/2 phosphorylated in threonine 202 and tyrosine 204) (pERK1/2 Thr202/Tyr204). The data correspond to the optical density in arbitrary units for each experimental condition normalized with respect to total ERK1/2 and the loading control (tubulin). For the Western Blot, 80µg of protein were loaded per well in 10% acrylamide gels. Tubulin was used as reference gene for loading control. The signal was detected by Chemidoc XRS+ System and images were treated by Image Lab 6.1 software. Results represents two biological replicates for WT and clones #7, #16 and #2 but just one for clone #6. MW = molecular weight.

4.8. TRIB3 inhibition does not affect AKT and ERK pathways under starvation in the U-118 cell line

Metabolic stress caused by starvation triggers responses to re-establish homeostasis and maintain cellular functions. In the absence of nutrients, the cell shuts down all the processes that consume energy[230]. For example, the mTOR pathway, usually activated when cells are proliferating, is inactivated when ATP levels are low in the cell[231].

TRIB3 is known to coordinate stress-adaptative mechanisms. It is described that TRIB3 is upregulated by stress-induced transcriptional factors, such as CHOP and ATP4 [178]. Studies also showed that the induction of TRIB3 by these transcription factors could suppress AKT signaling[232]. Therefore, we hypothesized that TRIB3 inhibition could affect the PI3K/AKT/mTOR pathway more acutely under starvation-induced stress.

Basely, U-118 TRIB3 KO cells showed no significant differences in the status of the PI3K/AKT and MAPK pathways. Therefore, we re-analyzed the status of these pathways upon inducing metabolic stress. Overall, our results showed that TRIB3 expression did not have any effect on the activity of these pathways after inducing metabolic stress (Figure 4.10). We concluded that, in the U-118 cell line, AKT and ERK pathways are not modulated by TRIB3 levels.

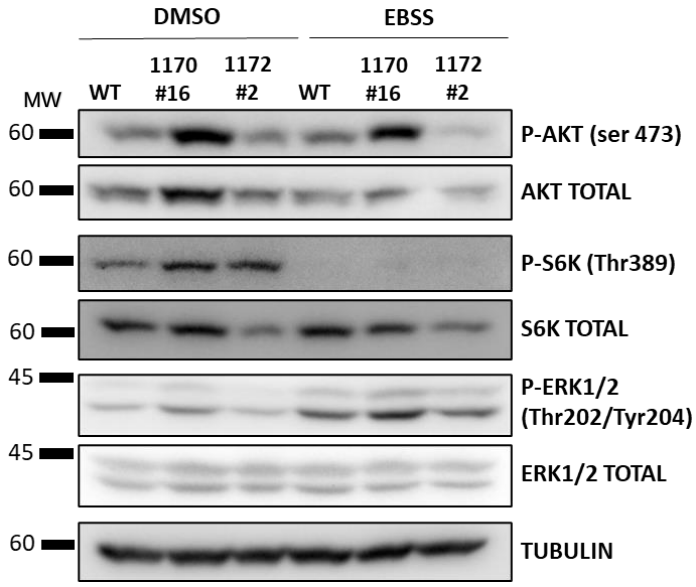

Figure 4.10 - Phosphorylation levels of key proteins from AKT and MAPK pathways in U-118 WT and TRIB3 KO cells upon starvation.

U-118 WT and TRIB3 KO cells were starved by EBSS incubation. After 6 hours, the pellet was collected for protein extraction. For the Western Blot, 80µg of protein were loaded per well in 10% acrylamide gels. Tubulin was used as reference gene for loading control. The signal was detected by Chemidoc XRS+ System and images were treated by Image Lab 6.1 software. MW = molecular weight.

4.9. U-118 cell viability and cell death upon TMZ treatment after TRIB3 inhibition

TMZ is the standard chemotherapy used for glioblastoma treatment. However, patients often recur and develop therapy resistance. To evaluate the effect of TRIB3 expression on cell resistance to TMZ, we performed proliferation assays (Trypan Blue exclusion assay) and cells' viability assays (crystal violet assay) upon TMZ treatment.

First, we exposed the U-118 parental cell to serial dilutions of TMZ concentration and performed a Crystal violet assay to assess the drug's half-maximum inhibitory concentration (IC50). The IC50 value indicates the amount of drug needed to produce half of its maximum effect. Our data show that IC50 for TMZ in the U-118 cell line is 500µM for 72h (Figure 4.11).

Studies showed that in the U-87 cell line, the most common cell line studied, the median TMZ IC50 value at 72h was 230.0 µM. However, TMZ sensitivity was inconsistent with other GBM cell lines[233]. Other reports indicate chemoresistance of U-118 cells to TMZ by escaping from TMZ-induced cell death through the PI3K/AKT and MAPK pathways[234], that together with a hypermethylated status of the MGMT promoter[235], could explain the high concentration IC50 levels that we established.

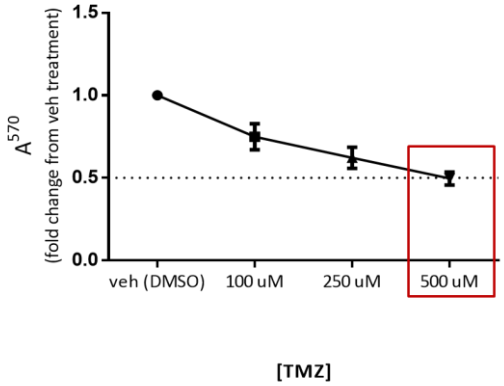

Figure 4.11 - TMZ concentration for IC50 in U-118 cell line.

10.000 cells of U-118 WT were plated in 24-wells plate. They were exposed to 100 - 500µM of TMZ. 24- and 48-hours treatments weren't effective. The figure represents the experiment after 72-hour treatment. Cells were fixed and stained with Crystal violet. The absorbance was read in the wavelength of 570nm. The results were normalized by the effect of DMSO, which is the drug vehicle. Results expressed in fold change from the vehicle treatment. Data was analyzed using GraphPad Prism 7.03 program.

4.9.1 Absence of TRIB3 expression does not alter cell sensitivity to TMZ

We hypothesized that TRIB3 has an oncogenic role in GBM. Thus, TRIB3 could be involved in the resistance of tumor cells to therapy. Therefore, inhibition of TRIB3 could result in decreased cell viability upon TMZ administration.

We analyzed the cell viability of U-118 WT and TRIB3 KO upon TMZ treatment (500µM) for 72 hours. Our results show that (1) inhibition of TRIB3 does not seem to increase the sensitivity of cells to TMZ, as the viability of TRIB3 KO cells is halved after treatment with TMZ, as well as in the control cells. However, (2) as TRIB3 inhibition under normal conditions already affects cell viability, TMZ

treatment turns out to be more effective when comparing the cell viability of TRIB3 KO cells with WT control cells (DMSO) (Figure 4.12).

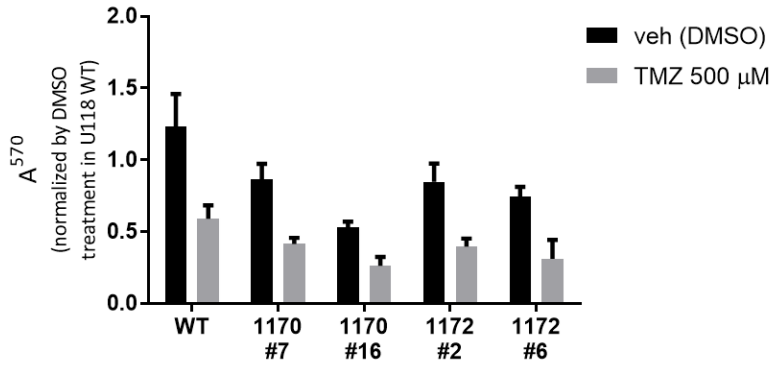

Figure 4.12 - Cell viability of U-118 TRIB3 KO cells after TMZ treatment.

U-118 TRIB3 KO cells were exposed to 500μM of TMZ for 72h. Four clones, two from each gRNA against TRIB3 were tested. Results are represented normalized from DMSO treatment, the diluent of the drug. Data was analysed using GraphPad Prism 7.03 program.

4.9.2. U-118 TRIB3 KO cell death by Trypan Blue exclusion assay upon TMZ treatment

Next, we performed a Trypan Blue exclusion assay to evaluate the contribution of TRIB3 expression on cell death induction after TMZ treatment. Overall, the absence of TRIB3 appears to induce more cell death upon TMZ treatment when compared to U-118 WT cells. However, only clone #1172 #2 showed a statistically significant increase, as shown in Figure 4.13, A. The total number of cells does not seem to vary between cells that express TRIB3 and cells that do not express TRIB3 in the presence of TMZ (Figure 4.13, B). Again, the total number of cells in the DMSO control samples is significantly higher than the total number of cells where TRIB3 has been depleted, as seen in our previous experiments (Figure 4.8, A). Therefore, the decrease in cell viability seen after TRIB3 inhibition is due to a decrease in cell proliferation of the U-118 cell line.

In summary, inhibition of TRIB3 does not significantly affect the cellular response of U-118 GBM cells after 72 hours of exposure to TMZ, the standard drug for GBM treatment. However, patients expressing low levels of TRIB3 could benefit from TMZ treatment compared to patients with high levels of TRIB3, as the decrease in TRIB3 reduces cell viability.

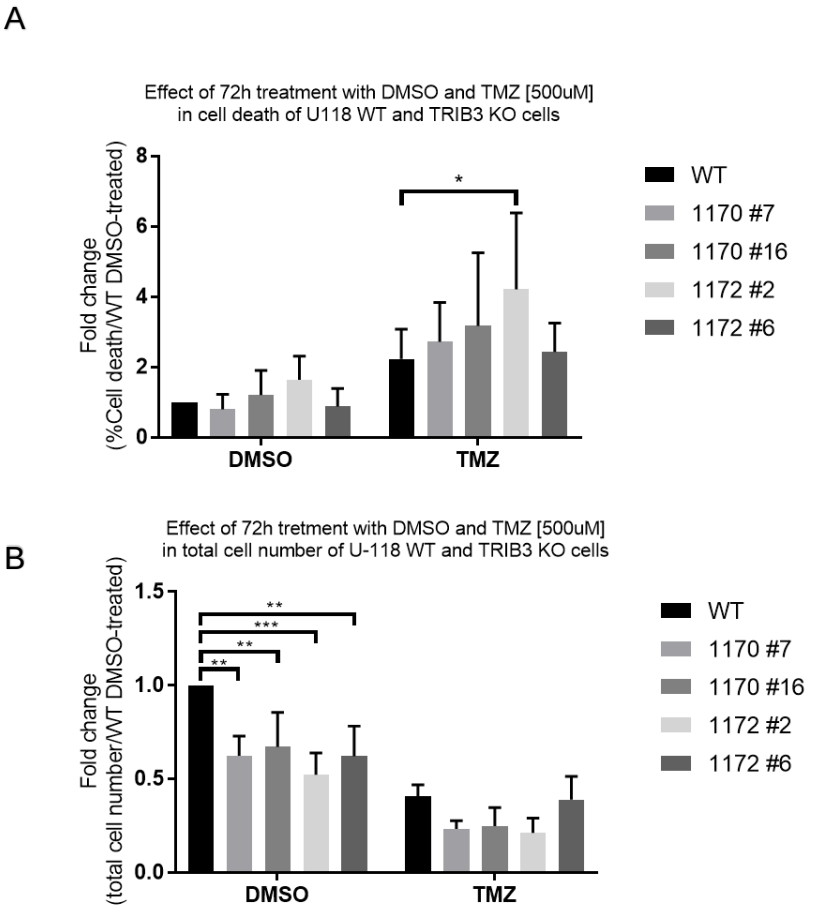

Figure 4.13 - Cell death by Trypan Blue of U-118 TRIB3 KO cells upon TMZ treatment.

Four clones from U-118 TRIB3 KO (#7, #16, #2 and #6) and U-118 WT cell line were exposed to DMSO and 500µM of TMZ. After 72-hours treatment, (A) dead cells and (B) total number of cells were counted with Trypan blue stain. Y axis shows fold change of the results from WT cells treated with DMSO. Data from 3 independent experiments was analysed with GraphPad Prism 7.03 program. Statistical significance was determined by 1way ANOVA (Dunnett's multiple comparisons) * $p \leq 0.05$; ** $p \leq 0.01$; *** $p \leq 0.001$.

4.10. Characterization of TRIB2 silencing in LN-229

This project aims to generate cell-based tools that allow us to study the role of Tribbles family members in GBM biology. So far, we have successfully generated TRIB3 KO cell lines. In the process of generating TRIB2 KO cells, we encountered technical problems that delayed the obtention of these cell lines. To overcome this problem, we have simultaneously modulated TRIB2 levels using siRNA. We used siRNA to silence TRIB2 in the LN-229 cell line, which has endogenously high expression levels of TRIB2 protein. With this approach, we were able to obtain preliminary data on the effects of TRIB2 silencing while we were generating a TRIB2 KO cell line.

TRIB2 silencing validation was done using a specific TRIB2 antibody (CST 13533. LN-229 cell line transfected with a siRNA against TRIB2 showed reduced levels of TRIB2 expression as expected (Figure 4.14). Our results showed no differences in the protein levels of FOXO3 nor AKT and ERK pathway activation (Figure 4.14). Taken together, the silencing of TRIB2 in LN-229 does not seem to affect the levels of these proteins. Moreover, TRIB2 may not be affecting the phosphorylation of AKT or MAPK pathways in the LN-229 cell line. However, this experiment was performed only once. It is necessary to have more biological replicates to verify the results obtained.

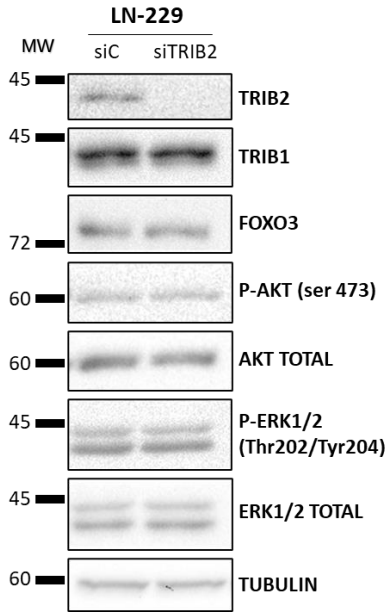

Figure 4.14 - Protein levels of siTRIB2 on LN-229 cell line.

TRIB2 protein was silenced with siRNA in L-229 cell line. The proteomic levels were assessed by Western Blot. First lane was loaded with LN-229 siCONTROL (siC) sample. The second lane was loaded with LN-229 transfected with siTRIB2. Transfection control was verified by TRIB2 specific antibody (CST 13533). The wells were loaded with 80µg of protein in 10% acrylamide gels. House-keeping gene Tubulin was used for loading control. The signal was detected by ImageQuant LAS 500 (GE Healthcare Bio-Sciences, Sweden) and images were treated by Image Lab 6.1 software. MW = molecular weight.

4.11. Generation of LN-229 TRIB2 KO cell line

Since TRIB3 modulation does not seem to have a significant impact on GBM cells, we decided to generate a TRIB2 KO cell line. To that end, we used CRISPR/Cas9 technology to generate the LN-229 TRIB2 KO cell line. It is important to note that this cell line was the cell line that showed the highest TRIB2 levels (Figure 4.4). After transfection of the CRISPRC/Cas9 plasmid to deplete TRIB2 expression, we screened for 8 clones using gRNA #1167 and 11 clones using gRNA #1169. From these, clones #1, #6, #7, #10, and #22 (from gRNA #1167), and clone #21 (from gRNA #1169) were positive for TRIB2 depletion (Figure 4.15). The parental cell line LN-229 WT was used as a control sample.

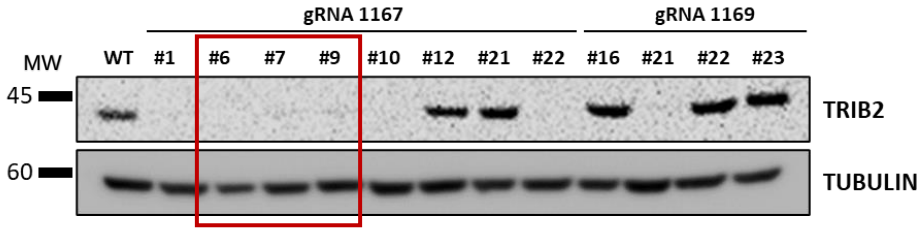

Figure 4.15 - Selection of LN-229 TRIB2 KO clones.

LN-229 cell line was transfected with plasmid PX459 containing gRNAs 1167 or 1169 for TRIB2 abrogation. First lane was loaded with control sample LN-229 WT. The other lanes were loaded with isolated clones obtained after plasmid transfection with Lipofactamine 2000. Specific antibody against TRIB2 (CST 13533) was used. Red box indicates the clones used for following experiments. A total of 80µg of protein were loaded per well in 10% acrylamide gels. Tubulin was used as reference gene for loading control. The signal was detected by ImageQuant LAS 500 and images were treated by Image Lab 6.1 software. MW = molecular weight.

4.12. LN-229 TRIB2 KO cell line protein characterization

The generation of an isogenic GBM cell line KO for TRIB2 was successfully achieved. LN-229 TRIB2 KO cell line now can be used to study the effects of TRIB2 abrogation on GBM cells.

We tested 3 clones (#6, #7, #9) that originated from the gRNA #1167 of CRISPR/Cas9 TRIB2 KO transfection to characterize them upon protein levels by Western Blot. However, this new analysis revealed that 2 of the selected clones (#7 and #9) were no longer TRIB2 KO, but showed reduced levels of TRIB2 protein compared to WT. Probably, these two clones were composed of a mosaic population, with cells that still express TRIB2 and cells TRIB KO. Due to this, after some passages, the TRIB2 expression was restored.

Despite not being the expected result for the KO experiment, cells with intermediate levels of TRIB2 offered us other tools to study the effect of TRIB2 modulation on GBM.

As described, Tribbles family members can modulate signaling pathways that regulate FOXOs protein activity. Thus, we wondered if TRIB2 modulation would affect FOXOs protein expression levels in this cell line. We saw no

differences in FOXOs expression levels between cell lines with and without TRIB2 (Figure 4.16).

Our data indicate that the reduction of TRIB2 levels may be inversely proportional to phosphorylation levels of AKT at serine 473 in the LN-229 cell line. Therefore, we would expect the activation of AKT downstream targets. However, our results also show that a reduction of at least half of TRIB2 levels is sufficient to inhibit phosphorylation of S6K in Threonine 389 (P-S6K Thr 389) in the LN-229 cell line (Figure 4.16), which indicates a downstream inhibition of the pathway. As already described, P-S6K Thr 389 is a marker for the activation status of mTORC1. Therefore, these data indicate that the reduction of TRIB2 protein levels in LN-229 is sufficient to cause mTOR shutdown.

Regarding ERK1/2 activation, our results showed no differences in the phosphorylation levels of ERK1/2 at Threonine 202 and Tyrosine 204 upon TRIB2 inhibition (Figure 4.16).

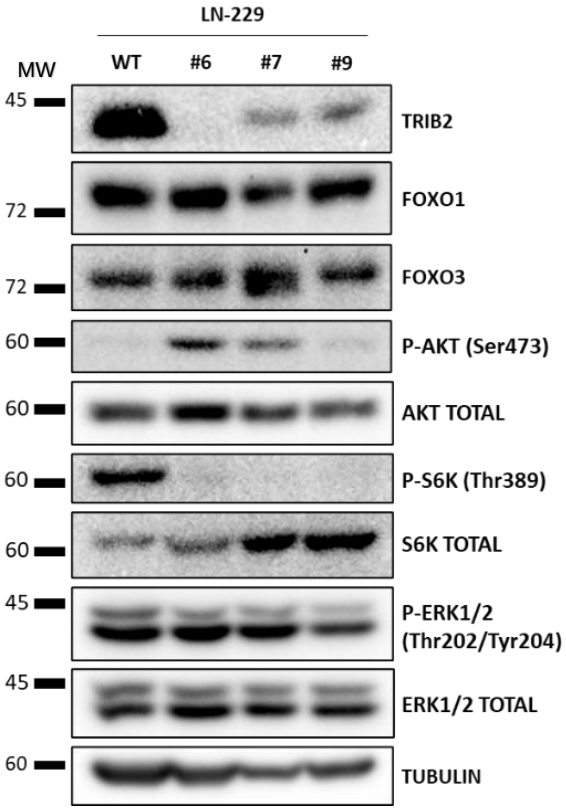

Figure 4.16 - Protein levels of LN-229 after TRIB2 modulation.

We loaded the first lane with WT for control. The other three lanes were loaded with LN-229 TRIB2 KO clones #6, #7 and #9, respectively, all from gRNA 1167. We used TRIB2 specific antibody as control for the KO transfection. It turned out that clones #7 and #9 were not KO clones, yet they present a reduction on TRIB2 levels. In this way we could analyse the effect of intermediate TRIB2 levels on the pathways studied. Tubulin was used as reference gene for loading control in 10% acrylamide gels. The signal was detected by ImageQuant LAS 500 and images were treated by Image Lab 6.1 software. MW = molecular weight.

4.13. Characterization of TRIB2 overexpression in U-87

To better understand the role of TRIB2 contribution to GBM biology, besides the generation of TRIB2 KO cells, we overexpressed TRIB2 in a GBM cell line with low levels of this protein. To do so, we selected the U-87 cell line and overexpressed TRIB2 by transfecting it with the pBABE-flag-TRIB2 construct.

We successfully generated the U-87 TRIB2 cell line (Figure 4.17). However, we did not see differences in the expression of TRIB1, FOXO3, or the

activation status of the PI3K/AKT pathway between the U-87 cells in which TRIB2 was overexpressed and the parental cell line.

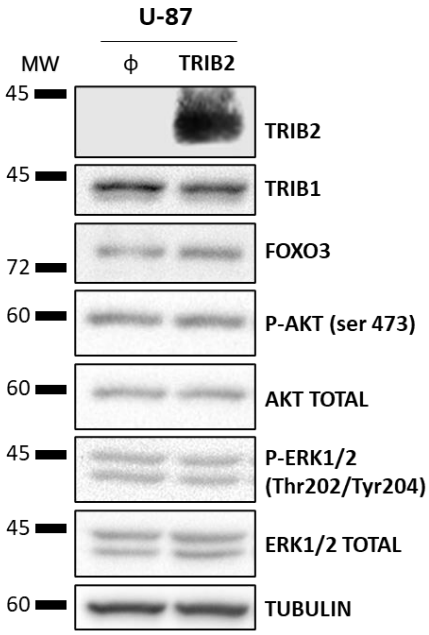

Figure 4.17 - Protein characterization after TRIB2 overexpression in U-87 cell line.

TRIB2 was overexpressed in U-87 cell line using pBABE-flag-TRIB2 vector. Protein levels were assessed by Western Blot. First lane was loaded with U-87 empty vector sample (φ). The second lane was loaded with U-87 transfected with TRIB2 plasmid. The wells were loaded with 80µg of protein in 10% acrylamide gels. Tubulin was used for loading control. The signal was detected by ImageQuant LAS 500 and images were treated by Image Lab 6.1 software. Figure representative from three biological replicates. MW = molecular weight.

5. DISCUSSION

GBMs are the most frequent and highly aggressive type of brain tumor that are difficult to treat and have a poor prognosis. Despite advances in surgical techniques and the standard therapy which includes radiation and chemotherapy, the average OS for patients with GBM is only 15 months after diagnosis[33]. Therefore, it is essential to deepen the knowledge of the genetic, molecular, and histopathological characteristics of GBM tumors to understand the biology of gliomagenesis better. In this way, we will be able to identify new prognostic biomarkers and therapeutic targets associated with these brain tumors that will contribute to advances in GBM treatment. A more accurate diagnosis that allows us to predict the probability of tumor recurrence added to more effective personalized treatments for the patient would contribute to a better outcome for GBM patients.

Tribbles family members are pseudokinases that have been shown to play a role in essential processes such as cell survival and proliferation. To do so, they can act as adapters regulating signaling pathways[138]. In this sense, it is understood that Tribbles dysregulation is associated with the progression of different types of cancer.

Although the pattern of expression and the role of each member of the Tribbles protein family depend on context and cell type, all isoforms have been described as important players in the process of tumor progression[125]. Precisely, studies have shown that high levels of TRIB2 are associated with tumor progression in melanoma[220], pancreatic cancer[236], liver cancer[133], leukemia[155], lung cancer[237], and ovarian cancer[238]. Relative to the TRIB3 homolog, high levels of expression of this protein are associated with tumorigenesis of renal carcinoma[163], oral squamous cell carcinoma[195], retinoblastoma[196], and bladder cancer[239]. However, some tumor suppressor properties were also associated with those proteins. Salomé *et al*. described that despite the oncogenic role of TRIB2 in leukemia, under stress conditions, TRIB2 deficiency contributed to growth and survival properties[215]. In the case of TRIB3, it was found that inhibition of TRIB3 increases tumorigenesis in cancer cells via FOXO inactivation[161].

In order to contribute to tumor progression, Tribbles proteins act by modulating different signaling pathways. For example, studies showed that TRIB3 could positively regulate Notch through activation of the MAPK/ERK pathway, contributing to tumor growth in breast cancer[169]. Moreover, it has been reported that the induction of oncogenic features by TRIB3 in retinoblastomas can be caused by the activation of the AKT/mTOR pathway. The study showed that TRIB3 overexpression increased AKT and mTOR phosphorylation levels. In contrast, TRIB3 knockdown decreased AKT and mTOR phosphorylation[196]. The AKT/mTOR pathway can also be regulated by TRIB2, as described in melanoma cells[159]. Studies also showed that FOXO3, a downstream target of AKT, is repressed by high levels of TRIB2 expression. In fact, this regulatory mechanism has been described as a possible inducer of resistance to cancer therapy. It has been described that high levels of TRIB2 lead to the activation of AKT, which in turn inhibits FOXO3 and P53 activity, conferring resistance to PI3K inhibitors[151]. Therefore, proteins from the Tribbles family may also be associated with treatment resistance. Taken together, these data highlight a potential prognostic biomarker value for Tribbles protein members.

Regarding the role and regulation of Tribbles protein members in GBM, the existing literature is still limited, and few studies have been published in the last decade. A preliminary analysis from the host lab indicated a relationship between the transcript expression of Tribbles family members and glioma grade, with it being higher in GBM. Considering these data and the background of the roles of Tribbles members in other cancers' contexts, we hypothesized that Tribbles proteins could contribute to tumorigenic properties in GBM development. Therefore, we proposed to study the role of Tribbles family members in GBM biology by generating cell-based tools that modulate Tribbles' expression levels.

To generate cell lines where Tribbles are differentially expressed, our first approach was to characterize a panel of five GBM cell lines according to the levels of Tribbles proteins. We proposed to create knock-out lines for Tribbles proteins. A suitable cell line should express considerable protein levels to be knocked out. Therefore, we chose to use the U-118 cell line to generate a TRIB3 knockout and the LN-229 line to generate a TRIB2 knockout, as they expressed high levels of TRIB3 and TRIB2, respectively. As none of the lines expressed

considerable levels of TRIB1, and we could not validate TRIB1 antibody, we chose not to modulate TRIB1. As stated earlier, Tribbles are capable of negatively regulating FOXOs proteins. In melanoma cells, for example, TRIB2 might induce tumorigenic properties through the abrogation of FOXO. Therefore, we also decided to verify the expression of FOXO proteins in GBM cell lines. We did not find an expression pattern that associated Tribbles with FOXOs. However, it is noteworthy that none of the lines tested showed detectable levels of FOXO4. In fact, this finding agrees with another study that described that FOXO4 expression is associated with the degree of gliomas[227]. Analyzes showed that FOXO4 expression levels were lower in GBM than in low-grade gliomas and normal tissue. Furthermore, the overexpression of FOXO4 in GBM cells promoted apoptosis and TMZ sensitivity in cancer cells, in addition to inhibiting cell migration and invasion[227]. Thus, FOXO4 may exhibit anti-tumorogenic activity in GBM.

After selecting the suitable cell lines, we used the CRISPR/Cas9 system to generate isogenic KO cell lines for TRIB3 (U-118 TRIB3 KO) and TRIB2 (LN-229 TRIB2 KO). To better understand this work, we decided to divide it into two topics, one focusing on TRIB3 and the other focusing on TRIB2.

5.1. TRIB3 inhibition

We successfully generated a U-118 TRIB3 KO clone. To minimize the off-target effect, we used two gRNAs against TRIB3. That is, clones of different gRNAs must show similar results for us to validate that the transfection affects only our gene of interest and is not binding to another gene. It has been described a similar oncogenic function between TRIB1 and TRIB2 in acute leukemia, suggesting that Tribbles members might have redundant functions[156]. To discard a possible compensation by other Tribble members after inhibiting TRIB3, we assessed the expression levels of all Tribbles homologs in the TRIB3 KO cells. Overall, our results showed that inhibition of TRIB3 does not appear to affect the other members of the Tribbles family in U-118.

As we hypothesized that TRIB3 has an oncogenic role in GBM, its inhibition should negatively affect cell viability and proliferation. The results from cell viability by crystal violet assay showed that cells with TRIB3 inhibition had a significant reduction in cell viability compared to the isogenic parental cell line. In addition, the Trypan Blue exclusion assay results demonstrated that TRIB3 inhibition reduced cell proliferation. Indeed, studies showed that TRIB3 knockdown, in addition to decreasing cell viability, also reduces colony formation, migration, and invasion of GBM cells[222]. To further assess whether the reduction in cell viability and proliferation in U-118 was due to the inhibition of TRIB3, the next step could be to reestablish the expression of TRIB3 in these cells and verify if the levels of viability and proliferation are also re-established. In this way, we could confirm that TRIB3 is indeed responsible for the modulation of cell proliferation in this cell line, possibly having an oncogenic role in GBM progression.

Studies described that the AKT signaling pathway is actively involved in the TRIB3-mediated promoting effect in retinoblastoma cells[196]. They showed that the downregulation of TRIB3 led to the inhibition of proliferation and invasiveness in retinoblastoma cells. On the other hand, TRIB3 overexpression promoted these cells' migratory and invasive capacities. Moreover, they described that the mechanism responsible for regulating TRIB3-induced proliferation occurred through the AKT/mTOR pathway induction. In other words, the downregulation of TRIB3 led to a reduction in the phosphorylation levels of AKT and mTOR, while the overexpression of TRIB3 produced the opposite effect, increasing the levels of phosphorylation of these proteins[196]. In ovarian cancer, a study described TRIB3 as a regulator of proliferation in cancer cells. Likewise, the down-regulation of TRIB3 inhibited cell proliferation. However, they observed that following the downregulation of TRIB3, the MEK and ERK phosphorylation levels were also reduced. Thus, these results indicate that TRIB3 regulates the proliferation of ovarian cancer cells through modulation of the ERK signaling pathway[228].

In this sense, we also verified the status of signaling pathways commonly associated with cell proliferation and frequently altered in GBM under baseline conditions and starvation conditions. The starvation condition causes metabolic

stress to the cell because it needs to shut down processes that consume high energy. Since TRIB3 regulates cellular metabolism and coordinates stress-adaptive mechanisms[178], we hypothesized that inhibition of TRIB3 could make cells more sensitive to the effects of starvation and have more impact on the proliferation pathways.

In terms of the AKT pathway, under baseline conditions, inhibition of TRIB3 appears to have slightly increased S6K phosphorylation. However, quantification did not show a significant difference. Under starvation, the AKT pathway did not show differences in the phosphorylation status of AKT as well. Overall, under both normal and starvation conditions, TRIB3 inhibition does not appear to significantly modulate the AKT signaling pathway in GBM cells.

The activation status of the MAPK pathway was also verified by analyzing the phosphorylation levels of ERK1/2. Under baseline conditions, the result showed increased levels of ERK1/2 phosphorylation, but it was clone-specific and not significant. Moreover, the levels of ERK1/2 phosphorylation after TRIB3 inhibition in the U-118 upon starvation did not differ. However, evaluating the activation status of intermediate proteins in these pathways, such as mTOR, a downstream target of the AKT pathway, or MAPK1/2 in the case of the MAPK pathway, could validate whether these pathways are in fact not being modulated by TRIB3 in GBM.

Overall, the results obtained in this study indicate that the reduced cell viability and proliferation caused by the inhibition of TRIB3 in the U-118 cell line is not being regulated by the PI3K/AKT or ERK1/2 pathways. To further understand the mechanisms underlying the reduction of cell proliferation after TRIB3 inhibition, it would be interesting to examine other signaling pathways involved in cell proliferation regulation. A study described that TRIB3 could interact with β-catenin and thus activate this pathway, promoting lung cancer progression[198]. Moreover, it has been described that TRIB3 increases glioma cell stemness by activating β-catenin signaling[240]. In this way, a potential candidate to verify is the Wnt signaling pathway, for example. These results would provide a more comprehensive understanding of the effects of TRIB3 inhibition on cell proliferation and could have important implications for the biology of GBM. By interacting with AKT, TRIB3 led to the inhibition of FOXO1 in breast cancer

cells[241]. Studies have described that TRIB3 can bind to AKT and thus inhibit the subsequent phosphorylation and degradation of FOXO1[241]. The accumulation of FOXO1, in turn, led to the induction of cancer stemness transcription factors. This regulation is associated with resistance mechanisms to therapy by breast cancer stem cells[241]. Taking this into account, and because resistance to therapy is one of the major reasons for GBM recurrence after therapy, we evaluated whether inhibition of TRIB3 could lead to an increased sensitivity of GBM cells upon TMZ treatment. However, our data show that inhibition of TRIB3 does not affect the GBM cells' sensitivity after 72 hours of treatment with TMZ. However, it would be interesting to evaluate other factors already described as regulators of therapy resistance in GBM, such as the MGMT promoter methylation status, after TRIB3 inhibition. As explained in the introduction, epigenetic silencing of MGMT is related to an increased sensitivity of GBM cells to TMZ[87]. A study showed that the U-118 cell line presents hypermethylation of the MGMT promoter[235]. If the MGMT methylation status is not altered by the TRIB3 inhibition, we can infer that in fact TRIB3 is not involved in the mechanism of resistance to TMZ therapy in the U-118 cell line.

Overall, the findings obtained with the results from this work confirm our hypothesis that TRIB3 has an oncogenic role in GBM progression since its inhibition decreases the proliferation and cell viability of GBM cells. However, it is necessary to study further the mechanisms that lead to this inhibition.

It is important to notice that our studies were performed with immortalized GBM cell lines. These lines grow in a monolayer and adhere to the substrate. However, cancer development depends on a set of factors involving cellular communication and the surrounding microenvironment[242]. In this sense, cell culture in spheres could provide a more reliable character regarding the expression of specific genes in the studied cell lines. In addition, genomic instability is one of the hallmarks of cancer, and therefore most primary tumors have a heterogeneous population of cells[4]. Nevertheless, immortalized lines are usually dominated by a single clone and are sometimes not representative of the original tumor from which they were isolated. In addition, after many passages and long periods of culture, these lines can also tend to a genetic drift, which

contributes to the lack of representativeness of the tumor of origin. In this sense, using primary lines would allow more reliable results from patients' samples.

5.2. TRIB2 inhibition

The generation of KO cells for TRIB2 resulted in more challenges with multiple transfections attempts and screening of a vast number of clones. We could think that the design of the gRNA used to generate the CRISPR/Cas9 could be compromised, but this construct has been successfully used in the past to generate TRIB2 KO cells in other tumor models. Alternatively, the difficulties in generating the KO line for TRIB2 may be due to altered cell repair mechanisms or copy number variation in the used cell line, LN-229. The cell viability of this cell line can also interfere with the single-cell expansion needed to develop a homogenous cell population.

In addition to generating a KO cell line for TRIB2, we also obtained cell clones with an intermediate expression of TRIB2. Initially, these intermediate-level cells showed TRIB2 inhibition. However, after a few passages, they showed some TRIB2 expression levels. Obtaining KO lines involves expanding the single-cell population to obtain clones. However, this is a technically challenging task to accomplish. Sometimes more than one clone grows in a population. The initially seen reduced TRIB2 phenotype may have been lost after a few passages of the cells due to the growth of cells that still expressed TRIB2. Despite not being the expected result for a KO experiment, these cells also showed modulation of TRIB2 levels and therefore served as a tool to study the intermediate levels of TRIB2.

Published studies have shown that high levels of TRIB2 are related to increased phosphorylation of AKT and FOXO3 in cancer cells[151]. Thus, TRIB2 can activate AKT and leads to the consequent inactivation of FOXO3, inducing tumorigenic properties. As we hypothesize that Tribbles proteins have an oncogenic role in GBM development, and agreement with other published studies, we expected that inhibition of TRIB2 would lead to decreased levels of AKT phosphorylation. However, our results showed that inhibition of TRIB2

resulted in increased AKT phosphorylation in the LN-229 cell line. Furthermore, the phosphorylation level appears to be inversely proportional to TRIB2 expression. Therefore, TRIB2 might be downregulating the AKT pathway. These findings do not relate to studies from our lab and others regarding the role of TRIB2 in tumor promotion, where high levels of TRIB2 upregulate the PI3K/AKT pathway by causing an increase in AKT phosphorylation[151,243]. However, the tumor models used referred to melanoma, breast cancer, and ovarian cancer and not GBM. Overall, this indicates that TRIB2 behaves in specific roles according to the cellular context involved.

Usually, activation of the AKT pathway results in consequent activation of mTOR. S6K phosphorylation can be a readout of mTOR phosphorylation, as it is a direct activator. However, our results showed that inhibition of TRIB2 inhibits S6K phosphorylation. More than that, only the reduction of TRIB2 levels could inhibit S6K phosphorylation. Therefore, our data indicate that the reduction of TRIB2 inhibits S6K and consequently inhibits the mTOR pathway.

Considering all these results, inhibition of TRIB2 appears to be inhibiting downstream targets of the AKT/mTOR pathway, despite inducing AKT phosphorylation. This can be explained due to other players involved in the pathway that may be mediating these proteins. To verify the pathways activation status, it would be necessary to evaluate the phosphorylation levels of intermediate proteins between AKT and S6K, such as TSC1/2, and even mTOR itself, by measuring the phosphorylation levels of Raptor. Only then could we confirm that TRIB2 inhibition shuts down the mTOR pathway.

Alteration in other regulators of the mTOR pathway could also make us better understand the results obtained. The action of negative pathway regulators, such as LKB1 and AMPKα, can activate TSC1/2 and inhibit mTOR signaling. LKB1 and AMPK function as metabolic checkpoints and are activated in the case of a lack of nutrients, for example. Therefore, LBK1/AMPK/mTOR signaling pathway connects the cellular metabolism and the energy state of the cell to processes such as cell proliferation, growth, and autophagy[244]. Thus, checking their activity after TRIB2 inhibition would also be interesting for a continuation of this work.

An essential point is that it was only possible to perform this experiment once due to lack of time. Therefore, it is necessary to obtain biological replicates that allow us to confirm these results. Moreover, it was not possible to perform other assays, such as verifying the proliferation and viability of these cells, and therefore it was not possible to attribute phenotypic changes to the differences in the expression levels of the studied pathway.

In summary, although we described that TRIB2 inhibition could modulate the AKT/mTOR pathway, with this result alone, it is not possible to confirm the hypothesis that TRIB2 has an oncogenic role in GBM progression. Thus, the oncogenic role of TRIB2 in GBM progression still needs to be explored. Despite our limitations, it is important to continue this work and further explore the potential role of TRIB2 in GBM. By improving our knowledge about the contribution of TRIB2 in GBM, we would be able to identify new therapeutic targets that would help in the development of new treatments. In conclusion, we partially confirm our hypothesis that members of the Tribbles family have an oncogenic character through the TRIB3 homolog since its inhibition resulted in the inhibition of tumorigenic properties. However, the main objective of this work was completed since we were able to modulate Tribbles levels and generate cell lines that will serve as tools to understand better the role of this family of pseudokinases in tumor progression.

6. CONCLUSIONS AND FUTURE PERSPECTIVES

We hypothesized that Tribbles family proteins have an oncogenic role in GBM, conferring tumorigenic properties on GBM cells. To study the role of Tribbles in GBM, it was necessary to modulate Tribbles' expression levels and generate stable cell lines to analyze this modulation's effect. In this sense, this work aimed to create tools to evaluate how Tribbles' modulation can affect tumorigenic properties in GBM cells.

The main objective of this work was accomplished as we were able to generate two CRISPR/Cas9 KO lines. We have successfully generated the U-118 TRIB3 KO and the LN-229 TRIB2 KO cell lines. In addition, we also obtained a line of GBM with overexpression of TRIB2.

Once we obtained our lines with modulated Tribbles levels, it was necessary to characterize them phenotypically so that we could assess the role of Tribbles in GBM. In this sense, we have partially achieved this objective. As we completed the TRIB3 KO cell line generation more quickly, we were able to assess its viability and cellular proliferation and compare them with the isogenic parental line that expresses TRIB3. We conclude that TRIB3 has oncogenic characteristics in GBM, as its inhibition led to reduced cell proliferation and viability.

We also assessed the role of Tribbles in the mechanism of resistance to TMZ treatment. In this regard, the inhibition of TRIB3 did not seem to alter the response of the cells studied compared to the parental line.

However, it would be interesting to perform future studies that evaluate the migratory capacity (through wound healing assay) and invasion (through matrigel assay), which are other properties related to tumor progression. Furthermore, since angiogenesis is a hallmark of GBM, assessing vessel formation would also be worthwhile. Finally, another hallmark of GBM is the presence of stem-like cells, and therefore the status of pluripotency markers could also be evaluated in KO cells to understand if the Tribbles family members act at this level.

We encountered some obstacles in the generation of the TRIB2 KO cell line. Still, we were able to generate the LN-229 TRIB2 cell line successfully. Despite this, the short time did not allow us to carry out assays beyond the protein characterization of this line compared to the parental LN-229 line.

Our results do not allow us to state the oncogenic role of TRIB2 in GBM cells. However, we have generated valuable tools to continue the studies on the role of TRIB2 in GBM. Again, it is interesting to evaluate phenotypic characteristics related to oncogenic properties, such as the ability of these cells to proliferate, invade and migrate.

It should be noted that the preliminary results obtained through the protein characterization of this line proved to be relevant. Only the reduction of TRIB2 could cause a shutdown of the mTOR signaling pathway, which is typically hyperactivated in the tumor context. However, further analysis is still needed to validate this result and understand how this regulation is taking place.

In summary, confirmation of the oncogenic role of the Tribbles pseudokinase family could be highly relevant in the context of GBM. Since GBM patients have a poor prognosis, unraveling the role of Tribbles in tumor progression could help identify new prognostic biomarkers for GBM patients. Moreover, the knowledge could contribute to developing targeted therapies against these proteins. In general, developing new therapeutic strategies and new druggable targets is extremely important to improve the treatment response and consequently increase the survival of patients with this still very lethal disease.

7. BIBLIOGRAPHY

1. Ritchie H. and Roser M. Causes of death. *Published online at OurWorldInData.org* https://ourworldindata.org/causes-of-death (2018).
2. Sung, H. *et al.* Global Cancer Statistics 2020: GLOBOCAN Estimates of Incidence and Mortality Worldwide for 36 Cancers in 185 Countries. *CA. Cancer J. Clin.* (2021) doi:10.3322/caac.21660.
3. Cancer Tomorrow. *International Agency for Cancer Research* https://gco.iarc.fr/tomorrow/en/dataviz/tables (2020).
4. Hanahan, D. & Weinberg, R. A. Hallmarks of Cancer: The Next Generation | Elsevier Enhanced Reader. *Cell* (2011).
5. Yokota, J. Tumor progression and metastasis. *Carcinogenesis* (2000) doi:10.1093/carcin/21.3.497.
6. Weinberg, R. A. *The Biology of Cancer: Second Edition.* (Garland Science, 2013).
7. Vogelstein, B. *et al.* Cancer genome landscapes. *Science* (2013) doi:10.1126/science.1235122.
8. Michor, F., Iwasa, Y. & Nowak, M. A. Dynamics of cancer progression. *Nature Reviews Cancer* (2004) doi:10.1038/nrc1295.
9. Perona, R. Cell signalling: Growth factors and tyrosine kinase receptors. *Clin. Transl. Oncol.* (2006) doi:10.1007/s12094-006-0162-1.
10. Sherr, C. J. & McCormick, F. The RB and p53 pathways in cancer. *Cancer Cell* (2002) doi:10.1016/S1535-6108(02)00102-2.
11. Lowe, S. W., Cepero, E. & Evan, G. Intrinsic tumour suppression. *Nature* (2004) doi:10.1038/nature03098.
12. Adams, J. M. & Cory, S. The Bcl-2 apoptotic switch in cancer development and therapy. *Oncogene* (2007) doi:10.1038/sj.onc.1210220.
13. Blasco, M. A. Telomeres and human disease: Ageing, cancer and beyond. *Nature Reviews Genetics* (2005) doi:10.1038/nrg1656.
14. Baeriswyl, V. & Christofori, G. The angiogenic switch in carcinogenesis. *Seminars in Cancer Biology* (2009) doi:10.1016/j.semcancer.2009.05.003.
15. DeBerardinis, R. J., Lum, J. J., Hatzivassiliou, G. & Thompson, C. B. The Biology of Cancer: Metabolic Reprogramming Fuels Cell Growth and Proliferation. *Cell Metabolism* (2008) doi:10.1016/j.cmet.2007.10.002.
16. Cavallaro, U. & Christofori, G. Cell adhesion and signalling by cadherins

and Ig-CAMs in cancer. *Nature Reviews Cancer* (2004) doi:10.1038/nrc1276.

17. Pagès, F. *et al.* Immune infiltration in human tumors: A prognostic factor that should not be ignored. *Oncogene* (2010) doi:10.1038/onc.2009.416.

18. Kim, R., Emi, M. & Tanabe, K. Cancer immunoediting from immune surveillance to immune escape. *Immunology* (2007) doi:10.1111/j.1365-2567.2007.02587.x.

19. Jackson, S. P. & Bartek, J. The DNA-damage response in human biology and disease. *Nature* (2009) doi:10.1038/nature08467.

20. Hanahan, D. Hallmarks of Cancer: New Dimensions. *Cancer Discovery* (2022) doi:10.1158/2159-8290.CD-21-1059.

21. Goodenberger, M. L. & Jenkins, R. B. Genetics of adult glioma. *Cancer Genetics* (2012) doi:10.1016/j.cancergen.2012.10.009.

22. Khazaei, Z. *et al.* The association between incidence and mortality of brain cancer and human development index (HDI): an ecological study. *BMC Public Health* (2020) doi:10.1186/s12889-020-09838-4.

23. Cancer Today. *International Agency for Cancer Research* https://gco.iarc.fr/today/ (2020).

24. Wilhelm, I., Molnár, J., Fazakas, C., Haskó, J. & Krizbai, I. A. Role of the blood-brain barrier in the formation of brain metastases. *International Journal of Molecular Sciences* (2013) doi:10.3390/ijms14011383.

25. Wu, S. Y. & Watabe, K. The roles of microglia/macrophages in tumor progression of brain cancer and metastatic disease. *Front. Biosci. - Landmark* (2017) doi:10.2741/4573.

26. Mo, F., Pellerino, A., Soffietti, R. & Rudà, R. Blood-brain barrier in brain tumors: Biology and clinical relevance. *International Journal of Molecular Sciences* (2021) doi:10.3390/ijms222312654.

27. Louis, D. N. *et al.* The 2021 WHO classification of tumors of the central nervous system: A summary. *Neuro. Oncol.* (2021) doi:10.1093/neuonc/noab106.

28. Louis, D. N. *et al.* The 2016 World Health Organization Classification of Tumors of the Central Nervous System: a summary. *Acta Neuropathologica* (2016) doi:10.1007/s00401-016-1545-1.

29. Vigneswaran, K., Neill, S. & Hadjipanayis, C. G. Beyond the World Health Organization grading of infiltrating gliomas: Advances in the molecular genetics of glioma classification. *Annals of Translational Medicine* (2015) doi:10.3978/j.issn.2305-5839.2015.03.57.

30. Zong, H., Verhaak, R. G. W. & Canolk, P. The cellular origin for malignant glioma and prospects for clinical advancements. *Expert Review of Molecular Diagnostics* (2012) doi:10.1586/erm.12.30.

31. Zong, H., Parada, L. F. & Baker, S. J. Cell of origin for malignant gliomas and its implication in therapeutic development. *Cold Spring Harb. Perspect. Biol.* (2015) doi:10.1101/cshperspect.a020610.

32. Ostrom, Q. T., Cioffi, G., Waite, K., Kruchko, C. & Barnholtz-Sloan, J. S. CBTRUS Statistical Report: Primary Brain and Other Central Nervous System Tumors Diagnosed in the United States in 2014-2018. *Neuro. Oncol.* (2021) doi:10.1093/neuonc/noab200.

33. Stupp, R. *et al.* Effects of radiotherapy with concomitant and adjuvant temozolomide versus radiotherapy alone on survival in glioblastoma in a randomised phase III study: 5-year analysis of the EORTC-NCIC trial. *Lancet Oncol.* (2009) doi:10.1016/S1470-2045(09)70025-7.

34. Ostrom, Q. T. *et al.* The epidemiology of glioma in adults: A state of the science review. *Neuro-Oncology* (2014) doi:10.1093/neuonc/nou087.

35. Eder, K. & Kalman, B. Molecular Heterogeneity of Glioblastoma and its Clinical Relevance. *Pathology and Oncology Research* (2014) doi:10.1007/s12253-014-9833-3.

36. Ignatova, T. N. *et al.* Human cortical glial tumors contain neural stem-like cells expressing astroglial and neuronal markers in vitro. *Glia* (2002) doi:10.1002/glia.10094.

37. Pearson, J. R. D. & Regad, T. Targeting cellular pathways in glioblastoma multiforme. *Signal Transduction and Targeted Therapy* (2017) doi:10.1038/sigtrans.2017.40.

38. McLendon, R. *et al.* Comprehensive genomic characterization defines human glioblastoma genes and core pathways. *Nature* (2008) doi:10.1038/nature07385.

39. Molina, J. R. & Adjei, A. A. The Ras/Raf/MAPK Pathway. *J. Thorac. Oncol.* (2006) doi:10.1016/s1556-0864(15)31506-9.

40. Porta, C., Paglino, C. & Mosca, A. Targeting PI3K/Akt/mTOR signaling in cancer. *Frontiers in Oncology* (2014) doi:10.3389/fonc.2014.00064.

41. Georgescu, M. M. Pten tumor suppressor network in PI3K-Akt pathway control. *Genes and Cancer* (2010) doi:10.1177/1947601911407325.

42. Nitulescu, G. M. *et al.* The Akt pathway in oncology therapy and beyond (Review). *International Journal of Oncology* (2018) doi:10.3892/ijo.2018.4597.

43. Tzivion, G., Dobson, M. & Ramakrishnan, G. FoxO transcription factors; Regulation by AKT and 14-3-3 proteins. *Biochimica et Biophysica Acta - Molecular Cell Research* (2011) doi:10.1016/j.bbamcr.2011.06.002.

44. Hatanpaa, K. J., Burma, S., Zhao, D. & Habib, A. A. Epidermal growth factor receptor in glioma: Signal transduction, neuropathology, imaging, and radioresistance1. *Neoplasia* (2010) doi:10.1593/neo.10688.

45. Verhaak, R. G. W. *et al.* Integrated Genomic Analysis Identifies Clinically Relevant Subtypes of Glioblastoma Characterized by Abnormalities in PDGFRA, IDH1, EGFR, and NF1. *Cancer Cell* (2010) doi:10.1016/j.ccr.2009.12.020.

46. Han, F. *et al.* PTEN gene mutations correlate to poor prognosis in glioma patients: A meta-analysis. *Onco. Targets. Ther.* (2016) doi:10.2147/OTT.S99942.

47. Holland, E. C. *et al.* Combined activation of Ras and Akt in neural progenitors induces glioblastoma formation in mice. *Nat. Genet.* (2000) doi:10.1038/75596.

48. Sonoda, Y. *et al.* Akt pathway activation converts anaplastic astrocytoma to glioblastoma multiforme in a human astrocyte model of glioma. *Cancer Res.* (2001).

49. Gallia, G. L. *et al.* Inhibition of Akt inhibits growth of glioblastoma and glioblastoma stem-like cells. *Mol. Cancer Ther.* (2009) doi:10.1158/1535-7163.MCT-08-0680.

50. Levine, A. J. p53, the cellular gatekeeper for growth and division. *Cell* (1997) doi:10.1016/S0092-8674(00)81871-1.

51. Wang, T. J. *et al.* Comparisons of tumor suppressor p53, p21, and p16 gene therapy effects on glioblastoma tumorigenicity in Situ. *Biochem. Biophys. Res. Commun.* (2001) doi:10.1006/bbrc.2001.5565.

52. Djuzenova, C. S. *et al.* Actin cytoskeleton organization, cell surface modification and invasion rate of 5 glioblastoma cell lines differing in PTEN and p53 status. *Exp. Cell Res.* (2015) doi:10.1016/j.yexcr.2014.08.013.

53. Van Den Heuvel, S. & Dyson, N. J. Conserved functions of the pRB and E2F families. *Nature Reviews Molecular Cell Biology* (2008) doi:10.1038/nrm2469.

54. Chkheidze, R. *et al.* Alterations in the RB Pathway With Inactivation of RB1 Characterize Glioblastomas With a Primitive Neuronal Component. *J. Neuropathol. Exp. Neurol.* (2021) doi:10.1093/jnen/nlab109.

55. Liu, W., Lv, G., Li, Y., Li, L. & Wang, B. Downregulation of CDKN2A and suppression of cyclin D1 gene expressions in malignant gliomas. *J. Exp.*

Clin. Cancer Res. (2011) doi:10.1186/1756-9966-30-76.

56. Ohgaki, H. & Kleihues, P. Genetic pathways to primary and secondary glioblastoma. *American Journal of Pathology* (2007) doi:10.2353/ajpath.2007.070011.

57. Fedøy, A. E., Yang, N., Martinez, A., Leiros, H. K. S. & Steen, I. H. Structural and Functional Properties of Isocitrate Dehydrogenase from the Psychrophilic Bacterium Desulfotalea psychrophila Reveal a Cold-active Enzyme with an Unusual High Thermal Stability. *J. Mol. Biol.* (2007) doi:10.1016/j.jmb.2007.06.040.

58. Niu, B. *et al.* Application of glutathione depletion in cancer therapy: Enhanced ROS-based therapy, ferroptosis, and chemotherapy. *Biomaterials* (2021) doi:10.1016/j.biomaterials.2021.121110.

59. Nobusawa, S., Watanabe, T., Kleihues, P. & Ohgaki, H. IDH1 mutations as molecular signature and predictive factor of secondary glioblastomas. *Clin. Cancer Res.* (2009) doi:10.1158/1078-0432.CCR-09-0715.

60. Parsons, D. W. *et al.* An integrated genomic analysis of human glioblastoma multiforme. *Science (80-.).* (2008) doi:10.1126/science.1164382.

61. Miller, J. J., Shih, H. A., Andronesi, O. C. & Cahill, D. P. Isocitrate dehydrogenase-mutant glioma: Evolving clinical and therapeutic implications. *Cancer* (2017) doi:10.1002/cncr.31039.

62. Shi, J. *et al.* An IDH1 mutation inhibits growth of glioma cells via GSH depletion and ROS generation. *Neurol. Sci.* (2014) doi:10.1007/s10072-013-1607-2.

63. Ohgaki, H. & Kleihues, P. The definition of primary and secondary glioblastoma. *Clinical Cancer Research* (2013) doi:10.1158/1078-0432.CCR-12-3002.

64. Jiao, Y. *et al.* Frequent ATRX, CIC, FUBP1 and IDH1 mutations refine the classification of malignant gliomas. *Oncotarget* (2012) doi:10.18632/oncotarget.588.

65. Kannan, K. *et al.* Whole exome sequencing identifies ATRX mutation as a key molecular determinant in lower-grade glioma. *Oncotarget* (2012) doi:10.18632/oncotarget.689.

66. Xue, Y. *et al.* The ATRX syndrome protein forms a chromatin-remodeling complex with Daxx and localizes in promyelocytic leukemia nuclear bodies. *Proc. Natl. Acad. Sci. U. S. A.* (2003) doi:10.1073/pnas.1937626100.

67. Koschmann, C., Lowenstein, P. R. & Castro, M. G. ATRX mutations and glioblastoma: Impaired DNA damage repair, alternative lengthening of

telomeres, and genetic instability. *Molecular and Cellular Oncology* (2016) doi:10.1080/23723556.2016.1167158.

68. Simińska, D. *et al.* Epidemiology of anthropometric factors in glioblastoma multiforme—literature review. *Brain Sciences* (2021) doi:10.3390/brainsci11010116.

69. Eckel-Passow, J. E. *et al.* Glioma Groups Based on 1p/19q, IDH , and TERT Promoter Mutations in Tumors . *N. Engl. J. Med.* (2015) doi:10.1056/nejmoa1407279.

70. Ohgaki, H. *et al.* Genetic pathways to glioblastoma: A population-based study. *Cancer Res.* (2004) doi:10.1158/0008-5472.CAN-04-1337.

71. Ohgaki, H. & Kleihues, P. Population-based studies on incidence, survival rates, and genetic alterations in astrocytic and oligodendroglial gliomas. *Journal of Neuropathology and Experimental Neurology* (2005) doi:10.1093/jnen/64.6.479.

72. Lam, S., Lin, Y., Zinn, P., Su, J. & Pan, I. W. Patient and treatment factors associated with survival among pediatric glioblastoma patients: A Surveillance, Epidemiology, and End Results study. *J. Clin. Neurosci.* (2018) doi:10.1016/j.jocn.2017.10.041.

73. Hecht, S. S. Tobacco carcinogens, their biomarkers and tobacco-induced cancer. *Nature Reviews Cancer* (2003) doi:10.1038/nrc1190.

74. Zheng, T., Cantor, K. P., Zhang, Y., Chiu, B. C. H. & Lynch, C. F. Risk of brain glioma not associated with cigarette smoking or use of other tobacco products in Iowa. *Cancer Epidemiol. Biomarkers Prev.* (2001).

75. Blowers, L., Preston-Martin, S. & Mack, W. J. Dietary and other lifestyle factors of women with brain gliomas in Los Angeles County (California, USA). *Cancer Causes Control* (1997) doi:10.1023/A:1018437031987.

76. Dubrow, R. *et al.* Dietary components related to N-nitroso compound formation: A prospective study of adult glioma. *Cancer Epidemiol. Biomarkers Prev.* (2010) doi:10.1158/1055-9965.EPI-10-0225.

77. Taylor, A. J. *et al.* Population-based risks of CNS tumors in survivors of childhood cancer: The British childhood cancer survivor study. *J. Clin. Oncol.* (2010) doi:10.1200/JCO.2009.27.0090.

78. Pearce, M. S. *et al.* Radiation exposure from CT scans in childhood and subsequent risk of leukaemia and brain tumours: A retrospective cohort study. *Lancet* (2012) doi:10.1016/S0140-6736(12)60815-0.

79. Santivasi, W. L. & Xia, F. Ionizing radiation-induced DNA damage, response, and repair. *Antioxidants and Redox Signaling* (2014) doi:10.1089/ars.2013.5668.

80. Olsson, A. *et al.* Survival of glioma patients in relation to mobile phone use in Denmark, Finland and Sweden. *J. Neurooncol.* (2019) doi:10.1007/s11060-018-03019-5.

81. Cardis, E. *et al.* Brain tumour risk in relation to mobile telephone use: Results of the INTERPHONE international case-control study. *Int. J. Epidemiol.* (2010) doi:10.1093/ije/dyq079.

82. Ghosh, M. *et al.* Survival and prognostic factors for glioblastoma multiforme: Retrospective single-institutional study. *Indian J. Cancer* (2017) doi:10.4103/ijc.IJC_157_17.

83. Young, R. M., Jamshidi, A., Davis, G. & Sherman, J. H. Current trends in the surgical management and treatment of adult glioblastoma. *Annals of Translational Medicine* (2015) doi:10.3978/j.issn.2305-5839.2015.05.10.

84. Server, A. *et al.* Quantitative apparent diffusion coefficients in the characterization of brain tumors and associated peritumoral edema. *Acta radiol.* (2009) doi:10.1080/02841850902933123.

85. Yamaguchi, S. *et al.* The impact of extent of resection and histological subtype on the outcome of adult patients with high-grade gliomas. *Jpn. J. Clin. Oncol.* (2012) doi:10.1093/jjco/hys016.

86. Stupp, R. *et al.* Radiotherapy plus Concomitant and Adjuvant Temozolomide for Glioblastoma. *N. Engl. J. Med.* (2005) doi:10.1056/nejmoa043330.

87. Zhang, J., F.G. Stevens, M. & D. Bradshaw, T. Temozolomide: Mechanisms of Action, Repair and Resistance. *Curr. Mol. Pharmacol.* (2012) doi:10.2174/1874-470211205010102.

88. Kaina, B., Christmann, M., Naumann, S. & Roos, W. P. MGMT: Key node in the battle against genotoxicity, carcinogenicity and apoptosis induced by alkylating agents. *DNA Repair (Amst).* (2007) doi:10.1016/j.dnarep.2007.03.008.

89. Chinot, O. L. *et al.* Correlation between O6-methylguanine-DNA methyltransferase and survival in inoperable newly diagnosed glioblastoma patients treated with neoadjuvant temozolomide. *J. Clin. Oncol.* (2007) doi:10.1200/JCO.2006.07.4807.

90. Hegi, M. E. *et al.* MGMT Gene Silencing and Benefit from Temozolomide in Glioblastoma . *N. Engl. J. Med.* (2005) doi:10.1056/nejmoa043331.

91. Villalva, C. *et al.* O6-methylguanine-methyltransferase (MGMT) promoter methylation status in glioma stem-like cells is correlated to temozolomide sensitivity under differentiation-promoting conditions. *Int. J. Mol. Sci.* (2012) doi:10.3390/ijms13066983.

92. Kuhnt, D. *et al.* Correlation of the extent of tumor volume resection and patient survival in surgery of glioblastoma multiforme with high-field intraoperative MRI guidance. *Neuro. Oncol.* (2011) doi:10.1093/neuonc/nor133.

93. Pignatti, F. *et al.* Prognostic factors for survival in adult patients with cerebral low-grade glioma. *J. Clin. Oncol.* (2002) doi:10.1200/JCO.2002.08.121.

94. Thakkar, J. P. *et al.* Epidemiologic and molecular prognostic review of glioblastoma. *Cancer Epidemiology Biomarkers and Prevention* (2014) doi:10.1158/1055-9965.EPI-14-0275.

95. Chen, W. *et al.* Optimal Therapies for Recurrent Glioblastoma: A Bayesian Network Meta-Analysis. *Front. Oncol.* (2021) doi:10.3389/fonc.2021.641878.

96. Kirson, E. D. *et al.* Disruption of Cancer Cell Replication by Alternating Electric Fields. *Cancer Res.* (2004) doi:10.1158/0008-5472.CAN-04-0083.

97. Stupp, R. *et al.* Maintenance therapy with tumor-Treating fields plus temozolomide vs temozolomide alone for glioblastoma a randomized clinical trial. *JAMA - J. Am. Med. Assoc.* (2015) doi:10.1001/jama.2015.16669.

98. Cohen, M. H., Shen, Y. L., Keegan, P. & Pazdur, R. FDA Drug Approval Summary: Bevacizumab (Avastin®) as Treatment of Recurrent Glioblastoma Multiforme. *Oncologist* (2009) doi:10.1634/theoncologist.2009-0121.

99. Salacz, M. E., Watson, K. R. & Schomas, D. A. Glioblastoma: Part I. Current state of affairs. *Missouri medicine* (2011).

100. Raizer, J. J. *et al.* A phase II trial of erlotinib in patients with recurrent malignant gliomas and nonprogressive glioblastoma multiforme postradiation therapy. *Neuro. Oncol.* (2010) doi:10.1093/neuonc/nop015.

101. Uhm, J. H. *et al.* Phase II evaluation of gefitinib in patients with newly diagnosed grade 4 astrocytoma: Mayo/north central cancer treatment group study n0074. *Int. J. Radiat. Oncol. Biol. Phys.* (2011) doi:10.1016/j.ijrobp.2010.01.070.

102. Chi, A. S. *et al.* Exploring Predictors of Response to Dacomitinib in EGFR -Amplified Recurrent Glioblastoma . *JCO Precis. Oncol.* (2020) doi:10.1200/po.19.00295.

103. Rajaratnam, V. *et al.* Glioblastoma: Pathogenesis and current status of chemotherapy and other novel treatments. *Cancers* (2020) doi:10.3390/cancers12040937.

104. Liau, L. M. *et al.* Association of Autologous Tumor Lysate-Loaded Dendritic Cell Vaccination With Extension of Survival Among Patients With Newly Diagnosed and Recurrent Glioblastoma: A Phase 3 Prospective Externally Controlled Cohort Trial. *JAMA Oncol.* (2022) doi:10.1001/jamaoncol.2022.5370.

105. Ricklefs, F. *et al.* Extracellular vesicles from high-grade glioma exchange diverse pro-oncogenic signals that maintain intratumoral heterogeneity. *Cancer Res.* (2016) doi:10.1158/0008-5472.CAN-15-3432.

106. Galli, R. *et al.* Isolation and characterization of tumorigenic, stem-like neural precursors from human glioblastoma. *Cancer Res.* (2004) doi:10.1158/0008-5472.CAN-04-1364.

107. Chen, J. *et al.* A restricted cell population propagates glioblastoma growth after chemotherapy. *Nature* (2012) doi:10.1038/nature11287.

108. Alves, A. L. V. *et al.* Role of glioblastoma stem cells in cancer therapeutic resistance: a perspective on antineoplastic agents from natural sources and chemical derivatives. *Stem Cell Research and Therapy* (2021) doi:10.1186/s13287-021-02231-x.

109. Vescovi, A. L., Galli, R. & Reynolds, B. A. Brain tumour stem cells. *Nature Reviews Cancer* (2006) doi:10.1038/nrc1889.

110. Shibue, T. & Weinberg, R. A. EMT, CSCs, and drug resistance: The mechanistic link and clinical implications. *Nature Reviews Clinical Oncology* (2017) doi:10.1038/nrclinonc.2017.44.

111. Sundar, S. J., Hsieh, J. K., Manjila, S., Lathia, J. D. & Sloan, A. The role of cancer stem cells in glioblastoma. *Neurosurg. Focus* (2014) doi:10.3171/2014.9.FOCUS14494.

112. Dongre, A. & Weinberg, R. A. New insights into the mechanisms of epithelial–mesenchymal transition and implications for cancer. *Nature Reviews Molecular Cell Biology* (2019) doi:10.1038/s41580-018-0080-4.

113. Dean, M., Fojo, T. & Bates, S. Tumour stem cells and drug resistance. *Nature Reviews Cancer* (2005) doi:10.1038/nrc1590.

114. Bleau, A. M. *et al.* PTEN/PI3K/Akt Pathway Regulates the Side Population Phenotype and ABCG2 Activity in Glioma Tumor Stem-like Cells. *Cell Stem Cell* (2009) doi:10.1016/j.stem.2009.01.007.

115. Happold, C. *et al.* Transcriptional control of O 6 -methylguanine DNA methyltransferase expression and temozolomide resistance in glioblastoma. *J. Neurochem.* (2018) doi:10.1111/jnc.14326.

116. Smiley, S. B. *et al.* Novel therapeutics and drug-delivery approaches in the modulation of glioblastoma stem cell resistance. *Ther. Deliv.* **13**, 249–273

(2022).

117. Hausmann, D. *et al.* Autonomous rhythmic activity in glioma networks drives brain tumour growth. *Nature* (2022) doi:10.1038/s41586-022-05520-4.

118. Hunter, T. The Age of Crosstalk: Phosphorylation, Ubiquitination, and Beyond. *Molecular Cell* (2007) doi:10.1016/j.molcel.2007.11.019.

119. Shaw, A. S., Kornev, A. P., Hu, J., Ahuja, L. G. & Taylor, S. S. Kinases and Pseudokinases: Lessons from RAF. *Mol. Cell. Biol.* (2014) doi:10.1128/mcb.00057-14.

120. Kung, J. E. & Jura, N. Prospects for pharmacological targeting of pseudokinases. *Nature Reviews Drug Discovery* (2019) doi:10.1038/s41573-019-0018-3.

121. Boudeau, J., Miranda-Saavedra, D., Barton, G. J. & Alessi, D. R. Emerging roles of pseudokinases. *Trends in Cell Biology* (2006) doi:10.1016/j.tcb.2006.07.003.

122. Pellicena, P. & Kuriyan, J. Protein-protein interactions in the allosteric regulation of protein kinases. *Current Opinion in Structural Biology* (2006) doi:10.1016/j.sbi.2006.10.007.

123. Zhang, X., Gureasko, J., Shen, K., Cole, P. A. & Kuriyan, J. An Allosteric Mechanism for Activation of the Kinase Domain of Epidermal Growth Factor Receptor. *Cell* (2006) doi:10.1016/j.cell.2006.05.013.

124. Murphy, J. M. *et al.* A robust methodology to subclassify pseudokinases based on their nucleotide-binding properties. *Biochem. J.* (2014) doi:10.1042/BJ20131174.

125. Zhang, H., Photiou, A., Grothey, A., Stebbing, J. & Giamas, G. The role of pseudokinases in cancer. *Cellular Signalling* (2012) doi:10.1016/j.cellsig.2012.01.017.

126. Reiterer, V., Eyers, P. A. & Farhan, H. Day of the dead: Pseudokinases and pseudophosphatases in physiology and disease. *Trends in Cell Biology* (2014) doi:10.1016/j.tcb.2014.03.008.

127. Eyers, P. A., Keeshan, K. & Kannan, N. Tribbles in the 21st Century: The Evolving Roles of Tribbles Pseudokinases in Biology and Disease. *Trends in Cell Biology* (2017) doi:10.1016/j.tcb.2016.11.002.

128. Mata, J., Curado, S., Ephrussi, A. & Rorth, P. Tribbles coordinates mitosis and morphogenesis in Drosophila by regulating string/CDC25 proteolysis. *Cell* (2000) doi:10.1016/S0092-8674(00)80861-2.

129. Cunard, R. Mammalian Tribbles Homologs at the Crossroads of

Endoplasmic Reticulum Stress and Mammalian Target of Rapamycin Pathways. *Scientifica (Cairo).* (2013) doi:10.1155/2013/750871.

130. Takasato, M. *et al.* Trb2, a mouse homolog of tribbles, is dispensable for kidney and mouse development. *Biochem. Biophys. Res. Commun.* (2008) doi:10.1016/j.bbrc.2008.06.088.

131. Hegedus, Z., Czibula, A. & Kiss-Toth, E. Tribbles: A family of kinase-like proteins with potent signalling regulatory function. *Cellular Signalling* (2007) doi:10.1016/j.cellsig.2006.06.010.

132. Jimenez, L. *et al.* Multiplexed cellular profiling identifies an organoselenium compound as an inhibitor of CRM1-mediated nuclear export. *Traffic* **23**, 587–599 (2022).

133. Wang, J. *et al.* Impaired phosphorylation and ubiquitination by p70 S6 kinase (p70S6K) and smad ubiquitination regulatory factor 1 (Smurf1) promote tribbles homolog 2 (TRIB2) stability and carcinogenic property in liver cancer. *J. Biol. Chem.* (2013) doi:10.1074/jbc.M113.503292.

134. Wennemers, M., Bussink, J., van den Beucken, T., Sweep, F. C. G. J. & Span, P. N. Regulation of TRIB3 mRNA and Protein in Breast Cancer. *PLoS One* (2012) doi:10.1371/journal.pone.0049439.

135. Macias, M. J., Wiesner, S. & Sudol, M. WW and SH3 domains, two different scaffolds to recognize proline-rich ligands. *FEBS Letters* (2002) doi:10.1016/S0014-5793(01)03290-2.

136. Modi, V. & Dunbrack, R. L. Defining a new nomenclature for the structures of active and inactive kinases. *Proc. Natl. Acad. Sci. U. S. A.* (2019) doi:10.1073/pnas.1814279116.

137. Hegedus, Z., Czibula, A. & Kiss-Toth, E. Tribbles: Novel regulators of cell function; evolutionary aspects. *Cellular and Molecular Life Sciences* (2006) doi:10.1007/s00018-006-6007-9.

138. Yokoyama, T. *et al.* Trib1 links the MEK1/ERK pathway in myeloid leukemogenesis. *Blood* (2010) doi:10.1182/blood-2009-10-246264.

139. Guan, H. *et al.* Competition between members of the tribbles pseudokinase protein family shapes their interactions with mitogen activated protein kinase pathways. *Sci. Rep.* (2016) doi:10.1038/srep32667.

140. Xu, S. *et al.* TRIB2 inhibits Wnt/β-Catenin/TCF4 signaling through its associated ubiquitin E3 ligases, β-TrCP, COP1 and Smurf1, in liver cancer cells. *FEBS Lett.* (2014) doi:10.1016/j.febslet.2014.09.042.

141. Dobens, L. L., Nauman, C., Fischer, Z. & Yao, X. Control of cell growth and proliferation by the tribbles pseudokinase: Lessons from Drosophila. *Cancers* (2021) doi:10.3390/cancers13040883.

142. Takahashi, Y., Ohoka, N., Hayashi, H. & Sato, R. TRB3 suppresses adipocyte differentiation by negatively regulating PPARγ transcriptional activity. *J. Lipid Res.* (2008) doi:10.1194/jlr.M700545-JLR200.

143. Qi, L. *et al.* TRB3 links the E3 ubiquitin ligase COF1 to lipid metabolism. *Science (80-.).* (2006) doi:10.1126/science.1123374.

144. Angyal, A. & Kiss-Toth, E. The tribbles gene family and lipoprotein metabolism. *Current Opinion in Lipidology* (2012) doi:10.1097/MOL.0b013e3283508c3b.

145. Johnston, J., Basatvat, S., Ilyas, Z., Francis, S. & Kiss-Toth, E. Tribbles in inflammation. *Biochem. Soc. Trans.* (2015) doi:10.1042/BST20150095.

146. Wei, S. C. *et al.* Tribbles 2 (Trib2) is a novel regulator of toll-like receptor 5 signaling. *Inflamm. Bowel Dis.* (2012) doi:10.1002/ibd.22883.

147. Jousse, C. *et al.* TRB3 inhibits the transcriptional activation of stress-regulated genes by a negative feedback on the ATF4 pathway. *J. Biol. Chem.* (2007) doi:10.1074/jbc.M611723200.

148. Mayoral-Varo, V., Jiménez, L. & Link, W. The critical role of trib2 in cancer and therapy resistance. *Cancers* (2021) doi:10.3390/cancers13112701.

149. Murphy, J. M. *et al.* Molecular Mechanism of CCAAT-Enhancer Binding Protein Recruitment by the TRIB1 Pseudokinase. *Structure* (2015) doi:10.1016/j.str.2015.08.017.

150. Li, K. *et al.* TRIB3 Promotes APL Progression through Stabilization of the Oncoprotein PML-RARα and Inhibition of p53-Mediated Senescence. *Cancer Cell* (2017) doi:10.1016/j.ccell.2017.04.006.

151. Hill, R. *et al.* TRIB2 confers resistance to anti-cancer therapy by activating the serine/threonine protein kinase AKT. *Nat. Commun.* (2017) doi:10.1038/ncomms14687.

152. Zareen, N., Biswas, S. C. & Greene, L. A. A feed-forward loop involving Trib3, Akt and FoxO mediates death of NGF-deprived neurons. *Cell Death Differ.* (2013) doi:10.1038/cdd.2013.128.

153. Liang, K. L., Rishi, L. & Keeshan, K. Tribbles in acute leukemia. *Blood* (2013) doi:10.1182/blood-2012-12-471300.

154. Yokoyama, T. *et al.* Identification of TRIB1 R107L gain-of-function mutation in human acute megakaryocytic leukemia. *Blood* (2012) doi:10.1182/blood-2010-12-324806.

155. Keeshan, K. *et al.* Tribbles Homolog 2 (Trib2) Inactivates C/EBPalpha and Causes Acute Myelogenous Leukemia. *Blood* (2006) doi:10.1182/blood.v108.11.776.776.

156. Dedhia, P. H. *et al.* Differential ability of Tribbles family members to promote degradation of C/EBPα and induce acute myelogenous leukemia. *Blood* (2010) doi:10.1182/blood-2009-07-229450.

157. Zhou, H. *et al.* Knockdown of TRB3 induces apoptosis in human lung adenocarcinoma cells through regulation of Notch 1 expression. *Mol. Med. Rep.* (2013) doi:10.3892/mmr.2013.1453.

158. Miyoshi, N. *et al.* Abnormal expression of TRIB3 in colorectal cancer: A novel marker for prognosis. *Br. J. Cancer* (2009) doi:10.1038/sj.bjc.6605361.

159. Zanella, F. *et al.* Human TRIB2 is a repressor of FOXO that contributes to the malignant phenotype of melanoma cells. *Oncogene* (2010) doi:10.1038/onc.2010.58.

160. Salazar, M. *et al.* TRIB3 suppresses tumorigenesis by controlling mTORC2/AKT/FOXO signaling. *Mol. Cell. Oncol.* (2015) doi:10.4161/23723556.2014.980134.

161. Salazar, M. *et al.* Loss of Tribbles pseudokinase-3 promotes Akt-driven tumorigenesis via FOXO inactivation. *Cell Death Differ.* (2015) doi:10.1038/cdd.2014.133.

162. O'Connor, C. *et al.* Trib2 expression in granulocyte-monocyte progenitors drives a highly drug resistant acute myeloid leukaemia linked to elevated Bcl2. *Oncotarget* (2018) doi:10.18632/oncotarget.24525.

163. Hong, B. *et al.* TRIB3 promotes the proliferation and invasion of renal cell carcinoma cells via activating MAPK signaling pathway. *Int. J. Biol. Sci.* (2019) doi:10.7150/ijbs.29737.

164. Dong, S. *et al.* Overexpression of TRIB3 promotes angiogenesis in human gastric cancer. *Oncol. Rep.* (2016) doi:10.3892/or.2016.5017.

165. Richmond, L. & Keeshan, K. Pseudokinases: a tribble-edged sword. *FEBS Journal* (2020) doi:10.1111/febs.15096.

166. Ord, T. & Ord, T. Mammalian Pseudokinase TRIB3 in Normal Physiology and Disease: Charting the Progress in Old and New Avenues. *Curr. Protein Pept. Sci.* (2017) doi:10.2174/1389203718666170406124547.

167. Mondal, D., Mathur, A. & Chandra, P. K. Tripping on TRIB3 at the junction of health, metabolic dysfunction and cancer. *Biochimie* (2016) doi:10.1016/j.biochi.2016.02.005.

168. Du, K., Herzig, S., Kulkarni, R. N. & Montminy, M. TRB3: A tribbles homolog that inhibits Akt/PKB activation by insulin in liver. *Science (80-.).* (2003) doi:10.1126/science.1079817.

169. Izrailit, J., Berman, H. K., Datti, A., Wrana, J. L. & Reedijk, M. High throughput kinase inhibitor screens reveal TRB3 and MAPK-ERK/TGFβ pathways as fundamental Notch regulators in breast cancer. *Proc. Natl. Acad. Sci. U. S. A.* (2013) doi:10.1073/pnas.1214014110.

170. Izrailit, J., Jaiswal, A., Zheng, W., Moran, M. F. & Reedijk, M. Cellular stress induces TRB3/USP9x-dependent Notch activation in cancer. *Oncogene* (2017) doi:10.1038/onc.2016.276.

171. Hughes, T. A. Regulation of gene expression by alternative untranslated regions. *Trends in Genetics* (2006) doi:10.1016/j.tig.2006.01.001.

172. Örd, D. & Örd, T. Characterization of human NIPK (TRB3, SKIP3) gene activation in stressful conditions. *Biochem. Biophys. Res. Commun.* (2005) doi:10.1016/j.bbrc.2005.02.149.

173. Yao, X. H. & Grégoire Nyomba, B. L. Hepatic insulin resistance induced by prenatal alcohol exposure is associated with reduced PTEN and TRB3 acetylation in adult rat offspring. *Am. J. Physiol. - Regul. Integr. Comp. Physiol.* (2008) doi:10.1152/ajpregu.00804.2007.

174. Rasmussen, T. L. *et al.* Smyd1 facilitates heart development by antagonizing oxidative and ER stress responses. *PLoS One* (2015) doi:10.1371/journal.pone.0121765.

175. Bailey, F. P. *et al.* The Tribbles 2 (TRB2) pseudokinase binds to ATP and autophosphorylates in a metal-independent manner. *Biochem. J.* (2015) doi:10.1042/BJ20141441.

176. Zhou, Y. *et al.* E3 ubiquitin ligase SIAH1 mediates ubiquitination and degradation of TRB3. *Cell. Signal.* (2008) doi:10.1016/j.cellsig.2008.01.010.

177. Ohoka, N., Sakai, S., Onozaki, K., Nakanishi, M. & Hayashi, H. Anaphase-promoting complex/cyclosome-cdh1 mediates the ubiquitination and degradation of TRB3. *Biochem. Biophys. Res. Commun.* (2010) doi:10.1016/j.bbrc.2009.12.175.

178. Schwarzer, R., Dames, S., Tondera, D., Klippel, A. & Kaufmann, J. TRB3 is a PI 3-kinase dependent indicator for nutrient starvation. *Cell. Signal.* (2006) doi:10.1016/j.cellsig.2005.08.002.

179. Bowers, A. J., Scully, S. & Boylan, J. F. SKIP3, a novel Drosophila tribbles ortholog, is overexpressed in human tumors and is regulated by hypoxia. *Oncogene* (2003) doi:10.1038/sj.onc.1206367.

180. Ohoka, N., Yoshii, S., Hattori, T., Onozaki, K. & Hayashi, H. TRB3, a novel ER stress-inducible gene, is induced via ATF4-CHOP pathway and is involved in cell death. *EMBO J.* (2005) doi:10.1038/sj.emboj.7600596.

181. Cravero, J. D. *et al.* Increased expression of the Akt/PKB inhibitor TRB3 in osteoarthritic chondrocytes inhibits insulin-like growth factor 1-mediated cell survival and proteoglycan synthesis. *Arthritis Rheum.* (2009) doi:10.1002/art.24225.

182. Humphrey, R. K. *et al.* Mixed lineage kinase-3 stabilizes and functionally cooperates with TRIBBLES-3 to compromise mitochondrial integrity in cytokine-induced death of pancreatic beta cells. *J. Biol. Chem.* (2010) doi:10.1074/jbc.M110.123786.

183. Zhang, J. *et al.* Inhibition of TRIB3 protects against neurotoxic injury induced by kainic acid in rats. *Front. Pharmacol.* (2019) doi:10.3389/fphar.2019.00585.

184. Saleem, S. & Biswas, S. C. Tribbles pseudokinase 3 induces both apoptosis and autophagy in amyloid-β-induced neuronal death. *J. Biol. Chem.* (2017) doi:10.1074/jbc.M116.744730.

185. Qu, J. *et al.* TRIB3 suppresses proliferation and invasion and promotes apoptosis of endometrial cancer cells by regulating the AKT signaling pathway. *Onco. Targets. Ther.* (2019) doi:10.2147/OTT.S189001.

186. Shang, Y. Y. *et al.* TRB3, upregulated by ox-LDL, mediates human monocyte-derived macrophage apoptosis. *FEBS J.* (2009) doi:10.1111/j.1742-4658.2009.06998.x.

187. Örd, T., Örd, D., Adler, P., Vilo, J. & Örd, T. TRIB3 enhances cell viability during glucose deprivation in HEK293-derived cells by upregulating IGFBP2, a novel nutrient deficiency survival factor. *Biochim. Biophys. Acta - Mol. Cell Res.* (2015) doi:10.1016/j.bbamcr.2015.06.006.

188. Sathyanarayana, P. *et al.* EPO receptor circuits for primary erythroblast survival. *Blood* (2008) doi:10.1182/blood-2007-10-119743.

189. Örd, T., Örd, D., Kuuse, S., Plaas, M. & Örd, T. Trib3 is regulated by IL-3 and affects bone marrow-derived mast cell survival and function. *Cell. Immunol.* (2012) doi:10.1016/j.cellimm.2012.11.011.

190. Sakai, S. *et al.* Dual mode of regulation of cell division cycle 25 a protein by TRB3. *Biol. Pharm. Bull.* (2010) doi:10.1248/bpb.33.1112.

191. Großhans, J. & Wieschaus, E. A genetic link between morphogenesis and cell division during formation of the ventral furrow in Drosophila. *Cell* (2000) doi:10.1016/S0092-8674(00)80862-4.

192. Morse, E., Selim, E. & Cunard, R. PPARα ligands cause lymphocyte depletion and cell cycle block and this is associated with augmented TRB3 and reduced Cyclin B1 expression. *Mol. Immunol.* (2009) doi:10.1016/j.molimm.2009.08.008.

193. Stefanovska, B., André, F. & Fromigué, O. Tribbles pseudokinase 3 regulation and contribution to cancer. *Cancers* (2021) doi:10.3390/cancers13081822.

194. Hua, F. *et al.* TRIB3 Interacts With β-Catenin and TCF4 to Increase Stem Cell Features of Colorectal Cancer Stem Cells and Tumorigenesis. *Gastroenterology* (2019) doi:10.1053/j.gastro.2018.10.031.

195. Shen, P., Zhang, T.-Y. & Wang, S.-Y. TRIB3 promotes oral squamous cell carcinoma cell proliferation by activating the AKT signaling pathway. *Exp. Ther. Med.* (2021) doi:10.3892/etm.2021.9744.

196. Bao, X. Y., Sun, M., Peng, T. T. & Han, D. M. TRIB3 promotes proliferation, migration, and invasion of retinoblastoma cells by activating the AKT/mTOR signaling pathway. *Cancer Biomarkers* (2021) doi:10.3233/CBM-200050.

197. Yu, J. jiao *et al.* TRIB3-EGFR interaction promotes lung cancer progression and defines a therapeutic target. *Nat. Commun.* (2020) doi:10.1038/s41467-020-17385-0.

198. Zhang, X., Zhong, N., Li, X. & Chen, M. bin. TRIB3 promotes lung cancer progression by activating β-catenin signaling. *Eur. J. Pharmacol.* (2019) doi:10.1016/j.ejphar.2019.172697.

199. Hua, F. *et al.* TRB3 interacts with SMAD3 promoting tumor cell migration and invasion. *J. Cell Sci.* (2011) doi:10.1242/jcs.082875.

200. Wennemers, M., Bussink, J., Grebenchtchikov, N., Sweep, F. C. G. J. & Span, P. N. TRIB3 protein denotes a good prognosis in breast cancer patients and is associated with hypoxia sensitivity. *Radiother. Oncol.* (2011) doi:10.1016/j.radonc.2011.05.057.

201. Liang, K. L., O'Connor, C., McCarthy, T. V. & Keeshan, K. Investigation of the role of TRIB2 in normal murine hematopoiesis. *Exp. Hematol.* (2015) doi:10.1016/j.exphem.2015.06.181.

202. Wang, J. *et al.* Combined elevation of TRIB2 and MAP3K1 indicates poor prognosis and chemoresistance to temozolomide in glioblastoma. *CNS Neurosci. Ther.* (2020) doi:10.1111/cns.13197.

203. Yokoyama, T. & Nakamura, T. Tribbles in disease: Signaling pathways important for cellular function and neoplastic transformation. *Cancer Science* (2011) doi:10.1111/j.1349-7006.2011.01914.x.

204. Foulkes, D. M. *et al.* Covalent inhibitors of EGFR family protein kinases induce degradation of human Tribbles 2 (TRIB2) pseudokinase in cancer cells. *Sci. Signal.* (2018) doi:10.1126/scisignal.aat7951.

205. Rishi, L. *et al.* Regulation of Trib2 by an E2F1-C/EBPα feedback loop in

AML cell proliferation. *Blood* (2014) doi:10.1182/blood-2013-07-511683.

206. Zhang, C. *et al.* miR-511 and miR-1297 Inhibit Human Lung Adenocarcinoma Cell Proliferation by Targeting Oncogene TRIB2. *PLoS One* (2012) doi:10.1371/journal.pone.0046090.

207. Liang, K. L. *et al.* Human TRIB2 oscillates during the cell cycle and promotes ubiquitination and degradation of CDC25C. *Int. J. Mol. Sci.* (2016) doi:10.3390/ijms17091378.

208. Fang, Y. *et al.* Tribbles homolog 2 (Trib2), a pseudo serine/threonine kinase in tumorigenesis and stem cell fate decisions. *Cell Communication and Signaling* (2021) doi:10.1186/s12964-021-00725-y.

209. Do, E. K. *et al.* Trib2 regulates the pluripotency of embryonic stem cells and enhances reprogramming efficiency. *Exp. Mol. Med.* (2017) doi:10.1038/emm.2017.191.

210. Andersen, M. O. *et al.* SiRNA nanoparticle functionalization of nanostructured scaffolds enables controlled multilineage differentiation of stem cells. *Mol. Ther.* (2010) doi:10.1038/mt.2010.166.

211. Naiki, T., Saijou, E., Miyaoka, Y., Sekine, K. & Miyajima, A. TRB2, a mouse tribbles ortholog, suppresses adipocyte differentiation by inhibiting AKT and C/EBP. *J. Biol. Chem.* (2007) doi:10.1074/jbc.M701409200.

212. Salomé, M., Hopcroft, L. & Keeshan, K. Inverse and correlative relationships between TRIBBLES genes indicate non-redundant functions during normal and malignant hemopoiesis. *Exp. Hematol.* (2018) doi:10.1016/j.exphem.2018.07.005.

213. Warma, A., Lussier, J. G. & Ndiaye, K. Tribbles pseudokinase 2 (Trib2) regulates expression of binding partners in bovine granulosa cells. *Int. J. Mol. Sci.* (2021) doi:10.3390/ijms22041533.

214. Basatvat, S., Carter, D. A. L., Kiss-Toth, E. & Fazeli, A. Tribbles role in reproduction. *Biochem. Soc. Trans.* (2015) doi:10.1042/BST20150121.

215. Salomé, M. *et al.* A Trib2-p38 axis controls myeloid leukaemia cell cycle and stress response signalling. *Cell Death Dis.* (2018) doi:10.1038/s41419-018-0467-3.

216. Keeshan, K. *et al.* Transformation by Tribbles homolog 2 (Trib2) requires both the Trib2 kinase domain and COP1 binding. *Blood* (2010) doi:10.1182/blood-2009-10-247361.

217. Hou, Z. *et al.* TRIB2 functions as novel oncogene in colorectal cancer by blocking cellular senescence through AP4/p21 signaling. *Mol. Cancer* (2018) doi:10.1186/s12943-018-0922-x.

218. Xiang, D. *et al.* Tribbles homolog 2 promotes hepatic fibrosis and hepatocarcinogenesis through phosphatase 1A-Mediated stabilization of yes-associated protein. *Liver Int.* (2021) doi:10.1111/liv.14782.

219. Wang, J. *et al.* TRIB2 acts downstream of Wnt/TCF in liver cancer cells to regulate YAP and C/EBPα function. *Mol. Cell* (2013) doi:10.1016/j.molcel.2013.05.013.

220. Hill, R. *et al.* Trib2 as a biomarker for diagnosis and progression of melanoma. *Carcinogenesis* (2014) doi:10.1093/carcin/bgv002.

221. Machado, S. *et al.* Harmine and piperlongumine revert TRIB2-mediated drug resistance. *Cancers (Basel).* (2020) doi:10.3390/cancers12123689.

222. Tang, Z. *et al.* TRIB3 facilitates glioblastoma progression via restraining autophagy. *Aging (Albany. NY).* (2020) doi:10.18632/aging.103969.

223. Tang, B. *et al.* Inhibition of tribbles protein-1 attenuates radioresistance in human glioma cells. *Sci. Rep.* (2015) doi:10.1038/srep15961.

224. Xiang, C. xiang *et al.* Identification of a glioma functional network from gene fitness data using machine learning. *J. Cell. Mol. Med.* (2022) doi:10.1111/jcmm.17182.

225. Best, B. P. Cryoprotectant Toxicity: Facts, Issues, and Questions. *Rejuvenation Res.* (2015) doi:10.1089/rej.2014.1656.

226. Buccitelli, C. & Selbach, M. mRNAs, proteins and the emerging principles of gene expression control. *Nature Reviews Genetics* (2020) doi:10.1038/s41576-020-0258-4.

227. Qi, M. *et al.* FOXO4 expression associates with glioblastoma development and FOXO4 expression inhibits cell malignant phenotypes in vitro and in vivo. *Life Sci.* (2020) doi:10.1016/j.lfs.2020.117436.

228. Wang, S. *et al.* Down-regulation of TRIB3 inhibits the progression of ovarian cancer via MEK/ERK signaling pathway. *Cancer Cell Int.* (2020) doi:10.1186/s12935-020-01509-z.

229. Wang, R.-Q. *et al.* Tribbles pseudokinase 3 (TRIB3) contributes to the progression of hepatocellular carcinoma by activating the mitogen-activated protein kinase pathway. *Ann. Transl. Med.* (2021) doi:10.21037/atm-21-2820.

230. Guo, J. Y. & White, E. Autophagy, metabolism, and cancer. *Cold Spring Harb. Symp. Quant. Biol.* (2016) doi:10.1101/sqb.2016.81.030981.

231. Leprivier, G. & Rotblat, B. How does mTOR sense glucose starvation? AMPK is the usual suspect. *Cell Death Discov.* (2020) doi:10.1038/s41420-020-0260-9.

232. Nicoletti-Carvalho, J. E. *et al.* UPR-mediated TRIB3 expression correlates with reduced AKT phosphorylation and inability of interleukin 6 to overcome palmitate-induced apoptosis in RINm5F cells. *J. Endocrinol.* (2010) doi:10.1677/JOE-09-0356.

233. Poon, M. T. C., Bruce, M., Simpson, J. E., Hannan, C. J. & Brennan, P. M. Temozolomide sensitivity of malignant glioma cell lines – a systematic review assessing consistencies between in vitro studies. *BMC Cancer* (2021) doi:10.1186/s12885-021-08972-5.

234. Carmo, A., Carvalheiro, H., Crespo, I., Nunes, I. & Lopes, M. C. Effect of temozolomide on the U-118 glioma cell line. *Oncol. Lett.* (2011) doi:10.3892/ol.2011.406.

235. Lorente, A. *et al.* Detection of methylation in promoter sequences by melting curve analysis-based semiquantitative real time PCR. *BMC Cancer* (2008) doi:10.1186/1471-2407-8-61.

236. Wei, G., Lu, T., Shen, J. & Wang, J. LncRNA ZEB1-AS1 promotes pancreatic cancer progression by regulating miR-505-3p/TRIB2 axis. *Biochem. Biophys. Res. Commun.* (2020) doi:10.1016/j.bbrc.2020.05.105.

237. Grandinetti, K. B. *et al.* Overexpression of TRIB2 in human lung cancers contributes to tumorigenesis through downregulation of C/EBPα. *Oncogene* (2011) doi:10.1038/onc.2011.57.

238. Kritsch, D. *et al.* Tribbles 2 mediates cisplatin sensitivity and DNA damage response in epithelial ovarian cancer. *Int. J. Cancer* (2017) doi:10.1002/ijc.30860.

239. Yang, J. *et al.* TRIB3 Promotes the Malignant Progression of Bladder Cancer: An Integrated Analysis of Bioinformatics and in vitro Experiments. *Front. Genet.* (2021) doi:10.3389/fgene.2021.649208.

240. Lu, Y. *et al.* TRIB3 confers glioma cell stemness via interacting with β-catenin. *Environ. Toxicol.* (2020) doi:10.1002/tox.22905.

241. Yu, J. mei *et al.* TRIB3 supports breast cancer stemness by suppressing FOXO1 degradation and enhancing SOX2 transcription. *Nat. Commun.* (2019) doi:10.1038/s41467-019-13700-6.

242. Baghban, R. *et al.* Tumor microenvironment complexity and therapeutic implications at a glance. *Cell Communication and Signaling* (2020) doi:10.1186/s12964-020-0530-4.

243. Kim, D. K. *et al.* TRIB2 stimulates cancer stem-like properties through activating the AKT-GSK3β-β-catenin signaling axis. *Mol. Cells* (2021) doi:10.14348/molcells.2021.0030.

244. Shackelford, D. B. & Shaw, R. J. The LKB1-AMPK pathway: Metabolism

and growth control in tumour suppression. *Nature Reviews Cancer* (2009) doi:10.1038/nrc2676.

APPENDIX

ANNEX I

Protocol for purification of RNA from animal and plant cells

This protocol describes how to purify one sample of total RNA on one column using the PureLink™ RNA Mini Kit. For detailed instructions see the PureLink™ RNA Mini Kit User Guide at thermofisher.com or contact Technical Support.

Important guidelines

- For samples with more than >1 mg of total RNA, divide the sample into aliquots containing <1 mg of total RNA for each Spin Cartridge used.
- Use proper RNA handling techniques when working with RNA.
- When purifying total RNA from fresh samples, keep fresh cell and tissue samples on ice immediately after harvesting and quickly proceed to homogenization step.

Recommended homogenization method

Cells/sample	Homogenizer type
≤5×10^6	Homogenizer, or syringe and needle, or rotor-stator homogenizer
5×10^6– 5×10^7	Rotor-stator homogenizer

Step		Action		
		Suspension cells	Monolayer cells	Frozen cell pellet
1	**Harvest cells**	a. Transfer cells to an RNase-free tube and centrifuge at 2,000 × g for 5 min at 4°C. Discard growth medium. b. Add the appropriate volume of Lysis Buffer with 2-mercaptoethanol to your sample (see **Prepare fresh Lysis Buffer**). c. Vortex at high speed until the cell pellet is completely dispersed and the cells appear lysed.	a. Remove the growth medium from the cells. b. Add the appropriate volume of Lysis Buffer with 2-mercaptoethanol to your sample (see **Prepare fresh Lysis Buffer**).	a. Place the frozen cell pellet into an appropriately sized RNase-free tube. b. Add the appropriate volume of Lysis Buffer with 2-mercaptoethanol to your sample (see **Prepare fresh Lysis Buffer**). c. Vortex at high speed until the cell pellet is completely dispersed and the cells appear lysed.
2	**Homogenize cells**	a. Perform one of the following homogenization options at room temperature (see **Recommended homogenization method**): • Transfer the lysate to a Homogenizer inserted in a Collection Tube and centrifuge at 12,000 × *g* for 2 min. • Transfer the lysate to a 1.5-mL tube and pass 5–10 times through an 18- to 21-gauge needle attached to a syringe. • Transfer the lysate to an appropriately RNase-free tube and homogenize using a rotor-stator homogenizer at maximum speed for >45 sec. Centrifuge the homogenate at ~2,600 × *g* for 5 min, then transfer the supernatant to a clean RNase-free tube.		
3	**Bind RNA**	a. Add 1.5 volumes of 100% ethanol and cell lysate to an appropriately sized RNase-free tube. b. Vortex to mix thoroughly and to disperse any visible precipitate that may form after adding ethanol. c. Transfer up to 700 µL of the sample (including any remaining precipitate) to the Spin Cartridge (with the Collection Tube). d. Centrifuge at 12,000 × *g* for 15 seconds at room temperature. Discard the flow-through, and reinsert the Spin Cartridge into the same Collection Tube. e. Repeat Steps c–d until the entire sample has been processed.		
4	**Wash RNA**	**No DNase treatment** a. Add 700 µL Wash Buffer I to the Spin Cartridge. b. Centrifuge at 12,000 × g for 15 sec at room temperature. c. Discard the flow-through and the Collection Tube. Place the Spin Cartridge into a new Collection Tube. d. Add 500 µL Wash Buffer II with ethanol to the Spin Cartridge. e. Centrifuge at 12,000 × g for 15 sec at room temperature. f. Discard the flow-through and reinsert the Spin Cartridge in the same Collection Tube. g. Repeat steps d–f one more time.	**On-column DNase treatment** a. Add 350 µL Wash Buffer I to the Spin Cartridge. b. Centrifuge at 12,000 × g for 15 sec at room temperature. c. Discard the flow-through and the Collection Tube. Place the Spin Cartridge into a new Collection Tube. d. Add 80 µL PureLink™ DNase Mixture onto the surface of the Spin Cartridge membrane. e. Incubate at room temperature for 15 min. f. Add 350 µL Wash Buffer I to the Spin Cartridge. g. Centrifuge at ~2,600 × *g* for 5 min at room temperature. h. Discard the flow-through and the Collection Tube. Place the Spin Cartridge into a new Collection Tube. i. Add 500 µL Wash Buffer II with ethanol to the Spin Cartridge. j. Centrifuge at 12,000 × g for 15 sec at room temperature. k. Discard the flow-through and reinsert the Spin Cartridge in the same Collection Tube. l. Repeat steps i–k one more time.
5	**Elute RNA**	a. Centrifuge the Spin Cartridge with Collection Tube at 12,000 × *g* for 1 min at room temperature. b. Discard the Collection Tube and insert the Spin Cartridge into a Recovery Tube. c. Add 30 µL to 3 × 100 µL RNase-Free Water to the center of the Spin Cartridge. d. Incubate at room temperature for 1 min. e. Centrifuge at 12,000 × g for 2 min at room temperature. Note: Collect all eluates into the same tube when performing serial elution.		
6	**Analyze RNA yield and quality**	Determine the quantity and quality of the purified total RNA using any of the following techniques (See the PureLink™ RNA Mini Kit User Guide for details). • UV absorbance at 260 nm • Fluorescence microplate reader with Quant-iT™ RiboGreen™ RNA Assay Kit		
7	**Store RNA**	• Keep purified RNA on ice if using the RNA within a few hours of isolation. • Store purified RNA at –80°C or long-term storage.		

ANNEX II

nzytech
genes & enzymes

NZY First-Strand cDNA Synthesis Kit

Catalogue number: MB12501, 50 reactions
MB12502, 250 reactions

Features

- Provides high yields of full-length cDNA products for use in RT-qPCR and two-step RT-PCR assays
- Formulated to increase sensitivity in RT-qPCR
- Primer type: oligo(dT)$_{18}$ and random hexamers
- Starting material: 1 ng to 5 µg of total RNA
- Optimal reaction temperature: 50 °C
- Convenient and reliable

Description

The NZY First-Strand cDNA Synthesis Kit is a system that includes all the necessary components to synthesize first-strand cDNA, except template RNA.

The resulting single-stranded cDNA is suitable for use in real-time quantitative Reverse Transcription PCR (RT-qPCR). NZY First-Strand cDNA Synthesis Kit is formulated to provide high yields of full-length cDNA products and to increase sensitivity in RT-qPCR.

Starting material can range from 1 ng up to 5 µg of total RNA. The kit includes a combination of random hexamers and oligo(dT)$_{18}$ primers in order to increase sensitivity. The primers are included in the NZYRT 2× Master Mix, which also contains dNTPs, $MgCl_2$ and an optimized RT buffer. NZYRT Enzyme Mix includes both the NZY Reverse Transcriptase (RNase H minus) and the NZY Ribonuclease Inhibitor in order to protect RNA against degradation due to ribonuclease contamination. RNase H (from *E. coli*) is provided in a separate tube to specifically degrade the RNA template in cDNA:RNA hybrids after the first-strand cDNA synthesis. This procedure will improve the sensitivity of subsequent RT-qPCR reaction since PCR primers will bind more easily to the cDNA.

Shipping conditions

NZY First-Strand cDNA Synthesis Kit is shipped on dry ice.

Storage conditions

Store all kit components at -20 °C in a freezer without defrost cycles. Stability can be extended by storing it at -80 °C. The kit is stable for up to 3 years.

System Components

Component	MB12501 (50 reactions)	MB12502 (250 reactions)
NZYRT Enzyme Mix (1)	100 µL	5 × 100 µL
NZYRT 2× Master Mix (2)	500 µL	5 × 500 µL
NZY RNase H (*E. coli*)	50 µL	5 × 50 µL
DEPC-treated H_2O	1 mL	2 × 1 mL

(1) Includes NZY Reverse Transcriptase and NZY Ribonuclease Inhibitor
(2) Includes oligo(dT)$_{18}$, random hexamers, $MgCl_2$ and dNTPs

Protocol for first-strand cDNA synthesis

1. On ice, add the following reaction components into a sterile, nuclease-free microcentrifuge tube (for multiple reactions, a master mix without RNA may be prepared):

NZYRT 2× Master Mix	10 µL
NZYRT Enzyme Mix	2 µL
RNA (up to 5 µg)	× µL
DEPC-treated H_2O	up to 20 µL

2. Mix gently and incubate at 25 °C for 10 min.

3. Incubate at 50 °C for 30 min.

4. Inactivate the reaction by heating at 85 °C for 5 min, and then chill on ice.

5. Add 1 µL of NZY RNase H (*E. coli*) and incubate at 37 °C for 20 min.

6. Use the cDNA product directly in PCR or qPCR diluted in TE buffer or undiluted; or store at -20 °C until required.

Important notes

- High quality intact RNA, free of residual genomic DNA and RNases is essential for full-length, high quality cDNA synthesis and accurate RNA quantification. For this reason, special precautions should be taken when working with RNA:
  - Aseptic conditions should be maintained: always wear gloves; change gloves whenever you suspect

ANNEX III

BIO-RAD

iTaq™ Universal SYBR® Green Supermix

Catalog #	Supermix Volume	Kit Size
172-5120	2 ml (2 x 1 ml vials)	200 x 20 µl reactions
172-5121	5 ml (5 x 1 ml vials)	500 x 20 µl reactions
172-5122	10 ml (10 x 1 ml vials)	1,000 x 20 µl reactions
172-5124	25 ml (5 x 5 ml vials)	2,500 x 20 µl reactions
172-5125	50 ml (10 x 5 ml vials)	5,000 x 20 µl reactions

For research purposes only.

Storage and Stability
Guaranteed for 12 months in a constant temperature freezer at –20°C protected from light. For convenience, this supermix can be stored at 4°C short-term or refrozen up to ten times.

Kit Contents
iTaq™ Universal SYBR® Green supermix is a 2x concentrated, ready-to-use reaction master mix optimized for dye-based quantitative PCR (qPCR) on any real-time PCR instrument (ROX-independent and ROX-dependent). It contains antibody-mediated hot-start iTaq DNA polymerase, dNTPs, $MgCl_2$, SYBR® Green I dye, enhancers, stabilizers, and a blend of passive reference dyes (including ROX and fluorescein).

Instrument Compatibility
This supermix is compatible with all Bio-Rad and ROX-dependent Applied Biosystems real-time PCR instruments, and with the Roche LightCycler LC480, QIAGEN Rotor-Gene Q, Eppendorf Mastercycler EP realplex, and Stratagene Mx real-time PCR systems.

Reaction Mix Preparation and Thermal Cycling Protocol

1. Thaw iTaq™ Universal SYBR® Green supermix and other frozen reaction components to room temperature. Mix thoroughly, centrifuge briefly to collect solutions at the bottom of tubes, and then store on ice protected from light.

2. Prepare (on ice or at room temperature) enough assay master mix for all reactions by adding all required components except the DNA template according to the following recommendations (Table 1).

Table 1. Reaction Setup*

Component	Volume per 20 µl Reaction	Volume per 10 µl Reaction	Final Concentration
iTaq™ Universal SYBR® Green supermix (2x)	10 µl	5 µl	1x
Forward and reverse primers	Variable	Variable	300–500 nM each
DNA template	Variable	Variable	cDNA: 100 ng–100 fg Genomic DNA: 50 ng–5 pg
H_2O	Variable	Variable	—
Total reaction mix volume	*20 µl*	*10 µl*	—

* Scale all components proportionally according to sample number and reaction volumes.

3. Mix the assay master mix thoroughly to ensure homogeneity and dispense equal aliquots into each qPCR tube or into the wells of a qPCR plate. Good pipetting practice must be employed to ensure assay precision and accuracy.

4. Add DNA samples (and DNase-free H_2O if needed) to the PCR tubes or wells containing assay master mix (Table 1), seal tubes or wells with flat caps or optically transparent film, and vortex 30 seconds or more to ensure thorough mixing of the reaction components. Spin the tubes or plate to remove any air bubbles and collect the reaction mixture in the vessel bottom.

5. Program thermal cycling protocol on the real-time PCR instrument according to Table 2.

6. Load the PCR tubes or plate onto the real-time PCR instrument and start the PCR run.

7. Perform data analysis according to the instrument-specific instructions.

Table 2. Thermal Cycling Protocol

Real-Time PCR System	Setting / Mode	Polymerase Activation & DNA Denaturation at 95°C	Amplification			Melt-Curve Analysis
			Denaturation at 95°C	Annealing /Extension + Plate Read at 60°C	Cycles	
Bio-Rad® CFX96™, CFX384™ CFX96 Touch™, CFX384 Touch™, CFX Connect™ systems	SYBR® only	20–30 sec for cDNA or 2–5 min for gDNA	2–5 sec	15–30 sec	35–40	65°C–95°C 0.5°C increment 2–5 sec/step (or use instrument default setting)
Bio-Rad® iQ™5, MiniOpticon™, Chromo-4™, MyiQ™	Standard		10–15 sec	15–30 sec		
ABI 7500, StepOne, StepOnePlus, 7900ht, and ViiA7	Fast		1–3 sec	20–30 sec		
	Standard		15 sec	60 sec		
ABI 7300 and 7000	Standard		15 sec	60 sec		
Roche LightCycler 480	Fast		2–5 sec	15–30 sec		
	Standard		15 sec	60 sec		
QIAGEN Rotor-Gene and Stratagene Mx series	Fast		2–5 sec	15–30 sec		